

Aggregate route choice models: The mental representation item approach

THÈSE N° 8004 (2017)

PRÉSENTÉE LE 10 NOVEMBRE 2017

À LA FACULTÉ DE L'ENVIRONNEMENT NATUREL, ARCHITECTURAL ET CONSTRUIT

LABORATOIRE TRANSPORT ET MOBILITÉ

PROGRAMME DOCTORAL EN GÉNIE CIVIL ET ENVIRONNEMENT

ÉCOLE POLYTECHNIQUE FÉDÉRALE DE LAUSANNE

POUR L'OBTENTION DU GRADE DE DOCTEUR ÈS SCIENCES

PAR

Evanthia KAZAGLI

acceptée sur proposition du jury:

Prof. A. Nussbaumer, président du jury

Prof. M. Bierlaire, directeur de thèse

Prof. . G. Flötteröd, rapporteur

Prof. O. Anker Nielsen, rapporteur

Prof. N. Geroliminis, rapporteur



ÉCOLE POLYTECHNIQUE
FÉDÉRALE DE LAUSANNE

Suisse
2017

“In the process of way-finding, the strategic link is the environmental image,
the generalised mental picture of the exterior physical world that is held by an
individual.”

— Kevin Lynch, 1960
The image of the city

Acknowledgements

This thesis has been supported by the Swiss Nation Science Foundation, under the project #200021_146621 *Capturing latent concepts with non invasive sensing systems*.

This thesis is the product of several years of work and effort, during which I was accompanied and supported by many colleagues, friends and family members, with whom I shared smiles and tears, intriguing conversations and funny moments. I am grateful to each one of them for being part of this journey.

First and foremost, I would like to thank my supervisor Prof. Michel Bierlaire, for being a great mentor and for accepting me in the Transport and Mobility Laboratory — an exceptional group to be part of and a stimulating environment to work in. I am grateful to him for his patience and guidance, and for all the things I learned by working at his side. His intelligence, insightful comments and constructive feedback have been boosting my work all the way through. He is a fantastic person to have known, worked with and befriended.

I would also like to thank the committee of my thesis: Prof. Alain Nussbaumer, Prof. Gunnar Flötteröd, Prof. Otto Anker Nielsen and Prof. Nikolas Geroliminis, for their constructive and insightful feedback that significantly contributed in improving my thesis.

I am grateful to Haris Koutsopoulos, for being an amazing teacher, person and researcher, who inspired me to pursue research in the first place, and to Gunnar Flötteröd for his encouragement, availability and for all the fruitful discussions that have been a source of both knowledge and inspiration to me.

I am especially thankful to Tien Mai and Emma Frejinger for providing the Borlänge data and the code for — and insights into — the recursive logit model, as well as to Prof. Luis Miranda-Moreno and Joshua Stipancic from McGill University, for the provision of the Québec data and additional resources.

Special thanks to Matthieu de Lapparent for his support and feedback, and to the current and former members and friends from the Transport and Mobility Laboratory; thank you for constantly and actively creating a fantastic working atmosphere, for sharing the

load and being supportive to each other: Marija and Tom, Anna and Stefan, Shadi and Yousef, Virginie, Meri, Nicholas, Nikola, Riccardo; Amanda, Ricardo, Jingmin, Bilge, Aurélie, Nitish, Antonin, Flurin, Dimitris, Jianghang, Bilal. Thank you Marianne, Mila and Anne for being by our side and taking care of us. Thank you greater TRANSP-OR family: Darko, Karen and Aitor for complementing our amazing group. Thank you Leonardo and dear members of LUTS for the intriguing collaborations. Thank you my dear LUTS lady Claudia.

I am particularly grateful to Anastasia, Irene, Albano, Sophia, Sofia, Matthias, Mario, Stefanos and Dimitris; and to Evi, Orion, Lydia, Effe, Alexandros, Katerina, Michalis, Stergios, Sotiris, Tatiana, Kostas, Bram, Eirini, Giannis, Nico, Antigoni, Elisavet and Aliki for making Lausanne home for me.

Special thanks to my beloved friends Lina, Eleftheria, Stella, Giorgos, Lefteris, Giorgos and Eirini in Athens, and Athina, Gerasimos, Iro, Dimitris, Panos, Nikos, Giannis and Andreas in Stockholm.

Last, but not least, I would like to thank my family — my father and mother, Tasos and Moscho, my brother Christos, my aunts Lola and Katerina, my uncle Christos and my grand-parents — for their love, constant encouragement and support. Finally, I could not thank you enough Iliya, for your unconditional care, love and support, for your encouragement, your understanding and for being by my side.

Lausanne, September 25, 2017

Evanthia Kazagli

Abstract

Route choice analysis concerns the understanding, modeling and prediction of the itinerary of an individual who travels from one position to another. In this thesis we elaborate on aggregate route choice analysis. The objective is the development of a flexible framework for analysing and predicting route choice behavior.

The research is motivated by the need to reduce the structural complexity of the state of the art route choice models and aims at facilitating their practical applications. Our approach is inspired by the environmental images of the physical space that individuals form in their minds. The framework is based on elements designed to mimic these representations. In this context, we introduce the concept of mental representation item (MRI) in route choice analysis. The MRIs represent the strategic decisions of individuals and constitute the building blocks of the alternatives of the aggregate model. They play the same role as the links do in the specification of a disaggregate model. In contrast to the links, the MRIs are not dictated by the definition of the network model. Their definition depends on the analyst, allowing her to control the trade-off between complexity and realism, according to the needs of the specific application and the data availability.

We start by presenting a methodology for the definition of operational random utility models based on MRIs. As a proof of concept, we define a simple model for the town of Borlänge, in Sweden, and test it using real data. We further discuss applications of the proposed model to traffic assignment and route guidance. The results demonstrate that the use of simple methods leads to a meaningful model that can be estimated and used in practice.

We then investigate the capability of the proposed MRI model to derive route choice indicators for practical applications, through comparison with a state of the art disaggregate model. The recursive logit (RL) model is selected as the representative of the existing disaggregate approaches. An extension of the MRI framework with the definition of a graph of MRI elements is presented and methods to derive route choice indicators from a model that does not correspond to the intended level of analysis are proposed. The evaluation of the models' performance at the aggregate level shows that the MRI model should be preferred against a disaggregate model that is subjected to aggregation, if an aggregate analysis is of interest.

To demonstrate the generalization and applicability of the framework, we use a dataset from the city of Québec, in Canada. Our approach is motivated by (i) the additional complexity in the definition of the model due to the size of the city, and (ii) the lack of a detailed disaggregate network model. The proposed model is (i) operationalized using simple techniques, (ii) compatible with the standard estimation procedures and (iii) by integration with the RL model, readily applied to the prediction of flows on the major segments of the network. This model is not as simple as the first MRI model, yet still of much lower structural complexity in comparison with the disaggregate approach, allowing for fast computation times. The results demonstrate its capability to reproduce the patterns in the observed flows.

This thesis contributes by (i) gradually addressing the challenges related to the definition, operationalization and application of aggregate route choice models and (ii) demonstrating their applicability and validity using real data. This is important as it has the potential (i) to reduce the structural complexity of the state of the art approaches, and (ii) to allow for project-specific models that do not require a detailed network model. In a broader context, the framework is relevant and can be adapted to pedestrian route and activity choice modeling.

Keywords: route choice analysis, operational aggregate models, discrete choice models, environmental images, applications, route choice indicators, revealed preference data, sensor data, flexible framework

Résumé

Dans cette thèse, nous proposons une approche agrégée pour l’analyse des choix individuels d’itinéraire. L’objectif est le développement d’un cadre flexible pour analyser et prédire les comportements de choix d’itinéraire.

Cette recherche est motivée par la nécessité de réduire la complexité structurelle des modèles de choix d’itinéraires contemporains. Elle vise aussi à faciliter leurs mises en œuvre pratiques. La démarche propose un cadre normatif d’analyse qui s’inspire de la construction de l’imaginaire personnel, en particulier des représentations subjectives de l’espace physique que les individus se créent. Le concept d’ “unité de représentation mentale” (MRI) est au cœur de cette approche. La spécification et l’assemblage de plusieurs de ces unités permet de mimer ces représentations. Les MRI caractérisent les décisions stratégiques des individus en termes de choix d’itinéraire. Ils constituent les éléments générateurs des choix potentiels d’itinéraire. Par analogie, ils jouent le même rôle que les choix d’arcs routiers dans les modèles conventionnels de choix d’itinéraires. Contrairement à ces derniers, les MRI ne dépendent pas de la structure précise d’un réseau routier. Leurs définitions et la manière dont ils sont assemblés dépendent de l’analyste, ce qui lui permet d’arbitrer entre degré d’abstraction et réalisme au vu de l’application souhaitée et des données disponibles.

Nous débutons par la définition d’une architecture générale combinant modèles de choix d’itinéraire, maximisation de l’utilité aléatoire, et “unités de représentation mentale” (MRI). Sur la base de données collectées dans la ville de Borlänge (Suède), un modèle simplifié sert de premier cas d’étude. Outre la spécification et l’estimation du modèle, nous discutons des performances attendu d’un tel modèle en terme d’affectation du trafic et de guidage routier. Les résultats montrent que l’utilisation de telles méthodes sont fiables et robustes dans un cadre opérationnel.

Nous comparons ensuite les capacités d’une telle approche à prédire les flux routiers et autres indicateurs avec l’état de l’art des modèles désagrégés de choix d’itinéraire: le modèle logit récursif. A ce titre, un graphe d’unités MRI est détaillé. Les résultats de comparaison montre qu’un modèle à base de MRI proprement sélectionnés est préférable à modèle désagrégé soumis à agrégation ultérieure.

Pour montrer l’extension et la mise en pratique de notre approche, nous utilisons un

ensemble de données de la ville de Québec (Canada). Ce cas d'étude est motivé par (i) la complexité supplémentaire dans la définition du modèle, i.e. des unités MRI, en raison de la taille de la ville, et (ii) l'absence d'un modèle de réseau désagrégé détaillé pour la ville. Le cadre est mis en œuvre en utilisant des techniques usuelles: compatibilité avec les procédures d'estimation standard et aisance quant à la prédiction des flux sur les principaux segments du réseau. Ce modèle n'est pas aussi simple que le premier modèle MRI. Sa complexité structurelle reste cependant beaucoup plus commode par rapport à l'approche désagrégée. Les résultats démontrent la capacité du modèle à reproduire les profils dans les flux observés.

La thèse contribue (i) à aborder progressivement les défis liés à la définition, à la mise en œuvre pratique et à l'application des modèles de choix d'itinéraires globaux et (ii) à démontrer leur validité et leur réalisme en utilisant des données empiriques. Ceci est important car une telle approche montre que l'on peut réduire la complexité structurelle des modèles de choix d'itinéraire sans perdre en qualité en termes de prévision des flux de trafic. Dans un contexte plus large, le cadre est pertinent et peut être adapté à la modélisation des itinéraires piétonniers et des choix d'activités.

Mots-clés: analyse de choix de route, modèles d'agrégats opérationnels, modèles de choix discrets, images environnementales, applications, indicateurs de choix de route, données de préférence révélées, données de capteurs, flexibilité

Contents

Acknowledgements	i
Abstract (English/Français)	iii
List of Figures	xi
List of Tables	xiii
1 Introduction	1
1.1 Context and motivation	1
1.2 Objectives	4
1.3 Contributions	5
1.4 Thesis structure	6
2 State of the Art	9
2.1 Route choice data	11
2.2 Choice set	13
2.3 Correlation of alternatives	14
2.4 Summary	16
3 Aggregate route choice	19
3.1 Methodological framework	20
3.1.1 The Mental Representation Item	20
3.1.2 Definition of the alternatives	22
3.1.3 Specification of the utility functions	23
3.1.4 Model estimation	25
3.1.5 Model application	25
3.2 Additional considerations	27
3.2.1 Defining the MRI	27
3.2.2 Model-to-data approach	28
3.2.3 Route guidance	29
3.3 Case study	29
3.3.1 Definition the choice problem	30
3.3.2 Model specification	36
3.3.3 Model estimation	38

3.3.4	Forecasting results & validation	40
3.3.5	Model Application	41
3.4	Discussions	42
3.4.1	Critical aspects of the MRI approach	45
3.4.2	Limitations of the case study	45
3.5	Summary	46
4	Derivation of route choice indicators	47
4.1	Disaggregate and aggregate route choice models	48
4.1.1	The recursive logit model	48
4.1.2	The mental representation items model	49
4.2	Deriving indicators	50
4.2.1	Disaggregate and aggregate route choice indicators	51
4.2.2	Deriving disaggregate indicators	51
4.2.3	Deriving aggregate indicators	53
4.3	Additional considerations	58
4.3.1	Evaluation at the aggregate level	58
4.3.2	Addressing the correlation of alternatives	59
4.4	Case study	60
4.4.1	The MRI graph of Borlänge	61
4.4.2	Operational aspects of the MRI model	62
4.4.3	Model specifications and estimation results	63
4.4.4	Route choice indicators	65
4.4.5	Performance at the aggregate level	69
4.4.6	Capturing correlation with the MRI model	71
4.5	Summary	74
5	Route choice in a large network: Québec city	77
5.1	Modeling	78
5.1.1	Available dataset	78
5.1.2	The mobility image in Québec city	80
5.1.3	Definitions	82
5.1.4	Attributes	86
5.1.5	Model specification and estimation approach	87
5.1.6	Model application	90
5.2	Results	92
5.2.1	Estimation results	92
5.2.2	Forecasting results and validation	93
5.2.3	Aggregate element flows	95
5.3	Discussions	95
5.4	Summary	99

6 Conclusion	101
6.1 Research summary	101
6.2 Theoretical and practical implications	103
6.3 Future research directions	104
A Specification of the assignment model	107
B Description of a work trip in Athens	109
C Additional figures	113
D Additional tables	117
Bibliography	128
Curriculum Vitae	129

List of Figures

3.1	Example of two MRIs and their components.	21
3.2	Example of an aggregate route alternative in the MRI framework.	23
3.3	Schematic representation of the specification of utilities through representative paths.	24
3.4	Illustration of the measurement equation.	26
3.5	Example of MRI sequences in the city of Stockholm.	28
3.6	Borlänge road network.	30
3.7	National roads, R50 and R.70, in Borlänge.	31
3.8	Example of route options provided by Google Maps Directions.	32
3.9	Example of route options provided by Google Maps Directions.	32
3.10	Representative points of the MRIs.	34
3.11	The two main streets in the city center.	34
3.12	Illustration of the MRI choice set with representative paths.	35
3.13	Distribution of travel time for the four MRIs.	37
3.14	Power series of degree three for the travel time of the CL and the CO alternatives.	38
3.15	Box plot of the market shares from the application in 20% of the data. . .	41
3.16	Link choice probabilities given the MRI choice set.	42
3.17	Link choice probabilities conditional on the choice of the AV alternative. .	43
3.18	Link choice probabilities conditional on the choice of the CC alternative. .	43
3.19	Link choice probabilities conditional on the choice of the CL alternative. .	44
3.20	Link choice probabilities conditional on the choice of the CO alternative. .	44
4.1	Illustration of notation for the RL model.	49
4.2	Illustrative example.	55
4.3	The underlying MRI nesting structure.	60
4.4	The MRI graph.	62
4.5	Link flows for a given <i>od</i> pair assuming a demand of one vehicle.	65
4.6	MRI choice probabilities as derived from the two aggregation approaches. .	67
4.7	MRI choice probabilities as computed from the two models.	67
4.8	Indicative example of an observation for which the RL is faced with low probability for the chosen alternative.	68

4.9	Indicative example of an observation for which the MRI model is faced with low probability for the chosen alternative.	69
4.10	Log likelihood of the training samples.	72
4.11	Log likelihood of the test samples.	72
4.12	Box plot of the log likelihood for the training samples.	73
4.13	Box plot of the log likelihood for the test samples.	73
4.14	Log likelihood of the training samples.	75
4.15	Predicted log likelihood of the test samples.	75
5.1	Québec city: origins and destinations in the data sample.	79
5.2	Observed trajectories and boundaries of the study area.	79
5.3	Most visited segments in the data sample.	80
5.4	Mobility versus accesibility.	81
5.5	Geographical span of the MRIs and the <i>OD</i> zones in Québec city.	84
5.6	The MRI graph of Québec city.	85
5.7	Illustration of a simple (m_1) and a complex (m_2) node.	87
5.8	Distribution of departure time in the data sample.	89
5.9	Observed trajectory and the corresponding mapping on \mathcal{G}^M	91
5.10	Distribution of the forecasted choice probabilities of the chosen alternative.	94
5.11	Distribution of the state (next node) choice probabilities.	94
5.12	Average test error over the training samples.	96
5.13	Average test error over the test samples.	96
5.14	Aggregate element flows.	97
5.15	Boxplot of the aggregate element flows over the validation samples.	97
5.16	Number of links in the map-matched trajectory versus the corresponding number of nodes of the MRI sequence.	99
B1	Sketch of the described route alternatives.	111
C1	The <i>OD</i> zones in Borlänge.	113
C2	Characteristic examples of observed trajectories in Borlänge.	114
C3	The geographical span of the MRIs in Borlänge.	115
C4	Example of MRI sequences in Borlänge.	115
C5	The <i>OD</i> zones in Québec city.	116

List of Tables

3.1	Descriptive statistics on attributes	36
3.2	Specification table with piecewise linear travel time formulation	39
3.3	Frequency of the chosen alternatives	39
3.4	Estimation results	40
4.1	Notations	51
4.2	Route choice indicators	52
4.3	Estimation results for the RL model	63
4.4	Estimation results of the MRI logit model	64
4.5	Estimation results	74
5.1	The prominent routes in Québec city	81
5.2	The MRIs in Québec city	83
5.3	The MRI attributes	88
5.4	Estimation results	93
D1	List of alternatives of the MRI model (Borlänge)	117
D2	Transfer times (non zero) between MRI pairs (Québec)	118

1

Introduction

In this chapter, we start by framing the thesis in its broader context and outlining the research motivation (Section 1.1). Sections 1.2 and 1.3, present respectively, the research objectives and the research contributions. Section 1.4 describes the structure of the thesis.

1.1 Context and motivation

Nowadays, a plethora of ceaselessly collected data accompanies the increasing interest in human behavior. Researchers and analysts strive to access and exploit this data in order to (i) understand and describe the processes of generating the observed patterns in human behavior and (ii) be able to anticipate future behaviors. A vast amount of the collected data pertains to human mobility (e.g. Cottrill et al., 2013), i.e. to the various dimensions of individuals' travel behavior through the transportation system. Travel behavior comprises the choices of individuals with respect to the usage of the transportation system, such as the choice of the location to perform a given activity, the choice of the mode of transport, and the choice of the route to reach the location of interest.

As urban areas continue to expand, an increase in the number and use of different transportation modes is taking place (Gallotti and Barthelemy, 2014). Likewise, transportation networks expand in order to serve the increasing demand for transport. The availability of large-scale data is a powerful tool in monitoring, analyzing the perfor-

mance and eventually optimizing, through efficient management, the operations of today's transport systems. The efforts towards this goal are focused on better understanding, describing and predicting the individual travel choices. Benefiting from the data abundance, a great deal of research has taken, and continues to be taking, place in the domain of travel demand modeling.

Route choice models are at the core of travel demand analysis. They are applied to predict the distribution of travelers on the transportation network, allowing for the identification of congestion and supporting a variety of mobility analyses for planning and management, as well as real-time operations — such as route guidance. Given an origin (o), a destination (d) and a transportation mode, the objective is to develop a model that describes how individuals select their itineraries between the o and d in the transportation network. A comprehensive review of the route choice modeling problem can be found in Bovy and Stern (1990) and Frejinger (2008).

The complexity of the transportation network, inherent in most modern cities, brings about challenges for individuals, during their navigation and way-finding tasks (Rosvall et al., 2005; Gallotti et al., 2016; Venigalla et al., 2016), as well as for transport analysts tackling route choice analysis. Regarding the modeling side, classical route choice models assume a mathematical representation of the network $\mathcal{G} = (\mathcal{A}, \mathcal{V})$, defined in terms of links (oriented arcs) \mathcal{A} and nodes (vertices) \mathcal{V} , and a number of link additive attributes associated with each link. Following this network representation, a route is defined as a sequence of links connecting the o and the d of the trip in the network model. It is commonly referred to as a *path*. The need to go beyond the initial shortest and fastest path models (Dijkstra, 1959) has triggered a great deal of research. Route choice analysis is commonly performed within the framework of discrete choice modeling (Ben-Akiva and Lerman, 1985). The primary element for the development of an operational random utility model consists in the definition of the choice set \mathcal{C}_n of each individual n in the data. The identification of the path alternatives that form the \mathcal{C}_n of a route choice model in a real network is an intricate task, as it is subjected to the high complexity of the transportation network. As a consequence, route choice models are characterized by high structural complexity and their application to large networks is computationally expensive.

Different heuristics have been proposed to generate subsets of paths, commonly referred to as consideration sets (Ben-Akiva et al., 1984; Azevedo et al., 1993; de la Barra et al., 1993; van der Zijpp and Fiorenzo Catalano, 2005; Friedrich et al., 2001; Hoogendoorn-Lanser, 2005; Prato and Bekhor, 2006), to which the observed path is subsequently added for the estimation of the model (Bekhor et al., 2006). The values of the parameter estimates are dependent on the definition of the choice sets (Frejinger et al., 2009) and may vary significantly for different instances of sampled sets. Considering all feasible paths in the choice set is hence an important assumption in order to avoid biases in the model (Frejinger et al., 2009). Sampling approaches considering all feasible paths

between each *od* pair and correction of paths utilities for sampling have been proposed for this reason (Frejinger et al., 2009; Flötteröd and Bierlaire, 2013; Lai and Bierlaire, 2015). Triggered by previous works developed in the context of traffic assignment (Akamatsu, 1996; Baillon and Cominetti, 2008), Fosgerau et al. (2013a) present the recursive logit (RL) model, where the path choice problem is formulated as a sequential link choice problem in a dynamic framework. The proposed technique avoids the full enumeration of paths and does not require sampling of alternatives. The RL model is the most tractable disaggregate approach to route choice analysis.

Besides the complexity that it entails for the specification and estimation of the model, the path representation is not quite consistent with the way individuals perceive and describe their itineraries (Golledge, 1999).

“As the accessible space is larger than the space that they can perceive and since most destinations are located beyond the perceptual boundaries, people need to break down the complexity and form representations of the surrounding space in order to move effectively and efficiently in the environment.”
Büchner (2011)

In the research fields of cognitive science, environmental psychology and geography, and in their attempt to answer questions such as *How individuals perceive and process information during travel in spatial networks*, one comes across concepts such as the *mental map*, the *mental representation*, or the *anchor point*, that had been first discussed by Tolman (1948) and extensively researched thereafter (see e.g. Chase, 1983; Couclelis et al., 1987; Taylor and Tversky, 1992; Golledge, 1999; Golledge and Gärling, 2003). Each field approaches these concepts from a different perspective and defines them accordingly. Lynch (1960) decomposes the image of the city into *paths*, *edges*, *districts*, *nodes* and *landmarks*. Suttles (1972) defines a cognitive map as the mixture of qualitative and spatial information that allows us to make decisions in a spatial context. Golledge (1999) argues that individuals relate to anchor points in the spatial environment and that the anchors have a dual role: (i) they serve as organizing elements of individuals’ mental maps, and (ii) they enable way-finding. Hannes et al. (2008), defines the mental map as *“The whole of spatial and travel related information used and stored in memory”*.

Arentze and Timmermans (2005) use the concept of mental maps in a micro-simulation model for activity choice. A few attempts to use perceptual concepts in route choice analysis include the labelling approach by Ben-Akiva et al. (1984) for path generation and sampling, and the subnetworks approach by Frejinger and Bierlaire (2007) to capture correlation of alternatives. Yet, the modeling element in these works is still a path. Outside the framework of discrete choice, Manley et al. (2015a) and Manley et al. (2015b) perform an empirical analysis of taxi data and propose a heuristic model for route choice based on the concept of anchor points.

A question with respect to the definition of the route choice problem within the context

of discrete choice analysis is then *How long does the description of the alternatives — associated with the representation of the route choice decisions of individuals — needs to be, in order to obtain a meaningful model that is adequate for relevant analysis?* Similarly to the way individuals make simplifications of the physical space to facilitate their navigation and way-finding, route choice analysts may make use of aggregate modeling elements — associated with the mental representations of individuals — to adjust the level of complexity of the model, depending on the needs of its application and the availability, or not, of an adequate detailed network model. To put this in context, route choice behavior of individuals manifests itself as flow in the transportation network. The *link* and *route* flows are the most important *route choice indicators*. From an application point of view, both disaggregate and aggregate indicators are of interest.

The general trend in the literature is to propose more and more complex models tackling route choice (Fosgerau et al., 2013a; Yang and Juang, 2014; Lai and Bierlaire, 2015; Ramos, 2015; Mai et al., 2015; Mai, 2016; Mai et al., 2017). In this thesis, we are investigating in the opposite direction, i.e. we aim at simplifying the problem. This is done by modeling the strategic decisions of individuals instead of the operational ones. We build a modeling framework that (i) has a level of complexity similar with the one handled by the individuals and (ii) attenuates the curse of dimensionality of the path-based formulation. Along these lines, we introduce a modeling element that designates the mental representations of the physical space formed by the individuals. It is called Mental Representation Item (MRI). To derive a systematic definition of the MRI as a modeling element we combine theory and data. Contrary to the research conducted in the disciplines pertaining to cognition, this thesis does not look at how the representations of space are formed or learned. It rather exploits the intuition gained from these fields to achieve the goal of a flexible and operational modeling framework for route choice analysis.

1.2 Objectives

The goal of this thesis is the development of a flexible framework that facilitates the analysis and prediction of route choice behavior, by allowing to control the level of aggregation in the representation of the alternatives. Within this context, we address the following:

1. Development of aggregate route choice models
 - (a) We use a confirmatory approach for the definition of the modeling elements, where the consistency of the theoretical behavioral framework is verified by the data.
 - (b) We define operational random utility models based on the aggregate modeling elements and
 - (c) identify suitable methods for the model specification.

- (d) Finally, we integrate the framework with state of the art estimation procedures.
- 2. Use of route choice models to derive route choice indicators for practical applications
 - (a) We describe methods to derive route choice indicators using both existing disaggregate approaches and the proposed aggregate approach.
 - (b) We then analyze the features of each approach in deriving the indicators of interest.
 - (c) Finally, we evaluate the adequacy of the proposed aggregate approach in deriving indicators for aggregate analysis, through comparison with a state of the art disaggregate approach that is subjected to aggregation.
- 3. Application
 - (a) We apply the models using real data, in order to evaluate the performance and validity of the framework.
 - (b) Our analysis allows to draw insights into the use of a specific model, depending on the needs of the application and the data availability.
 - (c) Finally, we demonstrate the generalisation and applicability of the framework to a large network.

1.3 Contributions

This thesis contributes towards simplifying the structure of route choice models and facilitating their use for practical applications. The main scientific contributions of the research include:

- 1. Development of aggregate route choice models
 - (a) *Mental representation item* (Chapter 3) The definition of a new modeling element for the representation/ definition of the alternatives in the model. It is designed to mimic the mental representations of individuals and allows to simplify the description of the alternatives.
 - (b) *Aggregate route choice* (Chapter 3) The definition of a route choice modeling framework that is based on the concept of a MRI and is compatible with the state of the art specification and estimation procedures. It contains the definition of an aggregate graph composed of MRI elements, that is the equivalent of \mathcal{G} of the disaggregate approach.
- 2. Use of route choice models to derive route choice indicators for practical applications
 - (a) *Derivation of route choice indicators* (Chapter 4) The provision of a practical scheme for the derivation of route choice indicators using both disaggregate and aggregate models.

- (b) *Method to evaluate the MRI approach* (Chapter 4) The scheme incorporates a method that allows to evaluate the performance of the MRI model for the purposes of aggregate analyses, through comparison with a disaggregate model.

3. Application

- (a) *Route choice analysis in a large network* (Chapter 5) A paradigm for the operationalization of the MRI approach, that illustrates its flexibility and applicability to large networks.

The proposed models are applied to the case study of Borlänge, that serves as a proof of concept, in order to demonstrate their validity and identify their advantages and disadvantages with respect to their applications. The use of simple methods for the operationalization of the proposed aggregate approach, leads to a meaningful model that can be estimated and used in practice. The evaluation of the performance of the models at the *aggregate level* of analysis shows that the MRI model should be preferred to a disaggregate model that is subjected to aggregation. The case study of Québec city is employed to demonstrate the capability of the proposed framework to adapt to a large scale application, while remaining computationally affordable. By integration with the RL model (Fosgerau et al., 2013a), the proposed model is readily applied to the prediction of flows on the major segments of the network.

1.4 Thesis structure

The thesis is structured as follows.

Chapter 2 is a literature review pertaining to route choice modeling.

The chapter borrows from the book chapter

Kazagli, E., Chen, J., and Bierlaire, M. (2014). *Individual Mobility Analysis Using Smartphone Data*. In Soora Rasouli and Harry Timmermans eds., *Mobile Technologies for Activity-Travel Data Collection and Analysis* pp.187-208. IGI Global.

Chapter 3 describes the methodology for the development of aggregate route choice models and illustrates its use for traffic assignment.

The preliminary ideas of the methodology presented in this chapter are published as

Kazagli, E., and Bierlaire, M. (2014). *Revisiting Route Choice Modeling: A Multi-Level Modeling Framework for Route Choice Behavior*. *Proceedings of the Swiss Transportation Research Conference (STRC)* 14-16 May, 2014.

Kazagli, E., and Bierlaire, M. (2015). A Route Choice Model based on Mental Representations. Proceedings of the Proceedings of the 15th Swiss Transport Research Conference (STRC) April 15-17, 2015.

Kazagli, E., Bierlaire, M., and Flötteröd, G. (2015). Revisiting the route choice problem: A modeling framework based on mental representations. *Technical report TRANSP-OR 150824*.

The chapter has been published as

Kazagli, E., Bierlaire, M., and Flötteröd, G. (2016). Revisiting the route choice problem: A modeling framework based on mental representations, *Journal of Choice Modelling* 19:1-23.

Chapter 4 investigates tractable route choice models and evaluates how they perform in deriving disaggregate and aggregate route choice indicators. An extension of the MRI framework with the definition of a graph of MRI elements is presented and MRI models incorporating the effect of correlation are tested.

The preliminary ideas of the methodology presented in this chapter are published as

Kazagli, E., and Bierlaire, M. (2016). Assessing complex route choice models using mental representations. Proceedings of the 16th Swiss Transport Research Conference (STRC) May 19-20, 2016, 2016.

The chapter is based on the article (under review)

Kazagli, E., Bierlaire, M., and Lapparent, M.(de) (2017). Operational route choice methodologies for practical applications. *Technical report TRANSP-OR 170526*.

Chapter 5 applies the framework to a large network. The model specification is enhanced by the inclusion of more variables. As an example, an attribute representing the complexity of a route is introduced. The model is estimated using the RL model formulation and is readily applied to the prediction of flows on the major segments of the network.

The chapter is based on the article (working paper)

Kazagli, E., Bierlaire, M. (2017). Route choice analysis in a large network: Québec city. *Working paper*.

Chapter 6 summarizes the contributions of the thesis and determines future research directions.

2

State of the Art

Discrete choice modeling, formulated within the random utility framework, is the most common modeling approach to route choice analysis. Probabilistic models are developed on the basis of the utility maximization decision rule and statistical methods — with maximum likelihood being the most common method for the estimation of the model parameters — are used for the estimation of the models. We refer the reader to the textbooks by Ben-Akiva and Lerman (1985) and Train (2003) for a comprehensive review of discrete choice theory. In the following we provide a short overview.

Within the random utility framework, each individual n is assumed to associate a random utility U_{in} with each alternative i in her choice set \mathcal{C}_n and subsequently chose the alternative with the highest utility. This is expressed as $P(i | \mathcal{C}_n) = P(U_{in} \geq U_{jn}, \forall j \in \mathcal{C}_n)$, with U_{in} being a latent construct, i.e. a component that is not observed by the analyst. It is decomposed as $U_{in} = V_{in} + \varepsilon_{in}$. V_{in} is called the deterministic or systematic part of the utility. It is defined as a function of observed factors, that is the attributes of the alternative x_{in} and the socioeconomic characteristics of the individual z_n . ε_{in} represents the random variation due to e.g. incomplete knowledge of the analyst about the individual preferences, heterogeneity of preferences, measurement errors. It captures the factors that affect the utility but are not included in V_{in} . It relies on the analyst to make an assumption about the distribution of ε_{in} relative to her representation of the choice context (Train, 2003). This determines the type of model.

The fundamental model within this framework is the logit model. It assumes that ε_{in}

are independent and identically distributed (i.i.d.) extreme value. The logit probability has a closed form and it is given by

$$P(i | \mathcal{C}_n) = \frac{e^{\mu V_{in}}}{\sum_{j \in \mathcal{C}_n} e^{\mu V_{jn}}}, \quad (2.1)$$

where μ is the scale of the distribution. $V_{in} = \beta(x_{in} + z_n)$ with β a vector of parameters to be estimated.

To estimate the unknown parameters β of the choice model

1. the availability of *choice data* is the first element that the modeler needs to *have*,
2. the *choice set* \mathcal{C}_n is the first element that the modeler needs to *define*.

Additionally, the correlation of alternatives needs to be incorporated in the model specification. This is particularly important in the context of route choice, as the definition of a *path* entails a high overlap among the possible itineraries between an *od* pair. Therefore, a logit model, assuming independence of the error terms, is usually not appropriate.

The two types of data used in the literature for choice modeling are revealed preference (RP) and stated preference (SP). RP data consists in observed behavior, i.e. in choices that individuals actually made and are requested to report. SP data consists in individual responses to hypothetical scenarios, that are constructed by the analyst and presented to them. The estimation of discrete choice models for route choice analysis with RP data involves specific challenges that are related to the three elements identified above, i.e. to the data itself, the choice set and the correlation of alternatives. In summary, the demanding requirements in data collection and processing, the combinatorial nature of the choice set, and the structural correlation due to the physical overlap of paths (Ben-Akiva and Bierlaire, 2003) are the main issues of the estimation with RP data. These issues apply to a much lesser extent to the estimation of models with stated preference (SP) data, which is therefore easier to handle. In this thesis we focus on RP data.

The remainder of this chapter provides an overview of the existing route choice data collection approaches and reviews approaches that deal with the choice set generation and correlation of alternatives. It is organized in four parts. The first part (Section 2.1) focuses on data acquisition and processing pertaining to route choice analysis with RP data. The second part (Section 2.2) summarizes approaches tackling the definition of the choice set. The third part (Section 2.3) summarizes approaches tackling the correlation of alternatives. Section 2.4 concludes the chapter.

2.1 Route choice data

This Section borrows from the book chapter

Kazagli, E., Chen, J., and Bierlaire, M. (2014). *Individual Mobility Analysis Using Smartphone Data*, in Soora Rasouli and Harry Timmermans eds., *Mobile Technologies for Activity-Travel Data Collection and Analysis*, IGI Global, chapter 2, pp.187-208.

The primary data elements for the specification and estimation of a route choice model are (i) route choice observations, (ii) a network model, and (iii) information about the network attributes.

Choice data is traditionally collected by means of surveys where people are asked — among other context information questions — to describe their travel choices, such as the route they followed for a specific trip, or the mode of transport they used to perform the trip. Traditional surveys are conducted via mail, telephone or computer assisted tools. They entail complex logistics and are costly, limited by accuracy of recall, reliability, and respondents' compliance. Route choice studies based on survey data include Ben-Akiva et al. (1984), Mahmassani et al. (1993), Abdel-Aty et al. (1997), Ramming (2002), Vrtic et al. (2006) and Prato et al. (2011).

Recent advances in data collection technologies based on global positioning system (GPS) and GPS-enabled smartphones provide a wealth of spatiotemporal data at the *individual level*. These methods have revolutionized the data acquisition and have become a powerful tool in studying mobility patterns (e.g. González et al., 2008), as well as extracting traffic information and analyzing the performance of the transportation network (e.g. Jenelius and Koutsopoulos, 2013; Stipancic et al., 2017). Examples of smartphone-based travel surveys include Hato and Asakura (2001), Eagle and Pentland (2006), Murakami et al. (2012), Cottrill et al. (2013) and Miranda-Moreno et al. (2015).

GPS technologies allow to collect choice observations through passive monitoring, i.e. by tracking users as they traverse the network. GPS tracking is hence particularly relevant to the collection of route choice data. The first route choice models based on GPS data are presented by Broach et al. (2012) modeling route choice behavior of cyclists, and Murakami and Wagner (1999), Jan et al. (2000), Li et al. (2005) modeling car drivers route choice behavior. Halldórsdóttir et al. (2014) use GPS data to evaluate the efficiency of choice set generation methods in the case of bicycle routes and test their ability to produce relevant and heterogeneous routes. Prato et al. (2014) use a big GPS data of route choices to estimate the values of congestion and reliability and identify their effect on travel behavior. More recently, various methodological advances in route choice modeling for car traffic have benefited from the availability of GPS data (see

Frejinger and Bierlaire, 2007; Bierlaire and Frejinger, 2008; Fosgerau et al., 2013a; Mai et al., 2015, 2016). Ramos (2015) models car route choice in a dynamic framework and investigates the effect of travel information using GPS data.

GPS-enabled smartphones have an advantage over the vehicle-based GPS loggers. This is because (i) there is no need to carry any additional device as, nowadays, most people carry a smartphone with them throughout the day, and (ii) smartphones are embedded with various other sensors such as accelerometers, Wifi and Bluetooth, and therefore, important context information, such as the trip purpose, that is typically missing from the GPS data (Stopher et al., 2007), can be inferred through the development of models (e.g. Bierlaire et al., 2013).

The main challenge related to route choice data — either this comes from traditional surveys, or from GPS records — is that, typically, it is not directly applicable to use in the model (Frejinger, 2008). The data in its raw format rarely corresponds to paths, which is the established modeling element.

“The concept of path, which is the core of a route choice model, is usually too abstract for a reliable data collection process.” Bierlaire and Frejinger (2008)

The observations need to be matched to the network that the modeler uses and the required processing entails a high risk of introducing biases in the later steps of estimation. Along these lines, Bierlaire and Frejinger (2008) develop a framework for estimating route choice models that combines “network-free” data with a network based model. The idea is that since the underlying route choices, as represented in the model, are based on paths — while the observations are not — there is a need to establish a link between them. This is accomplished by determining physical areas in the network where each piece of data, e.g. a reported location along a trip or a GPS point) is relevant. They are called domains of data relevance (DDRs). The framework treats the errors in a probabilistic manner. Measurement equations are used to associate the network-free data with the network through the DDRs. By allowing several paths to correspond to the same observation, data manipulation and assumptions on missing observations are avoided. Later work by Bierlaire et al. (2013) further exploited this idea to develop a probabilistic map-matching algorithm¹ tackling the inaccuracy and sparseness of the data by proposing several candidate paths — each associated with a likelihood to be the true one — corresponding to the same observed sequence of records.

In summary, obtaining the resolution of information required for disaggregate route choice analysis, that treats the route alternatives as link-by-link sequences, is a challenging task. In addition, network models are often incomplete, and detailed information about their attributes, e.g. link travel times, is not available. With respect to the

¹Technique from which the actual paths of the users are reconstructed from the GPS records (e.g. Quddus et al., 2007; Rahmani and Koutsopoulos, 2013).

network model, researchers often take advantage of open source models such as OpenStreetMaps. This is a valuable source as such, yet these models often require additional processing as the coding of the network is usually incomplete or inconsistent with the physical network. Finally, travel time estimation on the link level consists in a research topic per se. Hence, this type of information is usually not available and assumptions about link travel times or their distribution need to be made.

2.2 Choice set

The choice set of a route choice model is a latent construct and therefore needs to be defined by the analyst. Three approaches are proposed in the literature for the generation of the alternatives in the choice set. The first one relies on heuristics to construct the choice set that is assumed to be considered by the travelers (Bovy and Fiorenzo Catalano, 2007; Prato and Bekhor, 2007). Examples such as the labelling approach (Ben-Akiva et al., 1984), the link elimination (Azevedo et al., 1993), the link penalty (de la Barra et al., 1993), and the constrained k-shortest path approach (van der Zijpp and Fiorenzo Catalano, 2005) assume deterministic shortest paths to generate the choice set. Constrained enumeration approaches based on branch-and-bound are proposed by Friedrich et al. (2001), Hoogendoorn-Lanser (2005), and Prato and Bekhor (2006). However, Bekhor et al. (2006) showed that all methods fail to generate a set that is guaranteed to include the *observed* routes. More recently, Halldórsdóttir et al. (2014), Rasmussen et al. (2016) and Rasmussen et al. (2017) demonstrate good coverage of the observed routes using double stochastic methods respectively for bicycle, public transport and car route choice set generation.

The second approach assumes that the choice set contains all feasible paths between the origin and the destination. This is called the universal set, denoted by \mathcal{U} . The assumption of \mathcal{U} — although not necessarily realistic — allows to avoid biases in the model, as the values of the parameter estimates are dependent on the definition of the choice sets (Frejinger et al., 2009) and may vary significantly for different instances of sampled sets. \mathcal{U} cannot be defined explicitly. Therefore, to make this approach operational, sampling techniques have been proposed (Frejinger et al., 2009; Flötteröd and Bierlaire, 2013). Frejinger et al. (2009) proposes an importance sampling approach that simulates a random-walk on the network. The limitation of this approach is that it generates paths with loops. Flötteröd and Bierlaire (2013) propose an importance sampling approach based on the Metropolis-Hastings algorithm to sample non-cyclic paths with predefined sampling probabilities. Although the method is presented in the context of choice set generation, it is general and appropriate for various applications that require sampling of paths, such as dynamic traffic assignment and route guidance. We exploit this approach for the application of the proposed aggregate route choice model to the prediction of link flows in Chapter 3.

The third approach follows a technique that does not rely on sampling, while avoiding the full enumeration of paths. It has been proposed by Dial (1971) and more recently by Fosgerau et al. (2013a). Fosgerau et al. (2013a) build upon previous works developed in the context of traffic assignment (Akamatsu, 1996; Baillon and Cominetti, 2008), and present an approach that circumvents the challenge of choice set generation. The authors decompose the path choice problem into a Markovian link choice problem. It is called the recursive logit (RL) and is equivalent to a path-based logit model. The RL is solved in a dynamic discrete choice framework, given a directed connected graph $\mathcal{G} = (\mathcal{A}, \mathcal{V})$, where \mathcal{A} denotes the set of links and \mathcal{V} the set of nodes. At each state (link) k the individual n chooses the next state (next link) a that maximizes the sum of the instantaneous utility $u_n(a | k)$ and the expected downstream utility $V^{d'}(a)$ to the destination, with d' being a destination dummy link — that is an absorbing state with no successors. The instantaneous utility is given by

$$u_n(a | k) = v_n(a | k) + \mu \varepsilon_n(a), \quad (2.2)$$

where ε_n is i.i.d. extreme value type I with zero mean. μ is the scale parameter of the model. $v_n(a | k) = v(x_{n,a|k}; \beta)$, where $x_{n,a|k}$ is the vector of attributes associated with the link pair (k, a) and β the vector of parameters to be estimated. $v(d' | k) = 0, \forall k$ that are connected to d' . The next link choice probability is given by the logit model

$$P_n^{d'}(a | k) = \frac{e^{\frac{1}{\mu}(v_n(a|k) + V^{d'}(a))}}{\sum_{a' \in \mathcal{A}(k)} e^{\frac{1}{\mu}(v_n(a'|k) + V^{d'}(a'))}}, \quad (2.3)$$

where $\mathcal{A}(k)$ is the set of outgoing links from link k . $V^{d'}(a)$ are value functions computed using the Bellman equation (Bellman, 1957)

$$V^{d'}(k) = \mu \ln \sum_{a \in \mathcal{A}} \delta(a | k) e^{\frac{1}{\mu}(v_n(a|k) + V^{d'}(a))}, \quad \forall k \in \mathcal{A}. \quad (2.4)$$

Given its advantage over the classical route choice models, i.e. (i) it can be consistently and efficiently estimated on the universal set of paths without sampling of alternatives and (ii) it is equivalent to a logit model, the RL is selected as the representative of the disaggregate approaches in the investigation of route choice models for practical applications in Chapter 4.

2.3 Correlation of alternatives

A major challenge pertaining to route choice modeling concerns the structural correlation among the path alternatives, due to their physical overlap. The approaches proposed in the literature can be divided into two categories; those dealing with the correlation in the deterministic part of the utility function, and those dealing with it in the stochastic part. Examples of the former include the c-logit proposed by Cascetta et al. (1996) and

the path size logit proposed by Ben-Akiva and Bierlaire (1999). Examples of the latter include the multivariate extreme value (MEV) models, such as the paired combinatorial logit and cross-nested logit (CNL) (Vovsha and Bekhor, 1998; Lai and Bierlaire, 2015), as well as non-MEV models, such as the probit (Daganzo and Sheffi, 1977) and the logit kernel model (Bekhor et al., 2002; Frejinger and Bierlaire, 2007).

Tackling the correlation of alternatives in the stochastic part of the utility function entails higher model complexity and estimation times. For route choice analysis in particular, the estimation of the CNL or mixed logit models is cumbersome. The CNL belongs to the MEV family that was first proposed by McFadden (1978). Letting $i = 1, 2, \dots, J$ be an alternative in the choice set and $m = 1, 2, \dots, M$ be a nest, the choice probability generating function (CPGF) of the CNL is then given by

$$G(y) = \sum_{m=1}^M \left(\sum_{j=1}^J \alpha_{jm}^{\frac{\mu_m}{\mu}} y_j^{\mu_m} \right)^{\frac{\mu}{\mu_m}}, \quad (2.5)$$

where α_{jm} are parameters indicating the degree of membership of an alternative j to a nest m (also called inclusion coefficients), μ is the scale for the model, μ_m is the scale parameter associated with nest m , and $y_j = e^{V_j}$. For (2.5) to be a CPGF, the following conditions need to be satisfied (Bierlaire, 2006): (i) $\alpha_{im} \geq 0$, $\forall i, m$, (ii) $\sum_m \alpha_{im} > 0$, $\forall i$, and (iii) $0 < \mu < \mu_m$, $\forall m$. Finally, for the estimation of the inclusion coefficients the normalization $\sum_{m=1}^M \alpha_{im} = 1$, $\forall i = 1, \dots, J$ is applied.

The cross-nested logit probability is given by

$$P_n(i) = \sum_{m=1}^M \frac{\left(\sum_{j \in \mathcal{C}_n} \alpha_{jm}^{\frac{\mu_m}{\mu}} e^{\mu_m V_{jn}} \right)^{\frac{\mu}{\mu_m}}}{\sum_{p=1}^M \left(\sum_{j \in \mathcal{C}_n} \alpha_{jp}^{\frac{\mu_p}{\mu}} e^{\mu_p V_{jn}} \right)^{\frac{\mu}{\mu_p}}} \frac{\alpha_{im}^{\frac{\mu_m}{\mu}} e^{\mu_m V_{in}}}{\sum_{j \in \mathcal{C}_n} \alpha_{jm}^{\frac{\mu_m}{\mu}} e^{\mu_m V_{jn}}}, \quad (2.6)$$

that corresponds to

$$P_n(i) = \sum_{m=1}^M P_n(m | \mathcal{C}_n) P_n(i | m), \quad (2.7)$$

where $P_n(i | m)$ is the probability of an alternative i conditional to nest m and $P_n(m | \mathcal{C}_n)$ as the probability of nest m given the choice set \mathcal{C}_n of individual n . Vovsha and Bekhor (1998) are the first to use a CNL model, also known as the *link-nested model*, in the context of route choice analysis. According to their formulation, each link of the network corresponds to a nest m and each alternative i , i.e. each path, is allocated to nests according to α_{im} . The α_{im} parameters are fixed and assumed to be equal to $\frac{\text{length}_{link}}{\text{length}_{path}}$. This nesting structure entails a very big number of nests and renders the estimation of the model a challenging task. Nest specific coefficients cannot be estimated. Ramming (2002) estimated this model for a network of 34000 links, where the estimation

of nest-specific coefficients was impossible. Lai and Bierlaire (2015) tackle sampling of alternatives within a MEV model. They present a CNL model and adopt the Metropolis-Hastings algorithm proposed by Flötteröd and Bierlaire (2013) with an expansion factor inspired by Guevara and Ben-Akiva (2013) allowing to avoid the enumeration of paths. The estimation of this model in large networks remains a challenging task. Recently, Mai et al. (2017) have presented a dynamic programming approach allowing to estimate large network-based MEV models in reasonable computational times.

The error component (EC) model (Bolduc and Ben-Akiva, 1991) is a mixed logit model incorporating elements that cause correlations among the utilities of the alternatives. The utility function of alternative i is specified as

$$U_{in} = V_{in} + \zeta_n f_{in} + \varepsilon_{in}, \quad (2.8)$$

where V_{in} is a vector of deterministic utilities based on observed variables. $\zeta_n f_{in} + \varepsilon_{in}$ represents the stochastic part of the utility, where ζ_n is a vector of randomly distributed terms with zero mean, f_{in} are the error component terms that consist in observed variables relating to alternative i and ε_{in} is a vector of independently and identically distributed extreme value error terms. f_{in} are specified so that they capture the desired correlation pattern. Exploiting the notion of perceptual correlation of the alternatives, Frejinger and Bierlaire (2007) introduce the concept of *subnetworks* within a factor analytic specification of an EC model. A subnetwork component captures the perceptual correlation of alternatives passing through the same part of the network. The authors argue that they capture correlation in a behaviorally realistic way without increasing the complexity of the model. Yet, the estimation of such a model for large networks is cumbersome.

More recently, Mai et al. (2015), Mai (2016) and Mai et al. (2016) benefit from the tractability of the RL model by Fosgerau et al. (2013a) and extend it to account for correlation of alternatives by means of a nested, cross-nested and mixed logit formulation, respectively.

2.4 Summary

Most state of the art models are path based². The concept of path is evidently hard to handle due to the operational limitations discussed in this chapter. Hence, state of the art models are either very complex or often fail to capture observed behavior. No realistic yet simple model based on RP data has been proposed. This is where the contribution of this thesis lies. We propose an *aggregate* model, that is not based on paths, and exploits RP data. It uses modeling elements mimicking the mental representations that are formed by the individuals. They are called mental representation items (MRIs). They are

²Link-based probit stochastic user equilibrium models are proposed by Daganzo and Sheffi (1977), Sheffi and Powell (1982) and Sheffi (1984).

designed to give the analyst the flexibility to control the level of aggregation in the model specification. As such, the use of MRIs allows to reduce the combinatorial complexity of the model with respect to (i) the choice set, and (ii) the correlation of alternatives. Finally, the proposed approach is less dependent on detailed data, both with respect to the observations and the network model, yet useful for practical applications of the model.

In Chapter 3 we define the novel modeling element and we propose the methodology for the development of aggregate route choice models based on MRIs, within the context of discrete choice. In Chapter 4 we focus on route choice indicators, i.e. link and route flows, and consider their representation both at the disaggregate and the aggregate level. We use the RL and the MRI model to derive these indicators and identify the pros and cons of each approach in doing so. We present an extension of the MRI model by the definition of a MRI graph and we tackle the correlation of alternatives within the MRI framework. Chapter 5 presents the application of the approach to a large network and demonstrates its capability in dealing with the additional complexity, due to the size of the application, while remaining computationally affordable.

3

Aggregate route choice

This chapter is based on the article

Kazagli, E., Bierlaire, M., and Flötteröd, G. (2016). Revisiting the route choice problem: A modeling framework based on mental representations, *Journal of Choice Modelling* 19:1-23.

The work has been performed by the candidate under the supervision of Prof. Michel Bierlaire and the collaboration of Prof. Gunnar Flötteröd.

In this chapter, we propose a new approach to route choice modeling. We replace the path representation — used in most of the state of the art route choice models — by an aggregate representation that describes the strategic decisions of individuals. The approach associates the strategic decisions of individuals with the mental representations that they form during their travel in the transport system. In this context, we introduce the concept of Mental Representation Item (MRI) as a modeling element for aggregate route choice analysis, and present a methodology for the definition of operational random utility models based on MRIs.

The chapter is organized as follows. Section 3.1 describes the proposed methodology. Section 3.2 presents empirical evidence of the MRI assumption and discusses modeling considerations regarding data issues and applications of the model. Section 3.3 applies the framework to a real case study and illustrates its use for traffic assignment. Sec-

tion 3.4 discusses critical aspects of the proposed framework in general, and of the case study in particular. Finally, Section 3.5 summarizes the findings of the chapter.

3.1 Methodological framework

In this section, we outline the methodology for the definition of an aggregate route choice model based on mental representations. In addition to the *mental representations* themselves (Section 3.1.1), four main elements need to be defined for the development of an operational random utility model

1. the choice set \mathcal{C}_n (Section 3.1.2),
2. the utility functions (Section 3.1.3),
3. the likelihood function and the measurement equations that are necessary for the estimation of the model parameters (Section 3.1.4), and finally
4. the mapping of the modeling elements to the elements of the application of the route choice model (Section 3.1.5).

The key feature of the present framework is the representation of routes as sequences of MRIs. Contrary to the current state of the art route choice models, the MRI framework is of greater generality. For instance, it is possible to define a MRI model that is independent from a network model.

In what follows, we start by providing a formal definition of the MRI as a modeling element and proceed with a description of the procedure for the specification, estimation and application of an operational MRI model.

3.1.1 The Mental Representation Item

A “Mental Representation Item” is a modeling element that captures the strategic decisions of individuals. It is formally characterized by

1. a name,
2. a description,
3. a geographical span, and
4. a set of representative geocoded points.

The first two components capture the conceptual aspects, and the last two are needed for the model to be operational.

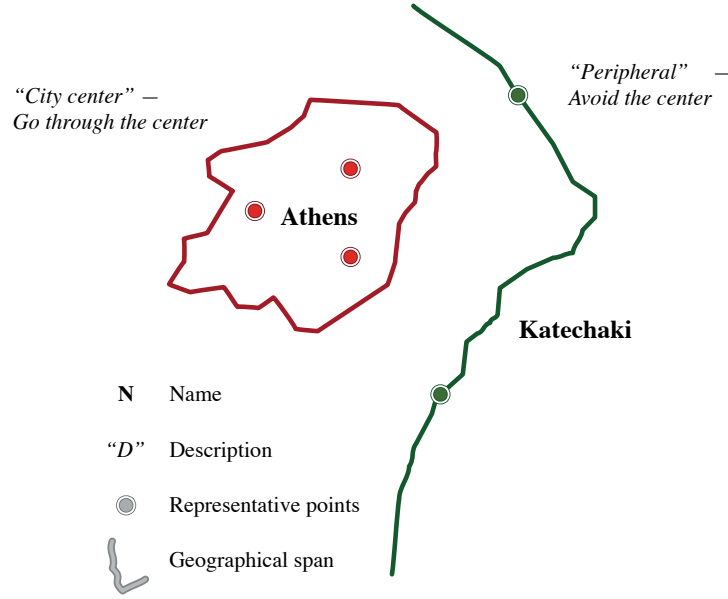


Figure 3.1: Example of two MRIs and their components.

3.1.1.1 The MRI components

Figure 3.1 provides an illustration of the four MRI components in the context of a route choice problem in the city of Athens. The choice consists in going through the city center or avoiding it. In what follows, we briefly discuss the purpose and use of each component and refer the reader to Section 3.2 for further insights and examples.

Conceptual components

1. The *name* is the label of the MRI that is determined based on a toponym, such as “Katechaki” in Figure 3.1. It is similar to the identification of a link in a network model. The difference is that the name of the MRI is not merely based on a numbering convention — as it is the case with the link identification. It characterizes the modeling element.
2. The *description* of the MRI completes the conceptual definition of the modeling element. It is typically a wording that would be used by an individual describing the itinerary to somebody, such as the “Peripheral” in Figure 3.1.

Operational components The operational components are designed to associate the MRI with a more objective representation, such as a map or a network.

3. The *geographical span* of the MRI may be an area, a polyline, or any other shape, convex or not, that determines the extent of the MRI on a map or a network model. If a network model is available, the span may be defined as a set of links or nodes. If not, it can be defined as a geomarked element on a map. The geographical span allows the analyst to relate the observations to MRIs.

4. A set of *representative points*. A representative point is any point or item that is characteristic for the MRI. It may be any landmark in the area of interest. Depending on the scope of the analysis, a representative point may be a major intersection in a city, or a city itself — in the case of urban and interurban route choice analysis, for instance. The representative points play a central role in the model specification as described in Section 3.1.3.

3.1.1.2 Modeling considerations

A MRI is associated with a prominent element of a city or an area, such as a highway, a city center, a bridge or a tunnel. Defining the MRI is a similar exercise as defining the alternatives of a choice model. It is context dependent and it may be complex. In the context of route choice, the complexity may depend on the size of the city, the dispersion of the origin-destination pairs, etc. The key difference is that the level of complexity is not constrained by the network topology as in a path-based formulation. The analyst has the flexibility to select the right level of complexity, consistently with the behavioral assumptions and the type of application of the model.

The definition of the MRI is the output of *modeling considerations* that draw insights from the relevant literature, the expert's knowledge of the area of interest and, ideally, travelers' description of their itineraries.

The MRI must be designed such that (i) it has a meaningful behavioral interpretation reflected by the *conceptual components* and (ii) its level of aggregation is high enough for the model to be simple and operational, yet low enough for the model to be useful — as reflected by the *operational components*. As a rule of thumb, the analyst should keep in mind that defining the MRIs to be geographically disjoint would allow for simpler model structures. It is also advisable to keep the number of MRIs low so that the number of MRI sequences is also low and can be enumerated to characterize the choice set.

3.1.2 Definition of the alternatives

Following the definition of the MRI, a route in the MRI framework is defined as

1. an origin,
2. an ordered sequence of MRIs (possibly only one), and
3. a destination.

An illustrative example of a MRI sequence connecting the origin and the destination is presented in Figure 3.2. The alternative is associated with two elements; the *East highway* and the *North bridge*. The case study presented in Section 3.3 deals with the simplest possible case, where each route is described by a single MRI and where there is a common choice set for all individuals. In Chapter 4, we define a graph of MRI

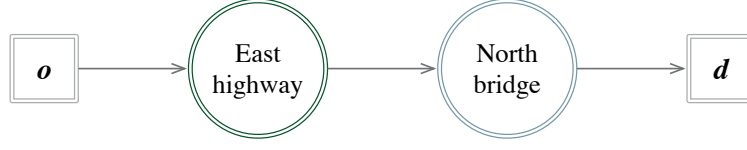


Figure 3.2: Example of an aggregate route alternative in the MRI framework.

elements on which sequences of MRIs can be generated, in the same way that paths are generated on a disaggregate network model, to define the choice set.

3.1.3 Specification of the utility functions

As soon as the MRIs are defined and the choice set (\mathcal{C}_n) is determined, we are able to specify a route choice model and define the choice probabilities $P(r \mid \mathcal{C}_n)$ for each alternative MRI r . Like for any random utility model, each alternative is associated with a utility, which is a function of the attributes of the alternatives x_{rn} and the characteristics of the individual z_n . Once the utility functions have been defined, any choice model $P(r \mid \mathcal{C}_n, x_{rn}, z_n)$ (logit, nested logit, cross-nested logit, etc.) can be considered.

As the main modeling elements are conceptual, the alternatives and their attributes are in general latent, that is, based more on perceptions than on objective measurements. The exact way to deal with this issue is application dependent. Below, we propose three simple methods to generate attributes for each alternative. The third one does not require a network model. More advanced specifications, exploiting the literature on perceptions, could be investigated as well.

3.1.3.1 A deterministic approach with representative paths

We assume that a network model of the area of interest is available and that the representative points of each MRI are nodes of this network. A unique representative path is associated with each alternative (Figure 3.3). The procedure consists of the following steps prior to the estimation of the model:

1. For each MRI and each choice context, select one of the representative points corresponding to a node in the network. The selected representative point can be different for different origin destination pairs, or for different individuals. Subsequently, for each individual and each alternative, there is a sequence of nodes connecting the origin and the destination of the trip.
2. Generate one path connecting the nodes for each observation. Typically, this can be done by connecting each pair of successive nodes by the shortest path according to a given metric, such as length, travel time, or any relevant performance

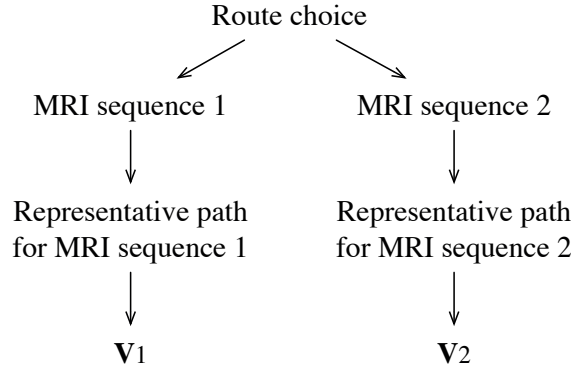


Figure 3.3: Schematic representation of the specification of utilities through representative paths.

measure³. The resulting path is the representative path of the MRI alternative.

3. The utility function of an alternative — that would be used in a classical route choice model — is specified as the utility function of the representative path.

We apply this approach in the case study presented in Section 3.3. The objective is to show that such a simple approach can provide meaningful results, although we acknowledge that more sophisticated procedures may be more appropriate. For instance, an extension of this procedure to a stochastic context is described below.

3.1.3.2 A stochastic multi-path approach

A direct generalization of the previous method would be to generate a set of paths associated with each MRI sequence. Each of these paths would be associated with a utility function, in a way similar to a classical path-based route choice model. Following the utility maximization principle, the utility associated with the MRI alternative would be the highest utility among these paths (expected maximum utility). If a MEV model is considered, generated by the function G , the expected maximum utility would be given by $\ln(G)$ (Fosgerau et al., 2013b).

3.1.3.3 A network-free approach

Within the MRI framework, it is not necessary to use a network model and paths. As each MRI is associated with a geographical span, it is possible to use attributes that are associated with a geographical area, such as the density of landmarks or points of interest. For example, Boarnet et al. (1998) propose a congestion index associated with

³During this step, it must be ensured that the geographical span of the MRIs that *do not* belong in the sequence is not traversed by the representative path. This can be done by associating the links belonging to the geographical span of the remaining MRIs with very high costs.

geographical areas. Along the same lines, and in the context of pedestrian route choice, Frank et al. (2009) propose a walkability index. The use of the MRI framework in a network-free context opens new research opportunities for route choice analysis and applications. We elaborate towards this direction in Chapter 5.

3.1.4 Model estimation

The estimation of the model parameters is accomplished by *maximum likelihood estimation*. In the MRI framework, the available data may not be expressed in terms of the MRIs. Consequently, the development of measurement equations is necessary.

3.1.4.1 Measurement equations

To estimate a MRI choice model, a *measurement equation* is necessary. It captures the contribution of each piece of data to the likelihood function. Let r be an alternative of the MRI model — that is an ordered sequence of MRIs — and y be an observation — it can be a reported sequence of places in a survey, or a GPS trace. Its contribution to the likelihood function is

$$\sum_{r \in \mathcal{C}_n} P(y | r) P(r | \mathcal{C}_n, x_{rn}, z_n), \quad (3.1)$$

where $P(r | \mathcal{C}_n, x_{rn}, z_n)$ is the MRI choice model, and $P(y | r)$ is the measurement equation. The latter models the data generation process, and is the probability to observe y given a MRI alternative r . The *geographical span* of a MRI plays an important role in the specification of the measurement equation. An observation y is deterministically associated with a MRI sequence r if it traverses the geographical span of all its MRIs in the correct order. A simple example involving only one MRI m in the sequence is presented in Figure 3.4. The exact definition of such measurement equations is application dependent. Examples of measurement equations can be found in Bierlaire and Frejinger (2008) and Chen and Bierlaire (2013).

3.1.5 Model application

The generality of the MRI framework may not allow a direct application of the model in a desired context. Similar to the necessity of measurement equations for the model estimation, it may be necessary to relate the MRIs to concrete elements for a given application. To illustrate that, consider the traffic assignment problem, which is a typical application of a route choice model.

Let us consider the assignment of a single traveler n with known origin and destination. We are interested in the probability $P(a | \mathcal{C}_n)$ that traveler n crosses any network link

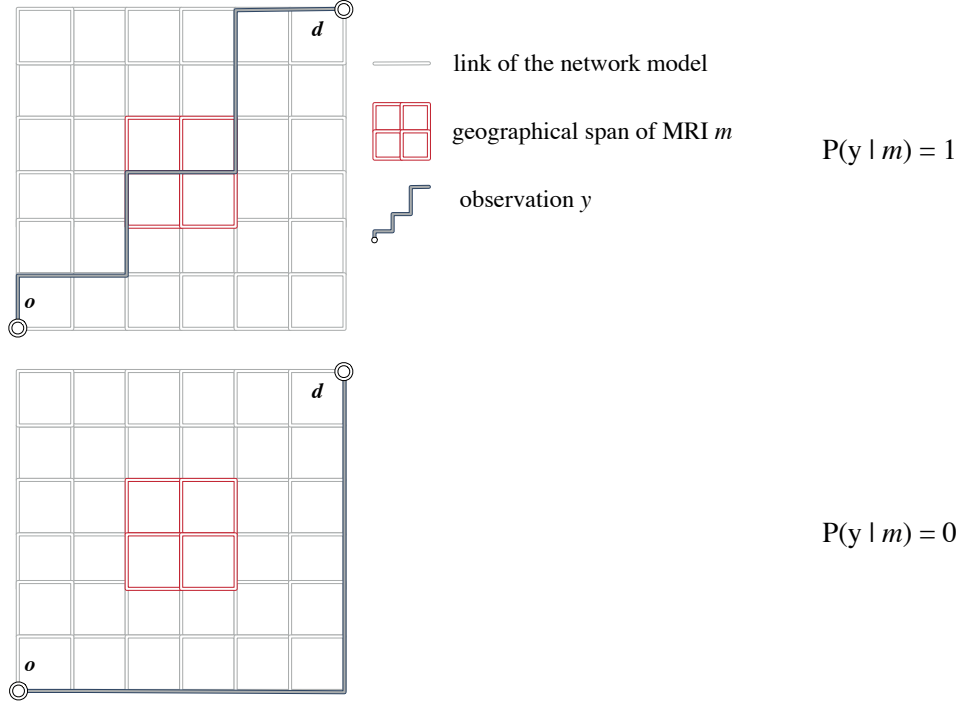


Figure 3.4: Illustration of the measurement equation.

a , given her choice set \mathcal{C}_n . In order to exploit the MRI choice model, this probability is written as

$$Prob(a \mid \mathcal{C}_n, x_{rn}, z_n) = \sum_{r \in \mathcal{C}_n} P(a \mid r) \cdot P(r \mid \mathcal{C}_n, x_{rn}, z_n), \quad (3.2)$$

where $P(r \mid \mathcal{C}_n, x_{rn}, z_n)$ is the MRI choice model, and $P(a \mid r)$ is the probability of using link a given MRI sequence r . $P(a \mid r)$ can be seen as the operational component, that is the implementation of decision r , while $P(r \mid \mathcal{C}_n, x_{rn}, z_n)$ is the behavioral component represented by the MRI choice model. One possibility to specify $P(a \mid r)$ consists in using a path-based representation. In that case, the specification would be

$$P(a \mid r) = \sum_p \delta_{ap} \cdot P(p \mid r) \quad (3.3)$$

where δ_{ap} is the zero/ one indicator of path p containing link a and $P(p \mid r)$ is the probability of traveling along path p given that MRI r is chosen. For the sake of illustration, a simple model specification is described in Appendix A. It is used in Section 3.3.5 to illustrate the application of the MRI model to traffic assignment for the case study of interest.

3.2 Additional considerations

In this section, we elaborate on specific features of the MRI approach. The discussions pertain to both the development and the application of a MRI model.

3.2.1 Defining the MRI

The flexibility of the framework allows to use various types of data for the estimation of the model. But data is also useful to drive the model specification and, in particular, the definition of the MRIs. Conducting interviews and surveys is particularly useful in this context. Reported itineraries are an ideal data source. In what follows, we present an example of a small qualitative survey providing insights into the MRI assumption.

In order to investigate how mental representations could be exploited for modeling purposes, we interviewed three drivers in the cities of Athens and Stockholm. Respondents were asked to give a description of the routes that they follow to go from home to work, or to a relative's place. We noted the wording they used to describe their itineraries.

All the respondents have good knowledge of the city's network and, if asked explicitly, they are able to describe the exact itinerary they follow in details, for instance: *"I go right in the first traffic light, continue straight for about 300 meters and turn left in the third traffic light that I encounter"*. However, in their initial response to the question *Describe your itinerary from home to work*, they never provide details. Instead, they identify two to three alternatives that they choose in rotation depending on the time of day — indicating different expectations of congestion — that are always associated with some conceivable element of the city, such as the *city center*, the *highway H*, the *neighborhood N*, the *bridge B*. These elements are used to identify alternatives. In some cases respondents also identify an alternative that they never choose; e.g. entering specific areas that are in the congestion pricing zone in Stockholm.

An example of a described itinerary is: *"I take E4 (major highway traversing Sweden) and then enter the city from the entrance in Solna (one of the main municipalities in Stockholm). I avoid Södermalm (district in central Stockholm) because of the tolls."*, or *"I go through Arsta (district in Stockholm) and then take the bridge to Kungsholmen (one of the islands that Stockholm comprises of)."*. The comparisons of these alternatives are described as *"longer but faster"*, *"faster because of less traffic lights"*, *"more pleasant"*, *"more boring"*, etc., meaning that not only the routes but also their attributes are perceived in an aggregated manner.

For the case of Athens, it appears that a natural example of a MRI is *"the city center"*. From the example of Stockholm, a possible MRI would be a bridge. Indeed, Stockholm spreads across 14 islands, which are connected through bridges and tunnels.

Figure 3.5 illustrates examples of MRI sequences in the city of Stockholm. The figure

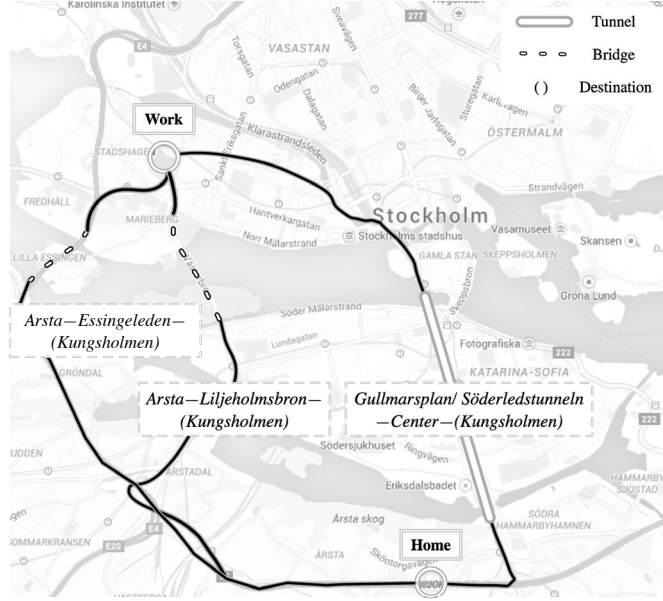


Figure 3.5: Example of MRI sequences in the city of Stockholm.

depicts three alternatives for a home to work trip, as identified by one of the drivers. Two of the alternatives first cross the district of Arsta and then entail a bridge choice either through Essingeleden, or through Liljeholmensbron, while the third alternative passes by the Gullmarsplan square (metro station), traverses the Söderledstunneln and then goes through the city center.

The experiments conducted in the two cities support the hypothesis that route choice takes place at a higher conceptual level and that the exact sequence of links — related to the concept of path — is the implementation of this decision at the operational level. In Appendix B we present one of the interviews for the city of Athens in details. Through the interviews we get (i) insight into peoples’ perception of route options, and (ii) intuition of how to define MRIs in a behaviorally realistic way.

3.2.2 Model-to-data approach

A MRI aims at representing how travel options are grouped and perceived; it does not necessarily aim at representing groups of realized travel patterns. Clustering GPS track segments may be a possible approach to defining MRIs if both groupings — of perception and realization — overlap. However, this is in general difficult to ascertain. Hence, the concrete choice of a MRI structure should be left to the analyst.

In the context of GPS records, we do not suggest a data-driven approach that automatically extracts MRIs from the records. Instead of answering the question “How to define the MRIs given the availability of GPS data?”, we suggest to address the question “Is

the definition of the MRIs consistent with the observations?” Our approach can be seen as “confirmatory”, as opposed to “exploratory”.

3.2.3 Route guidance

The proposed MRI approach is particularly relevant in the context of route guidance systems. The nature of the MRI makes it a natural way to provide information and guidance directly to users, without the necessity to use a navigation system. Variable Message Signs (VMS), radio announcements and oral instructions can benefit from the output of the model. Still, the model can be incorporated in navigation systems using the same decomposition as described in Section 3.1.5.

At the behavioral level, a recommendation of the sequence of MRIs is provided “*to go to the airport, avoid the city center and use the peripheral*”. If this recommendation must be transformed into a path, methods similar to those described above, exploiting the representative geocoded points, can be considered. Note that current navigation systems already work with this concept: if one provides as a destination the name of a city, without being more specific, the system itself selects a specific location in the city center and leads one there.

With the help of the MRI-based model, in-vehicle navigation systems could be adjusted according to the needs of the driver. As an example, drivers with good knowledge of the network do not always need step-by-step instructions to reach their destination, rather suggestions that would help them to avoid congestion in specific parts of the network (e.g. avoid the city center). In this context, the navigation systems could provide the option to choose between detailed itineraries in case of new destinations, or aggregate route suggestions in case of everyday trips, such as the trip to work, according to the current traffic conditions.

3.3 Case study

This case study serves as a proof of concept. The objective is to demonstrate that the model is applicable with real data. We focus on a case where only GPS data is available, and we show that, despite the need to use methods that may seem arbitrary in the first place, sensible results can be obtained. For this purpose, we use the network of Borlänge in Sweden (Figure 3.6). It consists of 3077 nodes and 7459 unidirectional links. The estimation results presented in this section are based on real GPS data collected from private vehicles in the city of Borlänge. The data had been previously processed to obtain map-matched trajectories useful for route choice analysis⁴. Each observation consists in a sequence of links from the origin to the destination. Apart from the map-matched

⁴We refer to (Frejinger and Bierlaire, 2007) and (Axhausen et al., 2003) for a description of the Borlänge dataset.

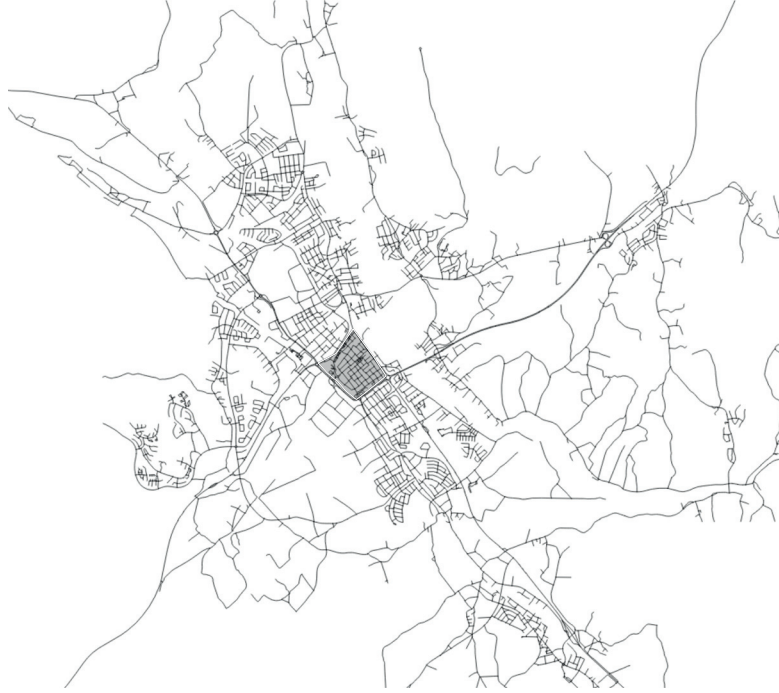


Figure 3.6: Borlänge road network.

trajectories, no further information regarding the trip and individual characteristics, such as departure time, trip purpose, age etc., is available.

The set of attributes for the network model of Borlänge includes the link lengths, the turning angles between each pair of links and the in- and out-degree of each node, allowing us to identify intersections. The travel time of each link had been computed as the ratio of the link length divided by an average speed, the latter being the average observed speed over all observations and all links with the same speed limit. A limitation of this case study is that the raw GPS data, with the timestamps of the records, is not available. Therefore, it is not possible to perform analysis that would allow to identify the effect of congestion on the link travel times.

In what follows, we present one possible way to operationalize the MRI choice model using the available network model, according to Section 3.1. Consistently with the objective of our research, we have tried on purpose to keep the modeling as simple as possible.

3.3.1 Definition the choice problem

In lack of survey data where people describe their itineraries, we rely on examining the network of Borlänge for the definition of the MRIs.

The center of the city (shaded area in Figure 3.6) is the first distinct element in the network of Borlänge. It is characterized by higher density of small streets in comparison with the rest of the network. This core is encircled by the national roads (R.50 and R.70) that are highlighted in Figure 3.7. In most of their parts, the national roads have four lanes — two in each direction — and the pavement is divided by guard-rails. These features signify higher operating speeds, as well as higher convenience, in comparison with the rest of the streets that have at most one lane per direction and lower speed limits.

Figures 3.8 and 3.9 show the output of Google Maps Directions API for route options given two arbitrarily selected origin-destination pairs. After investigating options provided by Google Maps for various origin-destination pairs, three high level possibilities appear: (i) going through the city center, (ii) following orbital routes around the city center and along its boundaries, and (iii) avoiding the city center. Patterns corresponding to these three possibilities have also been observed in the dataset.

Consequently, we identify three major elements: the “*city center*”, the “*perimeter of the city center*”, and the “*avoid the city center*”. We further separate the “*perimeter of the city center*” in two elements: (i) “*clockwise movement*”, and (ii) “*counter-clockwise movement*”, indicating left and right turn accordingly. These are two clear options for individuals as they approach the center. Therefore, we obtain four MRIs. We label them as CC, CL, CO and AV, equivalently for the “*city center*”, the “*clockwise movement*”, the “*counter-clockwise movement*” and the “*avoid the city center*”. Finally, we observe



Figure 3.7: National roads, R50 and R.70, in Borlänge.



Figure 3.8: Example of route options provided by Google Maps Directions.

that there is a river on the eastern boundary of the city. There are two bridges connecting the center of Borlänge to the neighboring settlements and the city of Falun. In this case study, we focus on trips within the city of Borlänge, while in Chapter 4 we extend the area of study to include trips between the two shores.



Figure 3.9: Example of route options provided by Google Maps Directions.

We now characterize the four MRIs. According to Section 3.1.1.1

1. the *name* for the
 - (a) CC corresponds to the “city center” of Borlänge,
 - (b) CL and CO corresponds to the name of the streets defining the perimeter; these are the Backaviadukten (south half of the perimeter), Siljansvägen (north-east part of the perimeter), and Ovanbrogatan (north-west part of the perimeter),
 - (c) AV may correspond to the name of any street that can be used to avoid the center.
2. the *description* for the
 - (a) CC would correspond to a sentence equivalent to “go through the center”,
 - (b) CL would correspond to a sentence equivalent to “take the national road on the left as approaching the city center”,
 - (c) CO would correspond to a sentence equivalent to “take the national road on the right as approaching the city center”,
 - (d) AV would correspond to a sentence equivalent to “take the peripheral to avoid the city center”.
3. the *geographical span* for the
 - (a) CC is the set of all links of the network that are inside the perimeter that defines the boundaries of the center,
 - (b) CL and CO is the set of all links on the perimeter defining the boundaries of the center,
 - (c) AV is the set of all the remaining links, that is, excluding the ones inside and on the perimeter of the center.
4. the *set of representative geocoded points* (Figure 3.10) for the
 - (a) CC consists in the two nodes that roughly correspond to the middle points of the two main streets in the center (Figure 3.11),
 - (b) CL and CO consists in the three nodes that roughly correspond to the middle points of the three streets.
 - (c) AV consists in the two nodes that correspond to the two main peripherals that can be used to avoid the center.

We consider the four elements to be mutually exclusive and consequently each alternative involves exactly one MRI. Moreover, the choice set is the same for every individual in the population, that is $\mathcal{C}_n = \{CC, CL, CO, AV\}$, for all n , independently of their origin and destination.

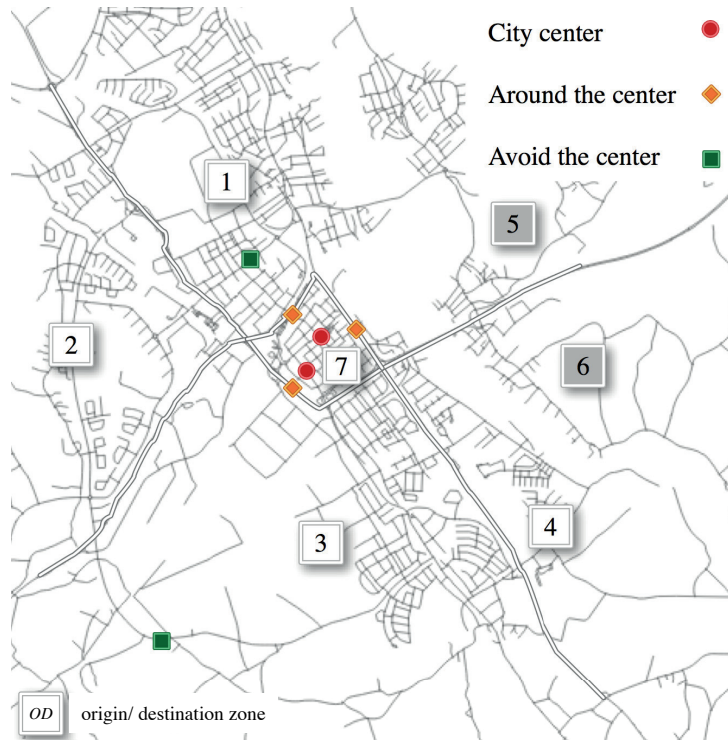


Figure 3.10: Representative points of the MRIs.



Figure 3.11: The two main streets in the city center.

3.3.1.1 Data processing

The network of Borlänge has been divided into 7 origin and destination zones, denoted respectively by O and D (Figure C1). The city center area serves both as a MRI and a zone (zone 7). Each observed trajectory is associated with an O and a D zone. The association of the trajectories with the OD zones is used to facilitate the selection of the representative points for each alternative and each observation. The operationalization of the MRI utility functions is dependent on this selection. A different representative point (Figure 3.10) for the same MRI alternative may be necessary depending on the O and D of the trip. As an example, avoiding the center usually corresponds to a long detour (Figure C2e). Indeed, for a trip with a direction from the south to the north part of the city, and vice versa, this is the only way to avoid the center, by using a rural street. Only for trips between the zones 1 and 2 it is possible to avoid the center through other streets. For these trips we have defined a different representative node⁵.

The method described in Section 3.1.3 is used for the specification of the utility functions. The *representative path* for each MRI is the fastest path. An indicative example of the four alternatives in the MRI choice set, as generated by this process, is depicted in Figure 3.12.

⁵An additional MRI alternative could be considered in this case, but due to the low number of observations we did not consider this demarcation.

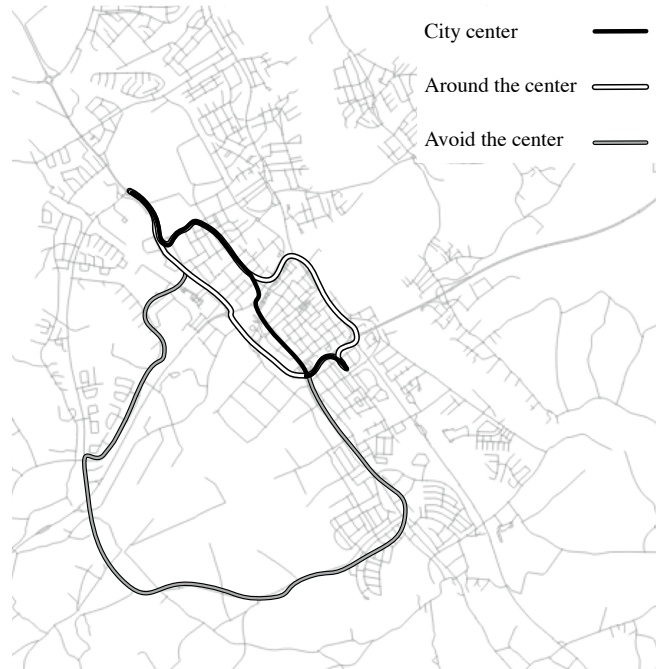


Figure 3.12: Illustration of the MRI choice set with representative paths.

Observations with a minimum length of 2 km are considered. The 2 km length threshold is adopted in order to obtain trips of relevant length, that can be associated with the strategic choices in the city of Borlänge. Due to the small size of the city, the majority of the observations concerns trips of less than 5 km. Recalling that in the present case study, we exclude trips between the two shores, we have a sample of 139 observations for the estimation of the model — out of the 1832 trips that are included in the dataset. Figure 3.13 shows the distribution of the travel times for the four MRI alternatives, while statistics on the attributes of the MRI alternatives are provided in Table 3.1.

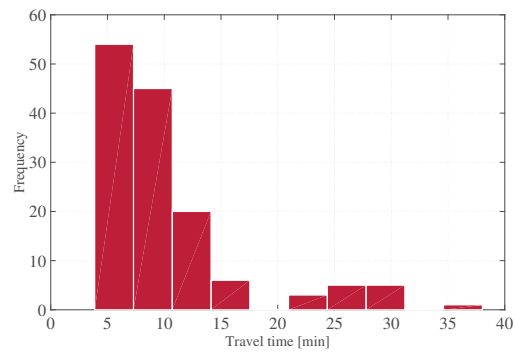
3.3.2 Model specification

From the distribution of travel times of the four alternatives in Figure 3.13, one can see that the deterministic travel times of the CC, CL and CO alternatives are quite similar. Furthermore, the travel times of the four alternatives are highly correlated with the corresponding lengths of the alternatives. This is a consequence of the way that the link travel times are computed (see the introduction paragraph of this section). Hence, only one of the two variables is included in the final specification of the model. This is a limitation of the case study that precludes the development of more advanced specifications that could tackle the trade-offs between length and time and that would allow to identify the effect of congestion on the choice of MRI alternatives. Yet, such specification can be estimated within the MRI framework. We elaborate further on this matter in the discussions section of the chapter.

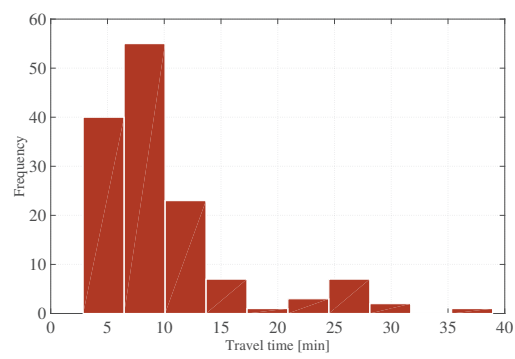
In order to test for nonlinearities of the utility function with respect to the travel time variable, we use a power series specification of degree three for the travel times of the four alternatives. We identify a non-linearity of the utility occurring for travel time intervals shorter and higher than 10 minutes in the case of the CL and the CO alternatives

Table 3.1: Descriptive statistics on attributes

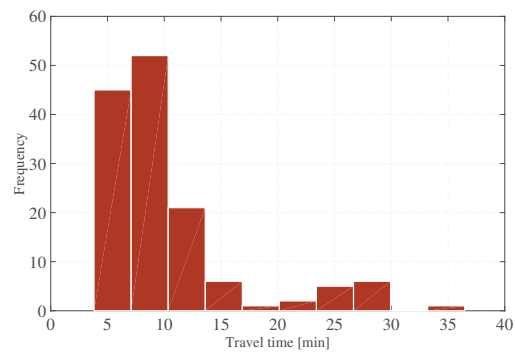
	mean	median	min	max	std. dev
Travel time CC (min)	10.18	8.38	3.88	38.03	6.41
Travel time CL (min)	9.98	8.18	2.86	38.93	6.32
Travel time CO (min)	10.21	8.37	3.81	36.47	6.23
Travel time AV (min)	11.80	13.12	2.66	38.58	11.81
Intersections CC (#)	27	26	9	51	9
Intersections CL (#)	25	24	6	58	10
Intersections CO (#)	26	26	4	48	11
Intersections AV (#)	34	37	10	75	15
left turns CC (#)	2	2	0	8	2
left turns CL (#)	2	2	0	5	1
left turns CO (#)	2	2	0	4	1
left turns AV (#)	3	3	0	9	2



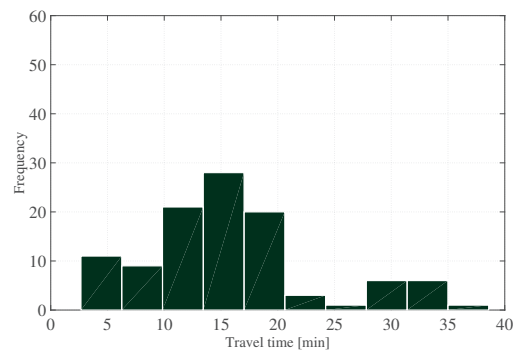
(a) CC



(b) CL



(c) CO



(d) AV

Figure 3.13: Distribution of travel time for the four MRIs.

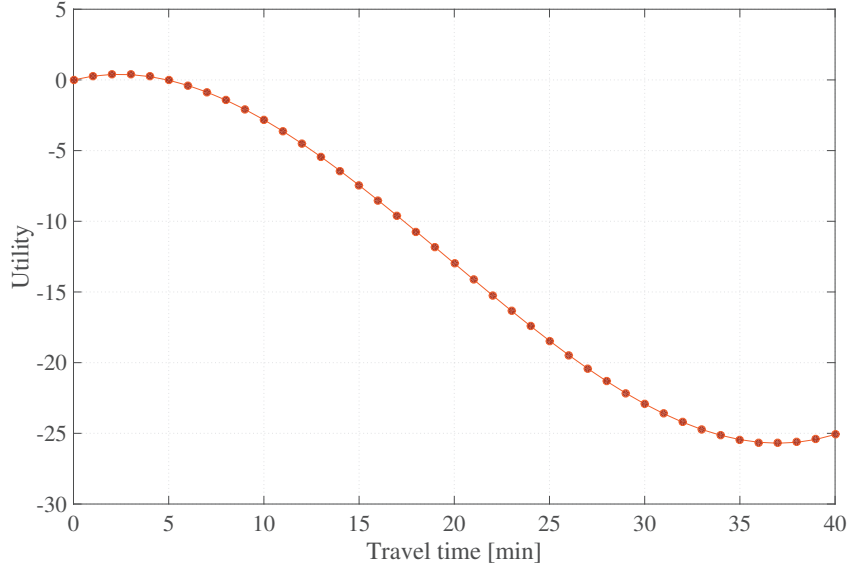


Figure 3.14: Power series of degree three for the travel time of the CL and the CO alternatives.

(Figure 3.14). To capture this effect, we consider a piecewise linear specification for the travel time variable of these two alternatives. We partition the travel times into two intervals, that is shorter than or equal to 10 minutes and longer than 10 minutes, and we define the corresponding coefficients. The corresponding results for the CC and the AV alternatives do not demonstrate nonlinearity.

Table 3.2 shows the specification of the model. We include the variables *number of left turns* (LEFT) and *number of intersections* (IS) in the specification. Finally, as the choice set consists of four alternatives, it is possible to estimate alternative specific constants (ASCs). The ASCs can partially account for the lack of the trade-offs between length and time in the specification.

The fact that the MRIs consist of physically disjoint network elements justifies the use of a logit model.

3.3.3 Model estimation

The available dataset of map-matched trajectories is transformed into a dataset consistent with the model specification. The measurement model defined by (3.1) is deterministic; each observation is associated with one alternative of the MRI model, according to the definition of the geographical span. Each r involves exactly one MRI in the sequence, as the four elements are mutually exclusive. More precisely, $P(y | r) = 1$, if the observed path traverses the geographical span of the MRI associated with r , and *zero* otherwise.

Table 3.2: Specification table with piecewise linear travel time formulation

Parameter	CC	CL	CO	AV
ASC_{CC}	0	0	0	0
$ASC_{CL, CO}$	0	1	1	0
ASC_{AV}	0	0	0	1
β_{TIME_CC}	TT (min)	0	0	0
$\beta_{TIME_CL, CO}^{[0-10min]}$	0	TT (min) ≤ 10	TT (min) ≤ 10	0
$\beta_{TIME_CL, CO}^{[>10min]}$	0	TT (min) > 10	TT (min) > 10	0
β_{TIME_AV}	0	0	0	TT (min)
β_{LEFT}	# left turns	# left turns	# left turns	# left turns
β_{IS}	# IS	# IS	# IS	# IS

Examples of observed routes, and the MRI that they correspond to, are provided in Figure C2a-e. Table 3.3 shows the number of times that each MRI is chosen.

The model is estimated using *Biogeme*, an open source software for discrete choice models (Bierlaire, 2003). The parameter estimates are presented in Table 3.4. Despite the small number of observations that is used for the estimation of the model, we are able to obtain significant parameters for the attributes of the alternatives, with their expected signs. The ASCs are not significant. The estimates of travel time parameters indicate that the users are more sensitive to travel time when they have to go through the center, in comparison with the rest of the alternatives. The piecewise specification of the travel time coefficients for the two *around* the CC alternatives reveals that the sensitivity of the users to changes in the travel time is smaller for shorter travel times — that is travel times shorter than 10 minutes — while it increases as the travel time becomes larger.

Intuitively, the CL and CO alternatives, that are associated with the orbital move-

Table 3.3: Frequency of the chosen alternatives

Choice	# times chosen
CC	13
CL	53
CO	51
AV	22
Total	139

Table 3.4: Estimation results

Parameter	Model 1
	Value (Rob. t -test 0)
ASC _{CL, CO}	-2.110 (-1.47)
ASC _{AV}	1.870 (0.89)
$\beta_{\text{TIME_CC}}$	-0.772 (-2.82)
$\beta_{\text{TIME_CL, CO}}^{[0-10min]}$	-0.286 (-1.74)
$\beta_{\text{TIME_CL, CO}}^{[>10min]}$	-0.616 (-2.86)
$\beta_{\text{TIME, AV}}$	-0.583 (-3.11)
β_{LEFT}	-0.288 (2.22)
β_{IS}	-0.047 (-2.16)
Number of observations	139
Number of parameters	8
$\bar{\rho}^2$	0.375
$\mathcal{LL}(0)$	-183.201
$\mathcal{LL}(\hat{\beta})$	-106.563

ments around the city center, may share unobserved attributes. In order to test this assumption, a nested logit formulation was specified and estimated. The nested logit was rejected by the likelihood ratio test against the logit model. The small sample of observations that is used for the estimation of the models may be the reason for not detecting the correlation between the two alternatives, according to our expectations.

3.3.4 Forecasting results & validation

In order to validate the model and test its performance with respect to the predicted choice probabilities, we adopt a cross validation approach. The procedure is outlined below

1. Randomly select 80% of the data for estimation.
2. Use the estimated model to predict the remaining 20%.
3. Repeat 100 times.

The results are summarized in the box plot in Figure 3.15, where we present the resulting sample shares for each alternative. In the same plot, we overlay the sample shares from the estimation on the full dataset (average probability), as well as their 5% and 95% percentiles. The average probability and its confidence interval are obtained via simulation, by drawing from the multivariate normal distribution $\mathcal{N}(\hat{\beta}, \hat{\Sigma})$, where $\hat{\beta}$

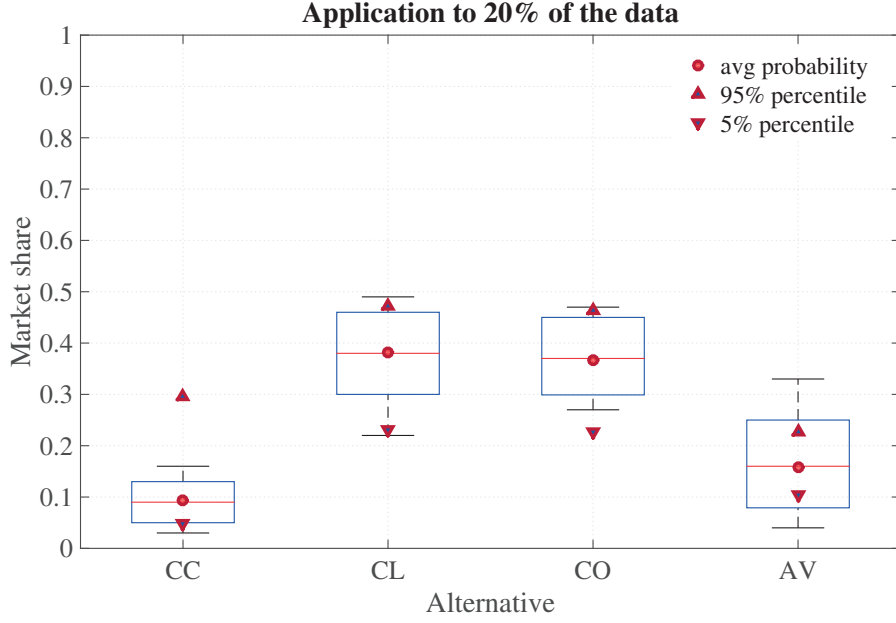


Figure 3.15: Box plot of the market shares from the application in 20% of the data.

where $\hat{\theta}$ is the vector of estimated parameters, and $\hat{\Sigma}$ is the variance-covariance matrix⁶.

The result is quite satisfying, as the level of precision for the forecast, using the point estimates of the parameters, is consistent with the confidence interval of the full model considering the distribution of the estimators.

3.3.5 Model Application

Following Section 3.1.5, and the specification of the model in Appendix A, we apply the MRI model to traffic assignment. For this illustration we assume a single traveler performing a trip from o , in the south of the center, to d , in the north of the center of Borlänge. The MRI choice probability $P(r | \mathcal{C}_n)$ follows the specification given in Section 3.3.2. For the selected od pair we obtain: $P(AV | \mathcal{C}) = 0.002$, $P(CC | \mathcal{C}) = 0.084$, $P(CL | \mathcal{C}) = 0.247$, $P(CO | \mathcal{C}) = 0.667$.

For the specification of $P(p | r)$ we have chosen $\kappa = 25$ and $\lambda = -2.5$. Figure 3.16 depicts for each link a of the network, the probability — as defined in (3.2) and approximated by (A.3) — that a single traveler executing a single trip passes through that link. On this figure one can identify the links that are most probable to be traversed by the traveler going from o to d with darker shades, while links with lower probability to be traversed are denoted by lighter shades. Figures 3.17 to 3.20 show the link choice probabilities — as defined in (3.3) and approximated by (A.2) — conditional on the choice of the

⁶The estimates are obtained from maximum likelihood, hence they are asymptotically normally distributed.

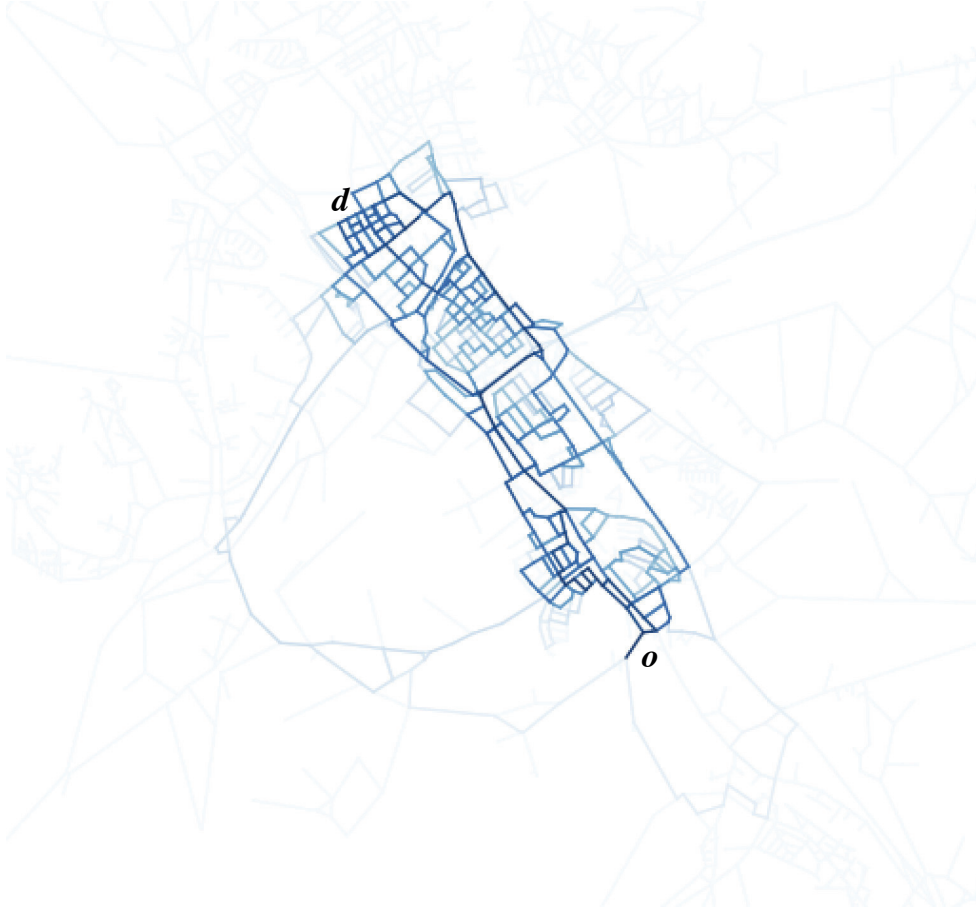


Figure 3.16: Link choice probabilities given the MRI choice set.

indicated MRI. On these figures one can identify the most attractive links for each MRI.

With respect to the sampling protocol, the selection of the value for the λ parameter — controlling, in the assignment context, the importance of travel time for the traveler — is manifested as variability in the sampled paths given a MRI alternative (Figures 3.17 to 3.20). More specifically, selecting a value for low sensitivity allows to obtain paths away from the fastest path, while selecting a value for high sensitivity restricts the sampled paths to be closer to the fastest path. More generally, in a simulation context for traffic assignment, this parameter can be calibrated on data.

3.4 Discussions

In this section, we identify (i) critical aspects of the MRI approach and (ii) limitations of the case study.



Figure 3.17: Link choice probabilities conditional on the choice of the AV alternative.



Figure 3.18: Link choice probabilities conditional on the choice of the CC alternative.



Figure 3.19: Link choice probabilities conditional on the choice of the CL alternative.



Figure 3.20: Link choice probabilities conditional on the choice of the CO alternative.

3.4.1 Critical aspects of the MRI approach

As discussed in this chapter, the framework has to be adapted on a case by case basis. While the definition of the MRI as a modeling element is context independent, the application is context and data dependent. The definition of a specific MRI draws from theory and knowledge about the context, and is confirmed by the data. It is the same exercise as defining an alternative in the choice set. When we model car choice for instance, the question is “*How do we characterize the car?*” Is it with the brand, and/or the year of construction, and/or the fuel type etc.? The exact answer to this question is context dependent, like for almost any modeling element. In this context, a potential danger associated with the MRI approach is that the analyst may not appropriately chose the *level of aggregation*, in accordance of the needs of the application.

The specification of the utility functions based on the representative paths approach may increase the complexity when it comes to the operationalization of the framework for large networks. That is, it may not be straightforward as in the present case (i) to identify the representative points for each alternative and observation, and (ii) to generate a unique representative path for each aggregate alternative without biasing the parameter estimates. We further elaborate on this matter in Chapters 5 and 6.

3.4.2 Limitations of the case study

The case study that is used as a proof of concept for the proposed framework entails some limitations with respect to the specification of the model. As the link lengths are used to compute the link travel times — and no information about congestion is available or can be derived — it is not possible to specify a model that captures the trade-offs between length and time/ speed. In practice, the trade-offs between shorter but slower and longer but faster routes are modeled using mixed logit formulations, for instance based on value of time distributions. The MRI approach can incorporate such specifications. We provide an example for the shake of illustration. Starting from $V = \beta \cdot \text{time} + \gamma \cdot \text{cost}$, and assuming that the total cost is a linear function of length, i.e. $\text{cost} = \bar{c} \cdot \text{length}$, with \bar{c} being the unit cost, the utility function of a MRI alternative can be written as

$$\begin{aligned} V &= \dots \beta \cdot \text{time} + \gamma \cdot \text{cost} \dots \Rightarrow \\ V &= \dots \beta \cdot \text{time} + \gamma \cdot \bar{c} \cdot \text{length} \dots \end{aligned} \tag{3.4}$$

the trade-off between time and length is then equal to $\frac{\beta}{\gamma \bar{c}}$. This corresponds to $\text{VoT} \cdot \frac{1}{\bar{c}}$, with VoT denoting the value of time. Equation (3.4) can be further decomposed as a

generalized cost function:

$$\begin{aligned}
 V &= \dots \beta \cdot \frac{\text{length}}{\text{speed}} + \gamma \cdot \bar{c} \cdot \text{length} \dots \Rightarrow \\
 V &= \dots \gamma \cdot \text{length} \cdot \left(\frac{\beta}{\gamma} \cdot \frac{1}{\text{speed}} + \bar{c} \right) \dots \Rightarrow \\
 V &= \dots \gamma \cdot \bar{c} \cdot \text{length} \cdot \left(\text{VoT} \cdot \frac{1}{\bar{c}} \cdot \frac{1}{\text{speed}} + 1 \right) \dots
 \end{aligned} \tag{3.5}$$

3.5 Summary

In this chapter, we present a new approach to route choice analysis that is designed to be flexible and simple. It explicitly separates the strategic decisions of individuals, associated with aggregate elements, from the operational decisions resulting in explicit paths. The concept of MRI as a modeling element is introduced, and a methodology to build and apply operational route choice models based on MRIs is outlined. We have shown, using a real case study and RP data, that the use of simple methods leads to a meaningful model that can be estimated and used in practice.

The MRI approach allows the analyst to control the level of complexity of the model. In particular, the definition of the MRIs for the city of Borlänge, allows to obviate the need for sampling of alternatives. Despite the limitations of the case study, the MRI approach is quite general and can handle various model specifications. It has the potential to provide better insights into the travel behaviour of individuals, if a relevant dataset to the problem at hand is available.

In Chapter 4, we extend the framework with the definition of a graph of MRI elements, and we build upon tractable disaggregate approaches proposed in the literature, in order to describe how both disaggregate and aggregate models can be used in practice to derive relevant indicators for route choice applications.

4

Derivation of route choice indicators

This chapter is based on the article

Kazagli, E., Bierlaire, M., and Lapparent, M.(de) (2017).
Operational route choice methodologies for practical applications.
Technical report TRANSP-OR 170526.

The work has been performed by the candidate under the supervision of Prof. Michel Bierlaire and Prof. Matthieu de Lapparent.

In this chapter, we focus on the application of tractable route choice models and present a set of methods for deriving relevant disaggregate and aggregate route choice indicators, namely link and route flows. Tractability is achieved at the disaggregate level by the recursive logit (RL) model (Fosgerau et al., 2013a), and at the aggregate level by the MRI approach, presented in Chapter 3. These two approaches are evaluated here. Extensions and specific features of the MRI approach are discussed. The analysis identifies the advantages and the limitations of each model and allows to draw insights into the use of a specific model, depending on the needs of the application and the data availability.

The chapter is organized as follows. Section 4.1 summarizes the RL model and presents an extension of the MRI model that concerns the definition of a graph of MRI elements. Section 4.2 describes the derivation of the indicators of interest using the *link-/ path-* and the MRI-based choice models. Section 4.3 presents (i) an evaluation process for the

performance of the models at the aggregate level of analysis and (ii) the incorporation of the correlation of alternatives within the MRI framework. Section 4.4 applies the models and methods presented in the previous sections and presents estimation and prediction results using real data. Section 4.5 summarizes the findings of the analysis.

4.1 Disaggregate and aggregate route choice models

We start by presenting the RL model. After a short recap of the MRI approach we proceed with the definition of the MRI graph.

4.1.1 The recursive logit model

Based on the literature review, the recursive logit (RL) model has an advantage over the classical route choice models, i.e. (i) it can be consistently and efficiently estimated on the universal set of paths without sampling of alternatives and (ii) it is equivalent to a logit model.

The RL model decomposes the route choice problem into a sequential link choice problem. The model has the Markov property and is solved in a dynamic discrete choice framework, given a directed connected graph $\mathcal{G} = (\mathcal{A}, \mathcal{V})$, where \mathcal{A} denotes the set of links and \mathcal{V} the set of nodes. At each state, that is at each link, k the individual n chooses the next state, that is the next link, a that maximizes the sum of the instantaneous utility $u_n(a | k)$ and the expected downstream utility $V^{d'}(a)$ to the destination. Figure 4.1 illustrates the relevant notation. d' denotes a dummy link that is defined for each destination in the data sample. The dummy links constitute the absorbing states of the network with no successors. The instantaneous utility is given by

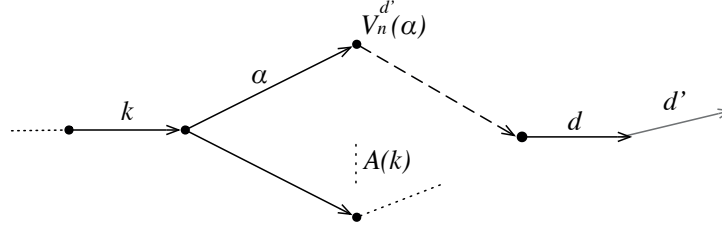
$$u_n(a | k) = v_n(a | k) + \mu \varepsilon_n(a), \quad (4.1)$$

where ε_n is independently and identically distributed (i.i.d.) extreme value type I with zero mean. μ is the scale parameter of the model. $v_n(a | k) = v(x_{n,a|k}; \beta)$, where $x_{n,a|k}$ is the vector of attributes associated with the link pair (k, a) and β the vector of parameters to be estimated. $v(d' | k) = 0$, $\forall k$ that are connected to d' . The next link choice probability is given by the logit model

$$P_n^{d'}(a | k) = \frac{e^{\frac{1}{\mu}(v_n(a|k) + V^{d'}(a))}}{\sum_{a' \in \mathcal{A}(k)} e^{\frac{1}{\mu}(v_n(a'|k) + V^{d'}(a'))}}, \quad (4.2)$$

where $\mathcal{A}(k)$ is the set of outgoing links from link k . $V^{d'}(a)$ are value functions computed using the Bellman equation (Bellman, 1957)

$$V^{d'}(k) = \mu \ln \sum_{a \in \mathcal{A}} \delta(a | k) e^{\frac{1}{\mu}(v_n(a|k) + V^{d'}(a))}, \quad \forall k \in \mathcal{A}. \quad (4.3)$$



Adapted from Fosgerau et al. (2013a).

Figure 4.1: Illustration of notation for the RL model.

As $\mathcal{A}(d') = \emptyset$, the value function at the destination is 0, $V^{d'}(k) = 0, \forall k = d'$. The link choice probabilities are organized in destination specific matrices denoted by $P^{d'}$. The model is estimated under the assumption of the universal set of paths \mathcal{U} . A path p is defined as a sequence of links and its probability is computed as the product of the link probabilities in the sequence

$$P_n^{d'}(p | \mathcal{U}) = \prod_{i=0}^{I-1} P^{d'}(k_{i+1} | k_i) \quad (4.4)$$

where k_0 is the origin and $k_I = d'$.

4.1.2 The mental representation items model

The definition of a MRI model is based on the identification and definition of the MRI elements for the case study of interest. They are the building blocks of the alternatives, in the same way that the links are for the paths. A route is defined as a sequence of MRIs that connects the origin to the destination of the trip. Consequently, the choice set \mathcal{C}_n of an individual n consists of MRI sequences.

A MRI characterizes the strategic decisions of travelers. It is associated with the mental representations used in daily language to describe a route. It may correspond to an area (e.g. the center of a city), a road segment (e.g. a major arterial) or any other prominent element in the transportation network that can be traversed, such as a bridge or a cordon. The definition of the items is context and application dependent.

In Chapter 3, we have presented a MRI model $P(r | \mathcal{C}_n, x_{rn}, z_n)$ where each alternative r involved exactly one MRI element in the sequence, and where the choice set \mathcal{C}_n consisted of four labeled alternatives, common for all individuals. These assumptions may not be applicable in a different and/or more complex choice context. The next paragraph presents the definition of a graph of MRI elements, which is the equivalent of $\mathcal{G} = (\mathcal{A}, \mathcal{V})$ of the disaggregate approach. The definition of the MRI allows for the generalization of the applicability of the approach.

4.1.2.1 The MRI graph

The MRI graph is denoted by $\mathcal{G}^{\mathcal{M}} = (\mathcal{L}', \mathcal{M}')$, where \mathcal{L}' is a set of links and \mathcal{M}' is a set of nodes. The definition of the graph observes the following steps:

1. Identification and definition of the MRI elements and the origin O and destination D zones for the case study of interest.

The set of MRIs \mathcal{M} , the set of origin zones \mathcal{O} and the set of destination zones \mathcal{D} compose the set of nodes \mathcal{M}' of the aggregate graph.

2. Determination of the possible transfers between pairs of nodes in \mathcal{M}' .

For each possible transfer between a pair of nodes in \mathcal{M}' , a link is added in \mathcal{L}' .

$\mathcal{G}^{\mathcal{M}}$ is a directed connected graph. It is defined in terms of aggregate nodes — that represent the MRIs and the origin and destination zones of the case study — and virtual links, that represent the possible transfers between pairs of nodes. We use capital letters to differentiate between the disaggregate representation of an od pair — that corresponds to specific locations on the network — and the aggregate representation of an OD pair — that corresponds to a zone (area) comprising several od pairs. Each $\mathbf{o} \in \mathcal{O}$ and $\mathbf{d} \in \mathcal{D}$ is a set of origins and destinations, that belong to the same O/D zone. An OD zone is defined as a geomarked area on a map or a network model and is represented by a centroid. A MRI alternative r is then defined on $\mathcal{G}^{\mathcal{M}}$ as $r = \mathbf{o}, m_1, \dots, m_h, \mathbf{d}$, where $m_i \in \mathcal{M}$ and h the number of nodes in the sequence.

A link in the MRI graph does not correspond to a single piece of infrastructure, as in the path-based approach defined on \mathcal{G} . This is why we refer to it as a virtual link. Unlike the path-based approach, the most important elements, for the specification of the model on $\mathcal{G}^{\mathcal{M}}$, are the nodes in \mathcal{M}' . We further discuss the implications of these features of $\mathcal{G}^{\mathcal{M}}$ in the remainder of the chapter.

4.2 Deriving indicators

The focus of this section is on the use of route choice models to derive useful indicators for practical applications. Both disaggregate and aggregate indicators are considered. We assume that a RL and/ or a MRI model are available, and present a set of methods aiming at bringing together and analyzing the results from the various levels of aggregation.

The derivation of disaggregate indicators from a disaggregate model, and of aggregate indicators from an aggregate model, is straightforward. On the other hand, the derivation of indicators from a model that does not correspond to the intended level of aggregation is not. An application of the aggregate MRI model to calculate disaggregate indicators is described in Section 3.1.5. We summarize it here and, in order to complete the toolbox, we present methods to assimilate the output of the disaggregate models to calculate ag-

gregate indicators. Although the RL model is link-based, we also present the derivation of aggregate indicators for a path-based formulation.

We begin by delineating the disaggregate and aggregate route choice indicators of interest. Table 4.1 summarizes some important notations for the remainder of this section.

4.2.1 Disaggregate and aggregate route choice indicators

The flow is the most important *route choice indicator*, as its distribution reflects the route choice behavior of individuals. Table 4.2 presents the “element” and the route at the disaggregate and aggregate level. At the disaggregate level, the *links* and the *paths* — defined on a detailed network model represented by \mathcal{G} — are the reference elements for which the flows shall be computed. At the aggregate level, it may not always be relevant to talk about link flows. Consistent with the definition of the MRI framework, it rather makes sense to talk about element flows. For a given origin-destination demand G and network configuration, the only ingredient for the computation of the flows are the *choice probabilities*. These are proportionate to the flows and the outcome of the route choice model on hand.

The scale of the application determines the relevant reference elements for which flows shall be computed. For instance, route flows may be distributed among highways between two cities or, among combinations of major arterials between two areas in one city. For high level of aggregation in the analysis, the route flows may degenerate to element flows, i.e. to flows across single elements. As an example, an aggregate analysis of the route flows between the cities of Geneva and Lausanne, in Switzerland, may only consider the split of flow between (i) the highway and (ii) the lake road. In this case, route flows are self-same to single element flows.

4.2.2 Deriving disaggregate indicators

4.2.2.1 Application of the RL model

The application of the RL model allows to compute disaggregate link flows in a straightforward way. The output of the model consists of destination specific link transition probability matrices $P^{d'}$ (see Section 4.1.1). The expected link flow $F(a)$ on link a is

Table 4.1: Notations

notation	element — quantity
p	disaggregate route representation, i.e. path in \mathcal{G}
r	aggregate route representation, i.e. MRI sequence in $\mathcal{G}^{\mathcal{M}}$
k, a	disaggregate element, i.e. link of \mathcal{G}
m	aggregate element, i.e. MRI node of $\mathcal{G}^{\mathcal{M}}$

Table 4.2: Route choice indicators

	route flows	element flows
disaggregate level	$F^{od}(p) = G^{od} \cdot P(p)$	$F(a) = \sum_p P(a p) \cdot F(p)$
aggregate level	$F^{OD}(r) = G^{OD} \cdot P(r)$	$F(m) = \sum_r P(m r) \cdot F(r)$

computed for a given destination as the summation of the flow originating at link a and the expected incoming flow, that is

$$F^{d'}(a) = G^{d'}(a) + \sum_{k \in \mathcal{A}} P^{d'}(a | k) \cdot F^{d'}(k), \quad (4.5)$$

where $G(a)$ is the demand originating at link a and ending at destination d' .

Link flows can be computed *for a specific destination* and multiple origins using the link transition probabilities by solving the following system of linear equations (Fosgerau et al., 2013a)

$$(I - P^T)F = G, \quad (4.6)$$

where I is the $|\mathcal{A}| \times |\mathcal{A}|$ identity matrix, P is the d' specific $|\mathcal{A}| \times |\mathcal{A}|$ link transition probability matrix, F is a $|\mathcal{A}| \times 1$ vector representing the expected link flow given by (4.5) and G is a $|\mathcal{A}| \times 1$ vector representing the demand $G(a)$ originating at any link $a \in \mathcal{A}$ and ending at d' .

Link flows for *multiple destinations* can then be computed by summation over the elemental link flows for specific destinations. The route flows $F(p)$ for a specific od pair are the product of the demand G^{od} and the route probabilities

$$F^{od}(p) = G^{od} \cdot P^{d'}(p | \mathcal{U}), \quad (4.7)$$

where $P(p | \mathcal{U})$ is given by (4.4).

4.2.2.2 Application of the MRI model

Given the choice probabilities $P(r | \mathcal{C}_n)$ of the MRI model, the probability that individual n , traveling from o to d , traverses link a can be computed as

$$Prob(a) = \sum_{r \in \mathcal{C}_n} P(a | r) \cdot P(r | \mathcal{C}_n), \quad (4.8)$$

where $P(a | r)$ is the probability of using link a given MRI sequence r . An example of model specification for $P(a | r)$ is proposed in Section 3.1.5. It relies on a path-based

representation and is specified as

$$P(a \mid r) = \sum_p \delta_{ap} \cdot P(p \mid r), \quad (4.9)$$

where δ_{ap} is the zero/ one link-path incidence and $P(p \mid r)$ is the probability of traveling along path p given MRI sequence r . A specification of $P(p \mid r)$ is presented in Appendix A. It incorporates two factors: (i) a consistency score of each path p for every MRI sequence r and (ii) a cost-dependency term favoring faster paths. As the number of paths with nonzero probability given a MRI r is too high to be enumerated, this specification requires sampling of paths. The Metropolis-Hastings algorithm proposed by Flötteröd and Bierlaire (2013) is used for this purpose, to sample a large number of paths for a given od pair. The flows for multiple od pairs can be computed by summation over the elemental link flows for specific od pairs.

The same specification of $P(p \mid r)$ applies to the computation of the disaggregate route choice probabilities that is given by

$$Prob(p) = \sum_{r \in \mathcal{C}_n} P(p \mid r) \cdot P(r \mid \mathcal{C}_n). \quad (4.10)$$

4.2.3 Deriving aggregate indicators

An aggregate route flow corresponds to the flow on a specific sequence of MRIs, e.g a sequence of major arterials in a city, while an aggregate element flow corresponds to the flow on a specific MRI, e.g. a specific arterial that is the sum of route flows passing through the arterial.

4.2.3.1 Application of the MRI model

The application of the MRI model allows to directly compute aggregate flows. The aggregate route flow is given by

$$F^{OD}(r) = G^{OD} \cdot P(r \mid \mathcal{C}_n), \quad (4.11)$$

and the aggregate element flow by

$$F(m) = \sum_r P(m \mid r) \cdot F(r), \quad (4.12)$$

independently of the OD , where $P(m \mid r)$ is a zero/ one MRI element-sequence incidence.

4.2.3.2 Application of the RL model

Consider the probability $P(r \mid \mathcal{C}_n)$ of a MRI sequence r as obtained from the MRI model. We are interested in reconstructing this probability using the output of a disaggregate model and use it to compute aggregate flows. This can be formulated as

$$Prob(r) = \sum_p P(r \mid p) \cdot P(p \mid \mathcal{U}), \quad (4.13)$$

where $P(r \mid p)$ is the probability of going through r given a path p , and $P(p \mid \mathcal{U})$ is the probability of p given the universal set of path \mathcal{U} ⁷.

If the MRIs are associated with a well identified geographical span, it is convenient to specify $P(r \mid p)$ as a deterministic zero/ one mapping of p to r : $P(r \mid p) = 1$, if p traverses the geographical span of the MRIs in the sequence r , and zero otherwise.

$P(p \mid \mathcal{U})$ is obtained from the disaggregate choice model on hand, e.g. from the RL model by applying (4.4), or from a path-based model. The sum in (4.13) spans over all paths for a given *od* pair. The number of paths may be too high, and consequently the computation of the sum over p may require sampling — if a RL model is not available. The following paragraphs propose two ways to derive $Prob(r)$ using the RL, with and without sampling.

From link to MRI sequence probabilities The link transition probability matrices obtained from the RL model can be exploited to compute MRI sequence probabilities. The method to derive the MRI sequence probabilities from the destination specific link transition probability matrices builds upon the routine for the computation of link flows given by (4.6) and, consistently with the RL formulation, it does not require sampling of paths. We start with a simple example to demonstrate the idea and then we present a general algorithm that, given a graph $\mathcal{G} = (\mathcal{A}, \mathcal{V})$ and the corresponding transition probabilities between each pair of links $k, a \in \mathcal{A}$, handles the derivation of MRI sequence probabilities.

The toy network presented in Figure 4.2 is used to illustrate the derivation of the aggregate probabilities, given the disaggregate link choice probabilities. The numbers above the edges denote the link transition probabilities given by the RL model. The numbers below the edges denote link flows, obtained by applying the RL model. Dashed arrows signify links that are connected to the destination. The derivation of an aggregate probability assumes a demand of *one* vehicle at the origin link $G(o) = 1$, and *zero* at any other link of the network, that is $G(k) = 0$ for all $k \neq o$. The flow $F(d')$ at the destination link is then proportionate to a probability.

⁷The assumption of \mathcal{U} is not necessary, but important following the discussions in Chapter 2. Hence, we adopt it throughout the thesis, when dealing with the choice set of a disaggregate model.

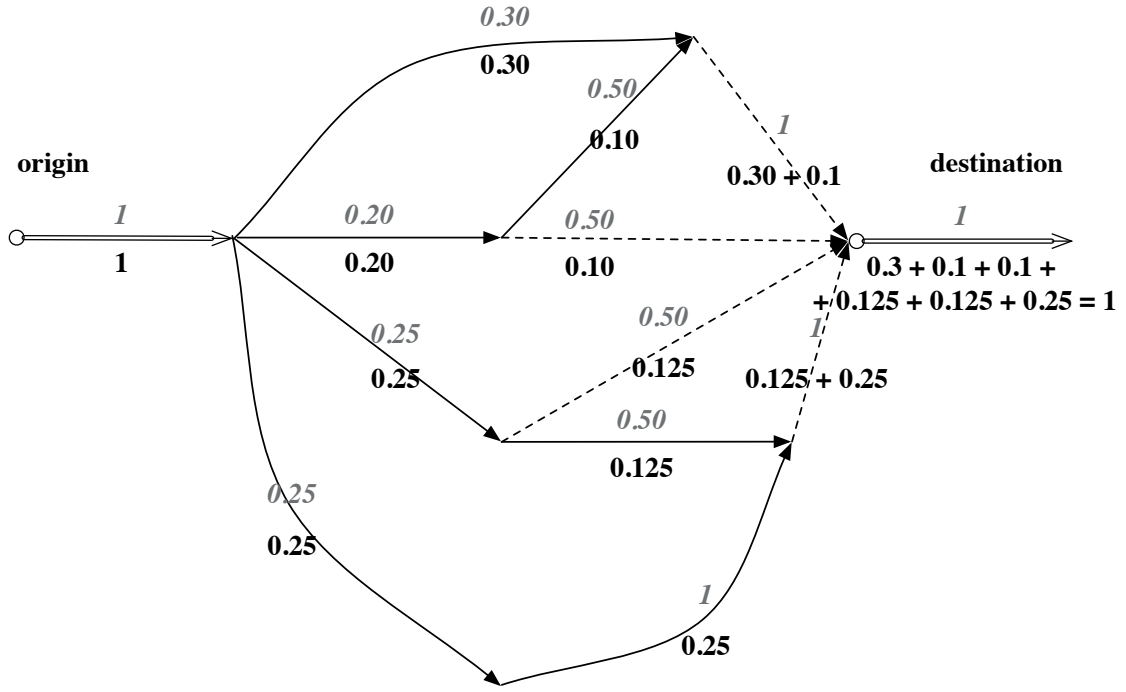
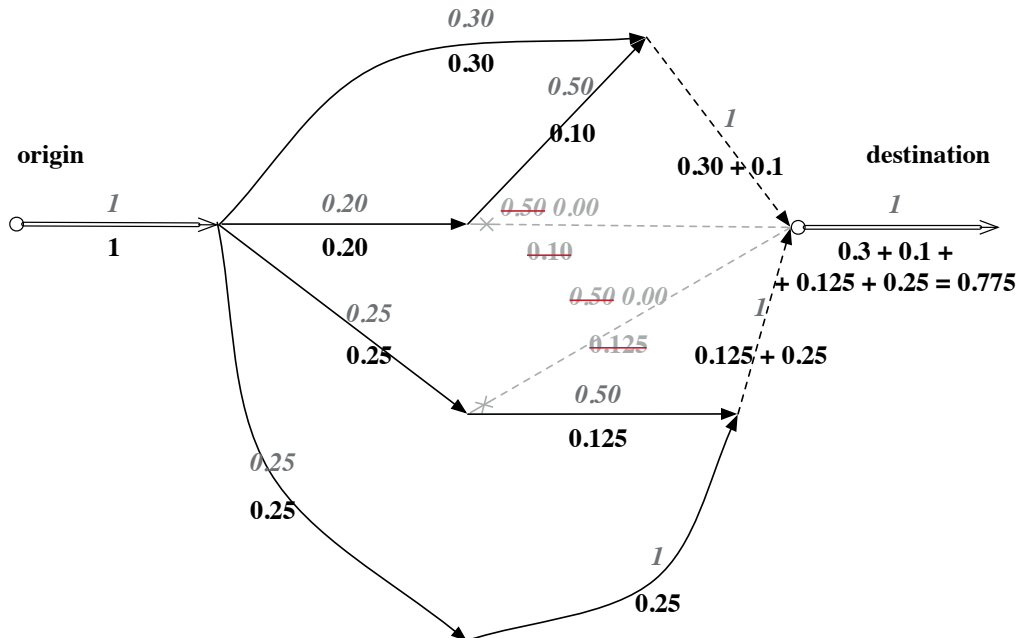
(a) The unit flow reaches d .(b) Setting $P(a | k) = 0, \forall a \in \{\text{city center}\}$ results in $F(d) < 1$.

Figure 4.2: Illustrative example.

Assume now that the toy network is demarcated into two MRIs, namely the *city center* and the *avoid the city center*. Each link is assigned to the geographical span of one of the two MRIs. We are interested in the probability of each MRI to be traversed. Let $\mathcal{M} = \{\text{CC}, \text{AV}\}$ be the set of MRIs in the choice context⁸. Let \mathcal{H}_{CC} and \mathcal{H}_{AV} denote the set of links defining the geographical span of the two MRIs, respectively for the city center and the avoid the city center options. Not passing through the *city center* entails using links in \mathcal{H}_{AV} only⁹.

The probabilities of the two MRIs can be computed as follows

1. Block the *city center* MRI by setting the transition probabilities to all links in \mathcal{H}_{CC} to 0:

$$P(a \mid k) = 0, \forall a \in \mathcal{H}_{\text{CC}}.$$

2. Calculate $F(d')$ using (4.6):

$$\text{This corresponds to } F^{\text{avoid}}(d').$$

3. Set $\text{Prob}(\text{avoid}) = F^{\text{avoid}}(d')$.

4. Compute $\text{Prob}(\text{city center})$:

$$\text{Prob}(\text{city center}) = 1 - \text{Prob}(\text{avoid}).$$

This process does not affect the link transition probabilities that have been previously estimated from the RL model. It only results in a loss of flow entering the *city center* area (Figure 4.2b). This flow does not reach the destination and therefore $F(d')$ is lower than 1. The flow that reaches d' corresponds to the probability of choosing to *avoid* the city center. In this example $\text{Prob}(\text{avoid}) = 0.775$. Then, the probability of the *city center* is simply $\text{Prob}(\text{city center}) = 1 - 0.775 = 0.225$. This process can be generalized to handle more MRIs and sequences of MRIs. Algorithm 1 summarizes the process. It does not specifically capture the sequence of the elements in r , but if the link transition probabilities of going backwards or forming loops are negligible¹⁰, we end up with a reasonable approximation of the sequence of interest. Note that, the MRIs should be disjoint for this method to be operational.

The method outlined here gives direct access to an approximation of $\text{Prob}(r)$ for a given *od* pair.

From path to MRI sequence probabilities The method that we propose in this paragraph applies to any path-based model through the use of a sampling approach. It relies on the fact that several paths in the road network may be associated with the

⁸In this example, $\mathcal{M} = \mathcal{C}_n$, as there are only two mutually exclusive MRIs and no possibility to follow a sequence of them.

⁹In this specific example $\mathcal{H}_{\text{CC}} \cup \mathcal{H}_{\text{AV}} = \mathcal{A}$. From an operational perspective, the links that define the span of *avoid* must be used to reach the *city center*.

¹⁰Under the assumption that most observations do not contain loops, the disaggregate model shall assign very low probabilities to paths with loops.

Algorithm 1: Derivation of $Prob(r)$ for a specific od using the output of the RL model.

- Input:** the origin link $o \in \mathcal{A}$ at the disaggregate level
- Input:** the d' specific link transition probability matrix $P_n^{d'}$ as obtained from the RL model estimation
- Input:** the set of the geographical spans of the MRIs in the choice context
 $\mathcal{H} = \{\mathcal{H}_1, \dots, \mathcal{H}_{|\mathcal{M}|}\}$, where $\mathcal{H}_i \subset \mathcal{A}$, $\forall i \in \{1, \dots, |\mathcal{M}|\}$ and $\mathcal{H}_i \cap \mathcal{H}_j = \emptyset$, $\forall i \neq j$
- Input:** the MRI sequence of interest $r = m_1, \dots, m_h$, where $m_i \in \mathcal{M}$
- Output:** $Prob(r)$ the probability of MRI sequence r
- 1 Set $P = P_n^{d'}$
 - 2 Set $P(a | k) = 0$, $\forall a \in \mathcal{H}_i$, $\forall i \in \{1, \dots, |\mathcal{M}|\}$, i.e. block all the MRIs in the choice context
 - 3 Set $G(o) = 1$ and calculate $F(d')$ using (4.6)
 - 4 Set $\sum_q Prob(q) = F(d')$, where q any path whose links belong exclusively to $\mathcal{A} \setminus \{\mathcal{H}_1 \cup \dots \cup \mathcal{H}_{|\mathcal{M}|}\}$, i.e. $\sum_q Prob(q)$ corresponds to the probability of not using any MRI $m \in \mathcal{M}$
 - 5 Set $P = P_n^{d'}$
 - 6 Set $P(a | k) = 0$, $\forall a \in \mathcal{H}_i$, $\forall i \in \{1, \dots, |\mathcal{M}|\} : m_i \notin r$, i.e. block all MRIs except for the ones belonging to the sequence r
 - 7 Set $G(o) = 1$ and calculate $F(d')$ using (4.6)
 - 8 Set $Prob(r) = F(d') - \sum_q Prob(q)$
-

In the case where blocking a specific MRI, for instance a bridge, would result in a disconnected graph \mathcal{G} for a given od pair, the MRI must not be blocked. If more than one such element exists, e.g. several competing bridges, their probabilities must be identified in advance and taken into consideration in the computations as an extra step in the algorithm. This can be done in the same way as above — after noting that the sum of the probabilities of these elements is equal to one — by blocking each element m and computing $Prob(m) = 1 - F(d')$. Each of these probabilities has then to be multiplied by $Prob(q)$, in order to identify the cases of not using any other MRI except for a bridge. This product must then be subtracted from $F(d')$ in the last step of the algorithm for the computation of the probability $Prob(r)$ of the MRI sequence of interest.

same MRI sequence¹¹. The path choice probabilities are aggregated to MRI sequence probabilities using (4.13). The $P(r | p) = 0$ or 1 mapping of paths to MRI sequences is adopted.

For a given od pair, it may be possible to enumerate the number of MRI sequences in the MRI choice set \mathcal{C}_n , while it is mostly not possible to enumerate the number of paths in \mathcal{U} . Hence, sampling of paths is required to calculate the sum in (4.13). The procedure observes the following steps:

1. For each od pair, a large number of paths is sampled.
 - Simulation of a random walk on the network is used to draw from the RL link transition probabilities a large number of paths.

¹¹An equivalent statement would be that the choice of an MRI sequence may be implemented using various paths in the road network.

2. The probability $P(p \mid \mathcal{U})$ of each sampled path p is computed and corrected for sampling.
 - $P(p \mid \mathcal{U})$ are computed using (4.4).
 - The expansion factor w_p^{Lai} proposed by Lai and Bierlaire (2015) is used to correct for sampling (see Section 4.4): $w_p^{\text{Lai}} = \frac{k_p}{k_s} \frac{b(s)}{b(p)}$, where $k(p)$ is the number of times a path p is sampled and $b(p)$ is the sampling probability. s denotes the most sampled path, and each p is deterministically assigned to a MRI alternative.
3. The $P(r \mid p) = 0$ or 1 incidences are computed.
4. The $Prob(r)$ are computed using (4.13).

Remarks The flow-at-the-destination approach is significantly faster than the sampling approach. The latter requires sampling of a large number of paths and further processing to assign them to MRI sequences. Both tasks are computationally expensive. On the other hand, for the flow-at-the-destination approach matrix multiplications suffice. Both methods are applied to the RL model in Section 4.4. We show that, for a large number of sampled paths, the two methods provide equivalent results and we establish the flow-at-the-destination approach for the remaining steps of the analysis.

4.3 Additional considerations

This section identifies issues towards the consolidation of the aggregate route choice approach based on MRIs and proposes ways to address them.

4.3.1 Evaluation at the aggregate level

The aim of the process presented in this paragraph is to evaluate the adequacy of the MRI model that is intended for aggregate analyses. Along these lines, we are interested in whether or not the proposed aggregate model gives an adequate result in comparison with the disaggregate model that is subjected to aggregation.

An important performance indicator for any choice model is the probability of the chosen alternative. It may reveal limitations in the specification of the model and is used to compute the likelihood of the sample in order to evaluate the model fit. Note that both models that we investigate here are estimated using maximum likelihood estimation.

In order to test the performance of the models at the aggregate level of analysis we perform the following steps:

1. The output of the RL model is aggregated to compute the probabilities $Prob(r)$.
The aggregate route choice probabilities $Prob(r)$ are computed using the flow-at-the-destination approach (see Section 4.2.3.2).

2. $Prob(r)$ are used to calculate an aggregate log likelihood value for the RL model. We denote this likelihood as \mathcal{LL}^{RL} .
3. The log likelihood \mathcal{LL}^{MRI} of the MRI model is calculated from the choice probabilities $P(r | \mathcal{C}_n)$.
4. \mathcal{LL}^{RL} and \mathcal{LL}^{MRI} are compared.
The effect of small probabilities on the log likelihood values is identified and analyzed.
5. A cross validation approach is elaborated on the basis of the \mathcal{LL}^{RL} and the \mathcal{LL}^{MRI} .

4.3.2 Addressing the correlation of alternatives

The model presented in Fosgerau et al. (2013a) and the MRI model presented in Section 3.3 are logit models. Both the RL and the MRI models can be extended to account for the correlation among the alternatives. We refer the reader to Mai et al. (2015), Mai (2016) and Mai et al. (2016) for the extensions of the RL model accounting for correlation using nested, cross-nested and mixed logit formulations, respectively. In the following paragraphs, we describe how the MRI model addresses the correlation of alternatives.

4.3.2.1 The nested and cross-nested logit with MRIs

Consider a MRI graph as defined in Section 4.1.2.1 and a MRI model specified on this graph. The correlation of the alternatives in the choice set can be captured at the MRI level by a nested logit (NL) or a cross-nested logit (CNL) after noting that each MRI may correspond to a nest. An alternative r belongs to a nest \mathfrak{m} if the MRI m appears in the sequence r (Figure 4.3). This specification is similar to the link nested model proposed by Vovsha and Bekhor (1998). The difference is that the nests correspond to MRIs instead of links, allowing for a much lower level of model complexity. The estimation of nest specific scales is not precluded by the MRI nesting structure, as the number of nests is low and under the control of the modeler. In addition, it is possible to estimate the inclusion coefficients $\alpha_{r\mathfrak{m}}$ using, for instance, a parametrization as the one presented below

$$\alpha_{r\mathfrak{m}} = \frac{\delta_{r\mathfrak{m}} \cdot e^{w_{\mathfrak{m}}}}{\sum_{\mathfrak{m}} \delta_{j\mathfrak{m}} \cdot e^{w_{\mathfrak{m}}}}, \quad (4.14)$$

where $\delta_{r\mathfrak{m}}$ is 1 if alternative r uses MRI \mathfrak{m} , and zero otherwise, and $w_{\mathfrak{m}}$ is a nest-specific parameter to be estimated. As only $\mathfrak{m} - 1$ nest-specific parameters can be estimated, one has to be normalized to zero.

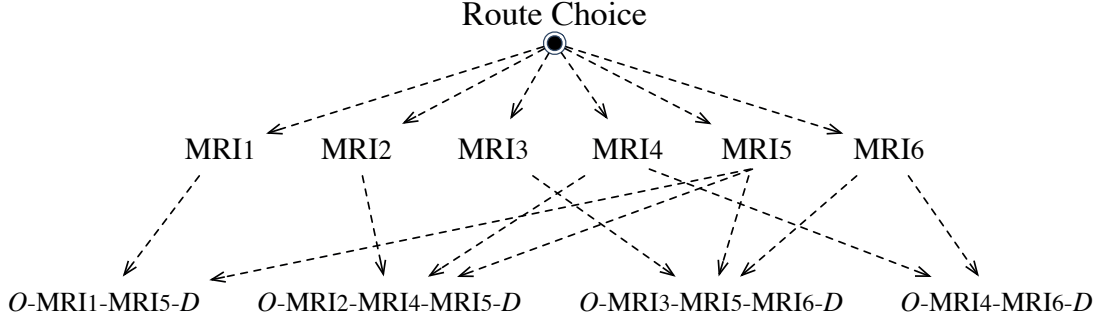


Figure 4.3: The underlying MRI nesting structure.

4.3.2.2 Error component model with MRIs

The error component (EC) model is a mixture of logit models incorporating elements that cause correlation among the utilities of the alternatives. Frejinger and Bierlaire (2007) introduced the concept of subnetworks within a factor analytic specification of an error component model. The subnetwork components capture the perceptual correlation of alternatives passing through the same part of the network.

This framework applies particularly well to the MRI model, where the correlation can be captured on the basis of aggregate elements. Each MRI is associated with an error component, and an alternative r is correlated with alternative j if they have at least one MRI in common. This is modeled by introducing MRI specific constants with which the random coefficients ζ are associated. The underlying assumption is that alternatives using the same MRI m share the random terms ζ_m . The random terms are assumed to be normally distributed $\sim \mathcal{N}(0, \sigma_m^2)$ and the σ_m parameter of each component is estimated from the data.

4.4 Case study

In this case study, we discuss specific features of, and compare, the RL and MRI models on the basis of the indicators presented in Section 4.2. We evaluate the performance of the models at the aggregate level and test for correlation of the MRI alternatives, following the process described in Section 4.3. We conclude with some remarks regarding critical aspects of the MRI approach.

The case study exploits the GPS dataset from the city of Borlänge¹² that has been used as a proof of concept in Chapter 3. It is extended here to include trips between the two shores, that is *OD* zones 5 and 6 are now in the study area. Consequently,

¹²The same dataset is used for the application of the RL model and its extension in Fosgerau et al. (2013a), Mai et al. (2015) and Mai (2016).

apart from the four MRIs identified in Chapter 3, two additional MRIs appear in the choice context. These are the two bridges. Recall that the network model of Borlänge (Figure 3.6) consists of 3077 nodes and 7459 unidirectional links, and each observation y is defined as a sequence of links from the origin to the destination.

A sample of 239 observations, with a minimum length of 2 km, is used for the estimation and validation of the model. The MRI-based models presented in this section are estimated using **Biogeme** (Bierlaire, 2003).

4.4.1 The MRI graph of Borlänge

The MRI graph depicted in Figure 4.4 is defined according to the following:

1. The city is divided into seven *OD* zones.
The natural barriers of the city are used to divide the zones. These are (i) the river, which splits the city in two parts and entails a bridge choice, and (ii) the main national roads (trunk highways R70, R50) passing through the city and granting its connection with the rest of the country (see Figure C1, of Appendix C).
2. Six MRIs are identified. These are:
1: the *city center* (CC), **2:** the *clockwise movement around the center* (CL), **3:** the *counter-clockwise movement around the center* (CO), **4:** the possibility to *avoid the center* (AV), **5:** the *secondary bridge* (B1), **6:** the *main bridge* (B2). The CC serves as an *OD* zone (zone 7), and a MRI.
3. For each MRI a node is added in \mathcal{M}' .
4. For each *OD* zone a node is added in \mathcal{M}' .
5. Links are defined according to the possible transfers between the MRIs themselves and the MRIs and the zones.
 - (a) A map of the city associating the *OD* zones and the MRIs is provided in Figure C3, of Appendix C.
 - (b) MRIs 1 to 4 that are associated with the city center are mutually exclusive, i.e. there are no common links among them. Evidently, the same counts for the two bridges.
 - (c) A decision among the four MRIs associated with the city center occurs for all trips originating or ending in zones 1 to 4.
 - (d) A bridge choice occurs for all trips originating or ending in zones 5 and 6.

In summary, the MRI graph consists of 12 nodes and 56 links, allowing for the enumeration of all the routes between an *OD* pair. Individuals with the same *OD* pair are faced with the same choice set of MRI sequences. The detailed list of alternatives is presented in Table D1, of Appendix D.

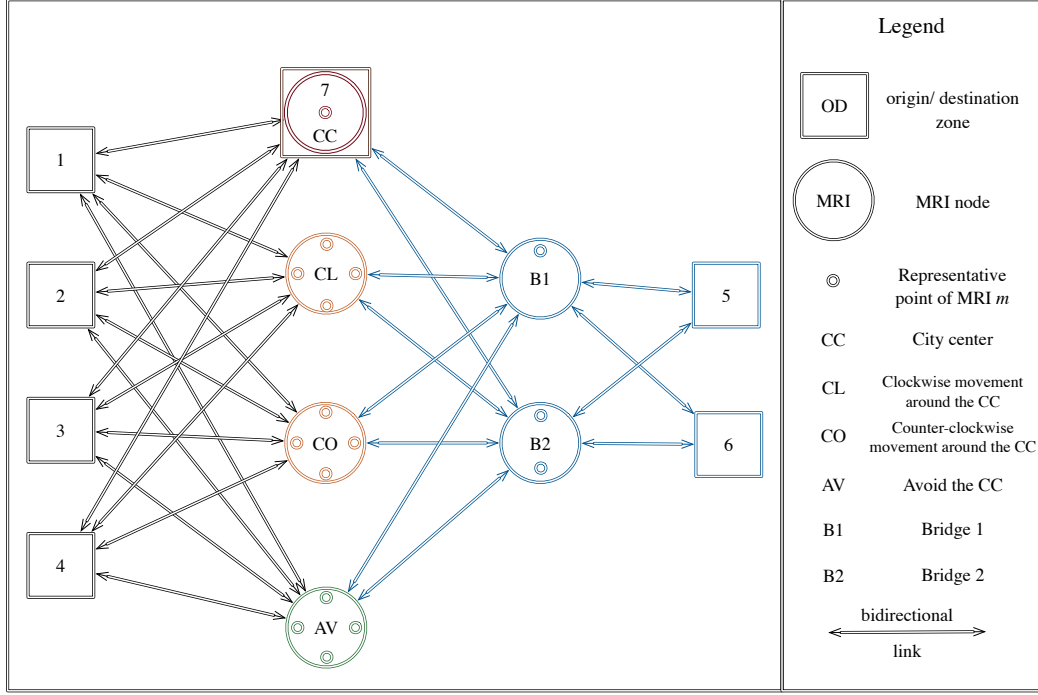


Figure 4.4: The MRI graph.

4.4.2 Operational aspects of the MRI model

Specification of utilities For the specification of the utility functions of the MRI model, we adopt the method proposed in Section 3.1.3. The representative points of the MRIs are used to generate a representative path for each observation and each alternative. This is done by connecting the origin and the destination of each individual, through the fastest path that passes through the representative points of the corresponding MRIs in the sequence.

The utility function of a specific MRI sequence is different for individuals with the same *OD* pair, as the attributes are computed for each individual based on the exact *od* at the disaggregate level. An example of representative paths associated with MRI sequences for a given *od* pair is presented in Figure C4, of Appendix C.

Measurement model Recall that the observations are represented at the disaggregate level by sequences of links from the origin to the destination of the trip. For the estimation of the MRI model, each observation y must be associated with an aggregate alternative, as described in Section 3.1.4.1. This mapping relies on the geographical span of the MRI elements. The geographical span of a MRI m is defined as a set of links $\mathcal{H}_m \subset \mathcal{A}$ in \mathcal{G} . An observation y is deterministically associated with a MRI sequence r if it traverses the span of all the MRIs in r in the correct order. The geographical span of the MRIs in Borlänge is depicted in Figure C3, of Appendix C.

4.4.3 Model specifications and estimation results

We first present the specifications and the estimation results for the two models. The RL and the MRI models are specified and estimated on \mathcal{G} and $\mathcal{G}^{\mathcal{M}}$, respectively. Note that both the RL and the MRI models estimated below are logit models, that is the correlation of alternatives is not taken into consideration.

4.4.3.1 RL model

The specification of the RL model is similar to the one proposed by Fosgerau et al. (2013a), including link travel times $TT(a)$, a constant $LC(a)$ which is equal to 1 for all links in order to penalize paths with many crossings, a left turn dummy $LT(a | k)$ that is equal to one if the turning angle from link k to link a is larger than 40 and less than 177, and zero otherwise, and a u-turn dummy $UT(a | k)$ if the turning angle is larger than 177. We let the parameter associated with the u-turn to be estimated, instead of fixing it to -20 (assumption in Fosgerau et al. (2013a)).

The instantaneous utility $v(a | k)$ of a link pair is given by the following expression

$$\begin{aligned} v(a | k) = & \beta_{TravelTime} TT(a) + \beta_{Penalty} LC(a) \\ & + \beta_{LeftTurn} LT(a | k) + \beta_{UTurn} UT(a | k). \end{aligned} \quad (4.15)$$

The estimation results are presented in Table 4.3. The estimated parameters are significant and have the expected signs. The estimates are approximately the same as the ones reported in Fosgerau et al. (2013a) using the dataset of 1832 observations¹³.

¹³Recall that here we consider observations with a minimum length of 2 km, that are relevant to the aggregate model.

Table 4.3: Estimation results for the RL model

Parameter	value (rob. t-test)
$\beta_{TravelTime}$	-2.91 (-13.15)
$\beta_{Penalty}$	-0.32 (-12.60)
$\beta_{LeftTurn}$	-1.00 (-16.10)
β_{UTurn}	-7.46 (-7.48)
Number of observations	239
Number of parameters	4
$\mathcal{LL}(\hat{\beta})$	-1255.538

4.4.3.2 MRI-based logit model

The utility functions of the MRI model are specified as follows:

$$V_{rn} = \beta_{TravelTime} TT_r + \text{dummy}_{AV} \delta_{rAV} + \text{dummy}_{Around} \delta_{rAround}, \quad (4.16)$$

$$V_{rn}^{\text{cross}} = \beta_{TravelTime} TT_r + \text{dummy}_{AV} \delta_{rAV} + \text{dummy}_{Around_{CL}} \delta_{rAround_{CL}} + \text{dummy}_{Around_{CO}} \delta_{rAround_{CO}} + \text{dummy}_{B2} \delta_{rB2}, \quad (4.17)$$

where δ_{rm} is 1 if alternative r includes MRI m , and 0 otherwise. V_{rn}^{cross} is specified for alternatives entailing a bridge choice. Apart from the necessary normalizations, dummy variables are associated with each MRI. dummy_{CC} and dummy_{B1} are normalized to zero. The parameters related to the number of left turns and number of intersections were tested and not found significant.

The estimation results are presented in Table 4.4. The travel time parameter is significant and negative. The dummy variables play a significant role in explaining the choice probability. As the trade-offs between length and time are not modeled here, their effect is captured by the dummy variables for the MRIs¹⁴. This limitation pertaining to the specification of the model cannot be circumvented due to the lack of relevant variables for the case study. We acknowledge this limitation of the case study in drawing better insights into the travel behavior of individuals. Yet, the focus of the chapter is on the illustration of the methods that allow for the transfers between disaggregate and aggregate representations — and the comparison of the corresponding outcomes — rather than advancing the specification of the models.

¹⁴As discussed in Section 3.3 the travel times in Borlänge are deterministic, computed based on length. Therefore, it is not possible to capture the trade-offs between the two variables in the case of congestion.

Table 4.4: Estimation results of the MRI logit model

Parameter	value (rob. t-test)
$\beta_{TravelTime}$	-0.991 (-7.47)
dummy_{AV}	3.93 (5.81)
dummy_{Around}	1.80 (3.37)
$\text{dummy}_{Around_{CL}}$	2.50 (3.16)
$\text{dummy}_{Around_{CO}}$	3.27 (4.48)
dummy_{B2}	-1.43 (-1.94)
Number of observations	239
Number of parameters	6
$\mathcal{LL}^{\text{MRI}}(\hat{\beta})$	-112.440

4.4.4 Route choice indicators

In the following paragraphs, we elaborate on the results of the models with respect to the derivation of the route choice indicators of interest. We particularly focus on the aggregation approaches, proposed in Section 4.2 to derive aggregate indicators. In lack of detailed demand information, we either omit it or make the assumption of a unit demand.

4.4.4.1 Disaggregate flows

The RL model is directly applicable to obtain link flows, according to Section 4.2.2.1, while the application of the MRI model is subjected to the model presented in Section 4.2.2.2.

Indicative links flows, assuming a demand of one vehicle for a given od pair, are presented in Figure 4.5 for (a) the RL and (b) the MRI model. The example concerns a trip from the south to the north of the city. Both models indicate that the bulk part of the choice probability (dark shade) is concentrated in the west perimeter of the center. It corresponds to the *clockwise movement around the center*. Although the two models agree on which part of the network is the most probable to be traversed, the RL model appears to be more conservative on the distribution of the link flows in comparison with the MRI model. The RL model is specified and estimated on the detailed network model, represented by \mathcal{G} . Its specification is mainly minimizing time. As we do not account for the correlation of alternatives due to path overlap, the RL tends to assign the choices



(a) Application of the RL model using (4.6). (b) Application of the MRI model using (4.8).

Figure 4.5: Link flows for a given od pair assuming a demand of one vehicle.

to one major alternative with local variants. Consequently, it is characterized by very high probabilities for specific itineraries, resulting in low probabilities for the remaining alternatives.

On the other hand, the specification of the MRI model is a product of aggregation, subjected to the assumptions regarding the operationalization of \mathcal{G}^M . The MRI model tends to distribute the probabilities among the aggregate alternatives. Its specification is less sensitive to small differences in the travel times of the alternatives. Now, the variability that is observed around each MRI alternative is the result of the sampling protocol. This variability can be controlled through the λ parameter that defines, in the assignment context, the importance of travel time for the traveler, as explained in Section 3.3.5. Selecting a value for low sensitivity allows to obtain paths away from the fastest path, while selecting a value for high sensitivity restricts the sampled paths to be closer to the fastest path, that is the representative path of each alternative.

To conclude, the high probabilities of the RL model restrict the flows on specific links, while the MRI probabilities, that are disaggregated to link probabilities based on the proposed mapping, allow for the flow to distribute among the possible itineraries.

4.4.4.2 Aggregate route flows

We now focus on the probabilities of the MRI sequences that are proportionate to aggregate route flows. Their computation is straightforward for the MRI model. For the RL model, the two methods presented in Section 4.2.3.2 are employed to compute $Prob(r)$. These are (i) the flow-at-the-destination and (ii) the sampling of paths approaches¹⁵.

Figure 4.6 illustrates the probabilities $Prob(r)$ of the *chosen* MRI alternatives for each observation in the data, as obtained from the two methods that handle the RL output. A deviation in the result as derived from the two methods is noted for three observations. Regressing the probabilities of the first approach against the ones of the second, and including an intercept, gives a coefficient estimate of 1.004 and an intercept ~ 0 . That is, the two methods give an equivalent result.

The probability of the chosen alternative is used as a reference to investigate the behavior of the two models in details. Figure 4.7 depicts for each observation the probability of the chosen MRI alternatives, as derived from the two models. The RL model forecasts, on average, marginally higher probability for the chosen alternatives. Both models are faced with low probabilities for the chosen alternative (bottom-left of the chart). Examining the instances for which low probabilities occur though, reveals that, in comparison with the MRI model, the RL model is faced with much lower probabilities, that for some observations are ~ 0 . In summary, the RL model is characterized by extreme instances

¹⁵500000 paths are sampled for each *od* pair, by simulating a random walk on the network to draw from the RL link transition probabilities.

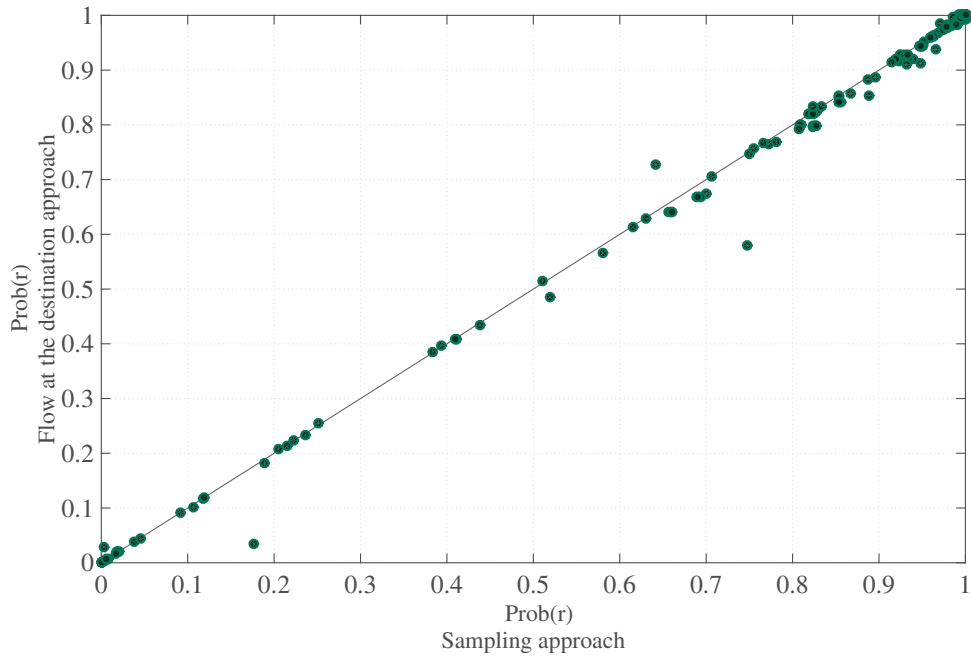


Figure 4.6: MRI choice probabilities as derived from the two aggregation approaches.

— concerning either high or low probabilities — while the MRI model is moderate.

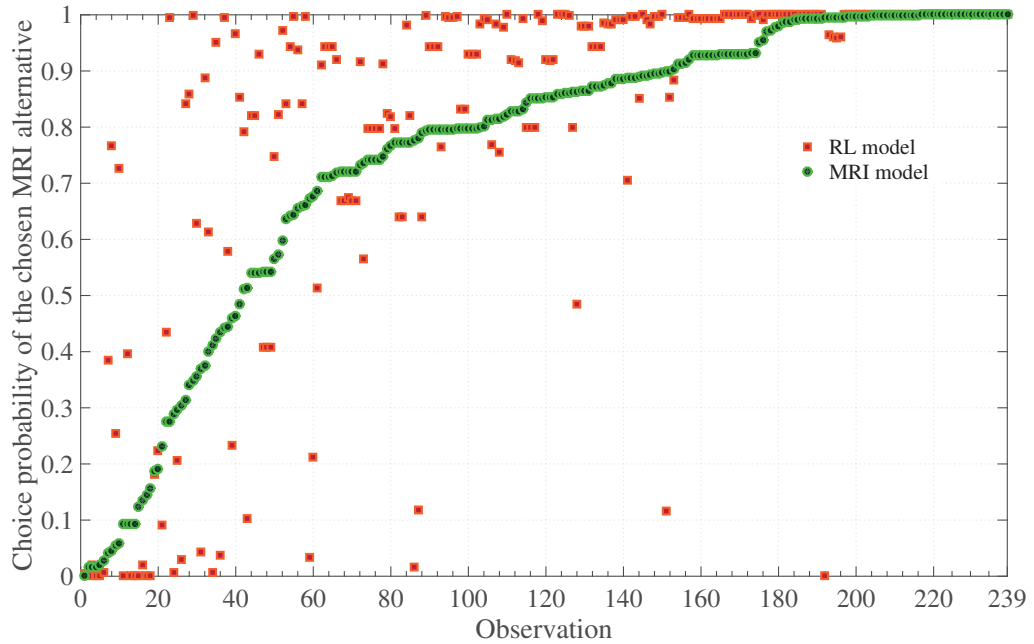


Figure 4.7: MRI choice probabilities as computed from the two models.



Figure 4.8: Indicative example of an observation for which the RL is faced with low probability for the chosen alternative.

For a few instances the RL model is outperformed by the MRI model. Figure 4.8 shows an indicative example. The dashed line denotes the observed path. The pale-color is an indicator of a low probability. The highlighted, dark line denotes the most probable path. Evidently, the RL model assigns a low probability to the chosen alternative at the disaggregate level.

Let us now examine what happens at the aggregate level. The observed path corresponds to choosing the AV alternative. Its probability according to the RL model is 0.117, against 0.454 for the CC, 0.429 for the CO, and ~ 0 for the CL. This is consistent with the output at the disaggregate level. On the other hand, the MRI model assigns a probability of 0.899 to the chosen alternative. The reason why the RL model is faced with low probabilities for the chosen alternative, both at a disaggregate and an aggregate level, is the low transition probability of the link (encircled on Figure 4.8) that grants access to (i) the observed path and (ii) to paths realizing the chosen MRI alternative, respectively for the disaggregate and aggregate levels. The low transition probability of specific links explains the instances for which the RL model is faced with low choice probabilities, even at an aggregate level when it is expected to perform better. The reason why these low link transition probabilities occur is not clear. One explanation is the small data sample that is used for the estimation of the models.

The MRI model is also faced with low probability for the chosen alternative. The source

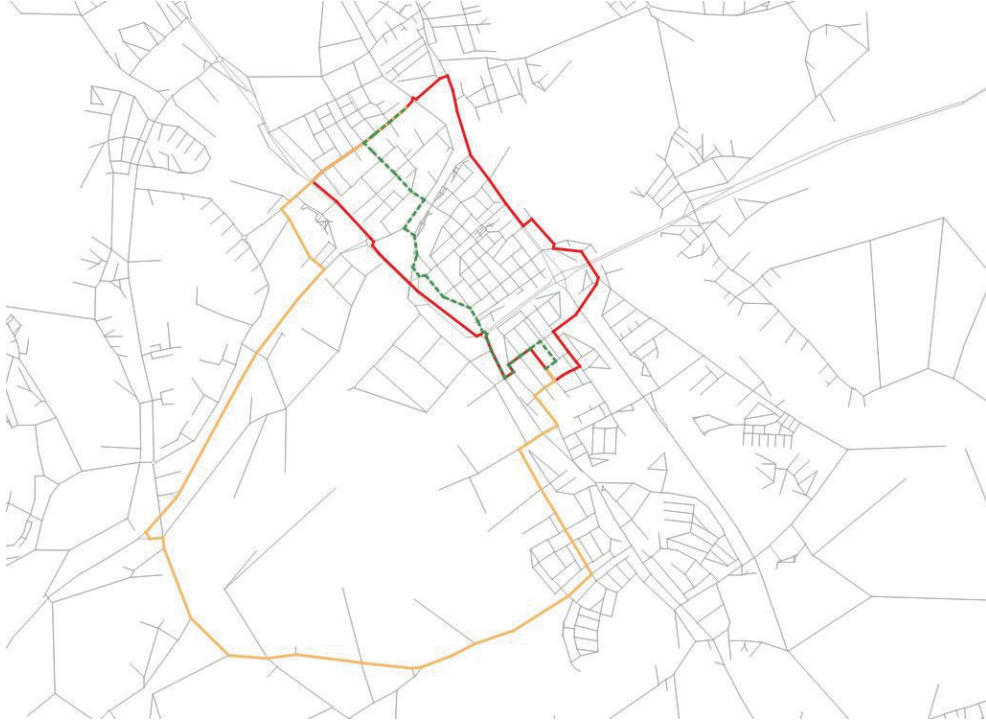


Figure 4.9: Indicative example of an observation for which the MRI model is faced with low probability for the chosen alternative.

of the problem in this case is the limited specification of the model. Travel time is the only attribute included in the utility function. Consequently, the dummy variables associated with the MRIs play an important role in the specification (see Table 4.4). If the travel times of two or more alternatives do not differ considerably, the dummy variables take over their choice probabilities. One such instance is depicted in Figure 4.9. The chosen MRI alternative is the CC (dashed line). Its travel time does not differ considerably from the ones of the *clockwise* and CO. As $\text{dummy}_{\text{Around}} = 1.80$, CL and CO are favored in expense of the CC alternative, for which the dummy variable is normalized to zero. The MRI model assigns a probability of 0.045 to CC, against 0.421, 0.533 and 0.001, accordingly for the CL, the CO and the AV alternatives. The RL model outperforms the MRI model in this case. It assigns 0.766, 0.133, 0.101 and ~ 0 , for the CC, the CL, the CO and the AV alternatives, respectively.

We further elaborate on the effect of the small probabilities on the performance of the models in the following section.

4.4.5 Performance at the aggregate level

The evaluation process outlined in Section 4.3.1 is conducted here. We start by commenting on the final aggregate log likelihood values of the two models, and identifying the

impact of small probabilities on them. We complete the analysis with a cross validation.

4.4.5.1 Final aggregate log likelihood

The final log likelihood of the MRI model is $\mathcal{LL}^{\text{MRI}} = -112.440$ (Table 4.4). The corresponding final log likelihood given by the RL model, computed based on $\text{Prob}(r)$, is $\mathcal{LL}^{\text{RL}} = -271.118$. We elaborate on this result and explain why one cannot claim that the MRI model has a better fit or predictive performance based on it.

Following up on the analysis of Section 4.4.4.2 and the discussions about Figure 4.7, the instances for which low probabilities occur in the case of the RL model are, in comparison with the MRI, more extreme, that is ~ 0 for some observations. This, results in a significant decrease of the log likelihood. Several instances of the RL model are characterized by decreases of more than 10, with the worst one being ~ 26 . On the other hand, the worst instance of the MRI model is characterized by a decrease of ~ 7.5 . The extreme instances concern 9 observations. Summing the logarithms of the probabilities of these 9 observations gives a downgrade of ~ 165 in the \mathcal{LL}^{RL} .

Excluding these 9 observations from the computation of the log likelihood values results in $\mathcal{LL}^{\text{MRI}} = -91.222$ and $\mathcal{LL}^{\text{RL}} = -94.446$. This is an important result as it demonstrates two things: (i) the two models give compatible results and (ii) the efficacy of the MRI model to produce meaningful results intended for an aggregate analysis.

4.4.5.2 Forecasted and predicted aggregate likelihood

A cross validation approach is used to evaluate the performance of the MRI and RL models with respect to the predicted MRI choice probabilities. 80% of the observations are randomly drawn and used to estimate the models, while the remaining 20% is used to apply them. 100 training and test samples are generated for this purpose. The same samples are used across all models. The resulting log likelihood values are conditional on the samples. The average of the log likelihood values over the samples is computed in order to obtain unconditional values as

$$\overline{\mathcal{LL}}_t = \frac{1}{t} \sum_{s=1}^t \mathcal{LL}_s, \quad \forall t = 1, \dots, 100 \quad (4.18)$$

where s is a sample. The values of $\overline{\mathcal{LL}}_t$ are plotted in Figures 4.10-4.13¹⁶. Figures 4.10 and 4.11 depict the final and the predicted log likelihood values of each replication for the training and the test samples, respectively. The MRI LL0 line shows the log likelihood of the null model corresponding to the MRI choice set¹⁷ and serves as a reference for

¹⁶The log likelihood converges to the unconditional value as long as $t \rightarrow \infty$. 100 samples are used so that the analysis can be conducted in a reasonable computational time.

¹⁷The null model predicts equal probabilities for all alternatives, as all its parameters are fixed to zero.

the performance of the models. The box plots in Figures 4.12 and 4.13 summarize the output of the 100 samples for each model.

The effect of the extreme instances, with probability of ~ 0 for the chosen alternative, on the performance of the RL model is manifest in Figures 4.10 and 4.11. Note that during the validation process we do not identify and exclude these observations. The output of the RL model is characterized by more variance. This is explained by the fact that it is estimated on the detailed network, and due to the small data sample, it is more sensitive to network attributes than the MRI model.

4.4.6 Capturing correlation with the MRI model

4.4.6.1 Model specifications

The logit model presented in Section 4.4.3.2 serves as a benchmark for testing for correlation within the MRI framework. We make the reasonable assumption that MRI sequences using the same MRI are correlated. It is tested using a NL and an EC specification. One nest, or component, is assumed accordingly for the NL and the EC models. It corresponds to the option of *going around the city center*, either using the *clockwise* or the *counter-clockwise* movement. Regarding the EC model, the underlying assumption is that alternatives using the same MRI m share the random terms ζ_m . ζ_m are normally distributed $\sim \mathcal{N}(0, \sigma_m^2)$ and the σ_m of each component is estimated from the data. The utility functions are specified as follows

$$V_{rn} = \beta_{TravelTime} TT_r + \text{dummy}_{AV} \delta_{rAV} + \text{dummy}_{Around} \delta_{rAround} + \zeta_{Around} \delta_{rAround}, \quad (4.19)$$

$$V_{rn}^{\text{cross}} = \beta_{TravelTime} TT_r + \text{dummy}_{AV} \delta_{rAV} + \text{dummy}_{Around_{CL}} \delta_{rAround_{CL}} + \text{dummy}_{Around_{CO}} \delta_{rAround_{CO}} + \text{dummy}_{B2} \delta_{rB2} + \zeta_{Around} \delta_{rAround}. \quad (4.20)$$

This specification is the same as the one of the logit model (see Section 4.4.3.2) with the inclusion of the error components. A CNL model, following the specification described in Section 4.3.2.1, was estimated and tested as well. It was not possible to obtain a specification for which the parameters corresponding to the scales μ_m of the nests were not hitting the bounds. This is attributed to the small sample that is used for the estimation.

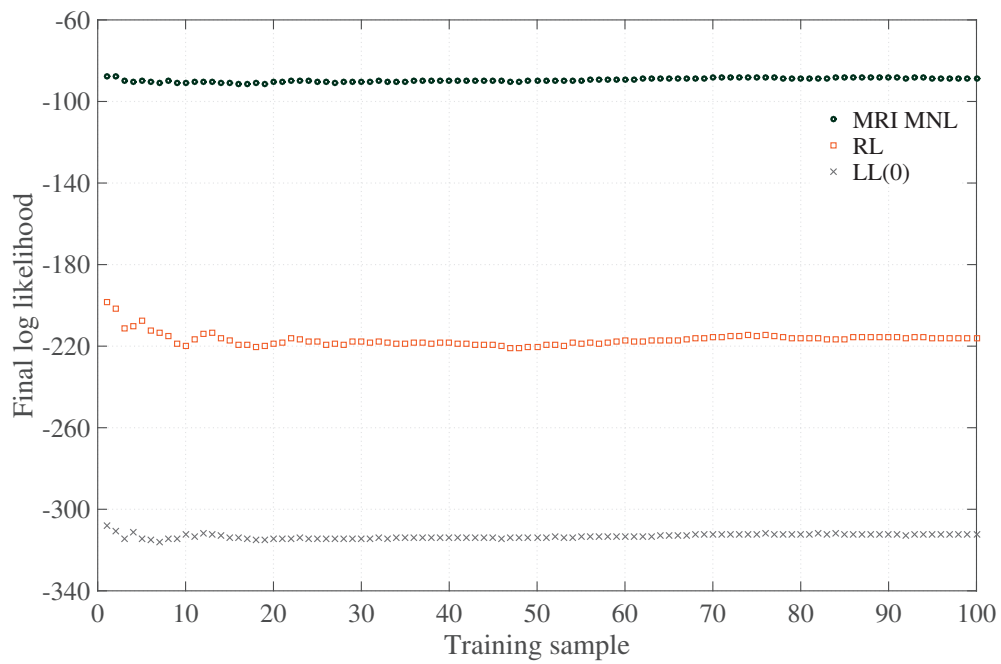


Figure 4.10: Log likelihood of the training samples.

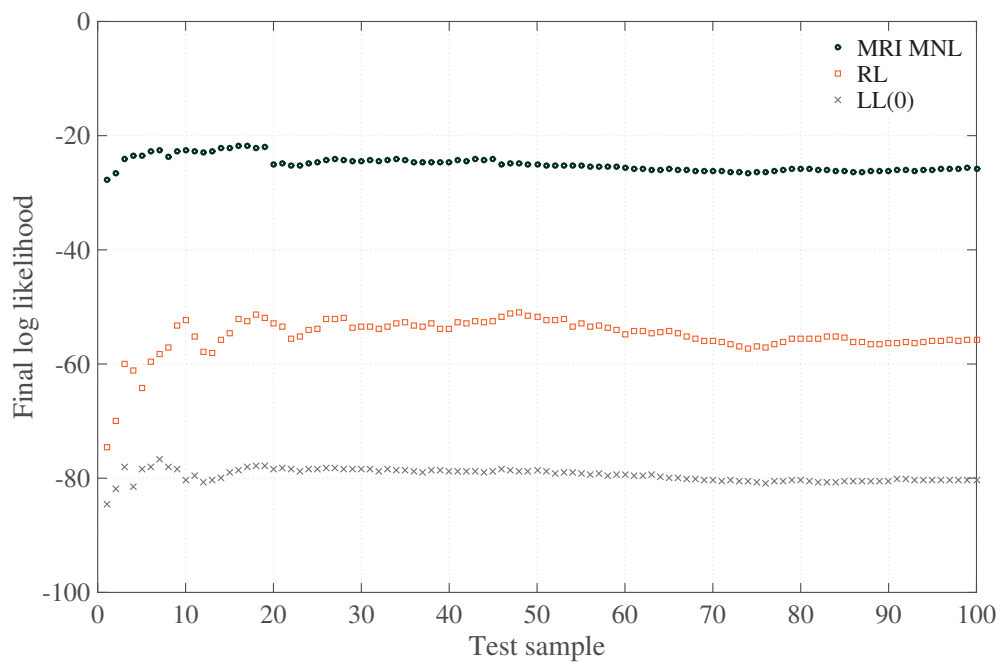


Figure 4.11: Log likelihood of the test samples.

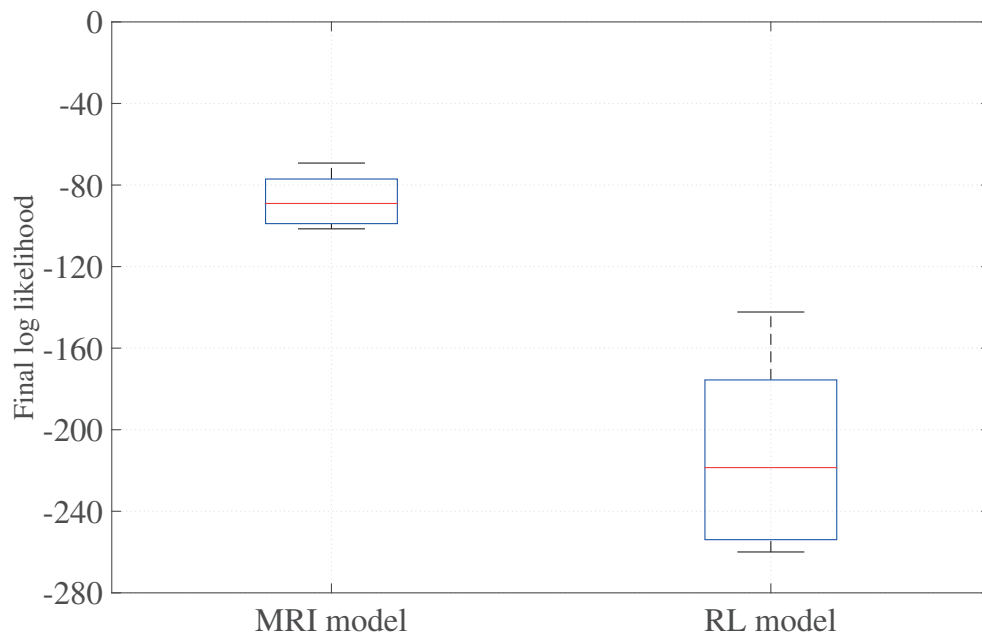


Figure 4.12: Box plot of the log likelihood for the training samples.

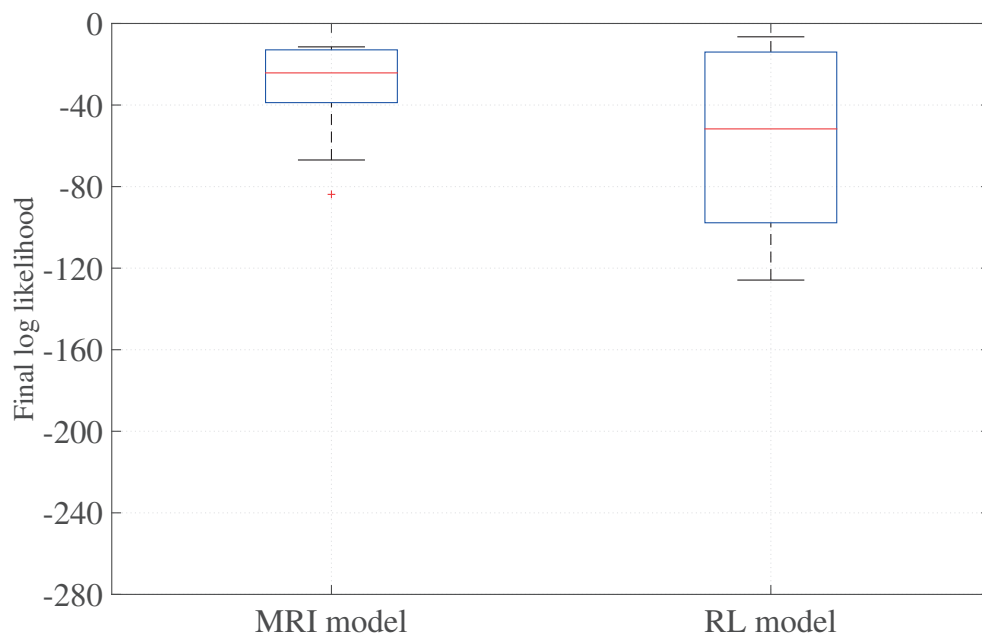


Figure 4.13: Box plot of the log likelihood for the test samples.

4.4.6.2 Estimation and forecasting results

Table 4.5 presents the parameter estimates for the three models. The parameters for travel time are significant and have the expected signs.

The parameters μ_{Around} and σ_{Around} are significant, indicating that the alternatives using the MRIs of *clockwise movement around the center* and the *counter-clockwise movement around the center* are correlated. Consistent with this result, there is an improvement in the final log likelihood of the NL and EC models, as compared to the logit model.

The cross validation approach (see Section 4.4.5.2) is also performed for the NL model. Figures 4.14 and 4.15 demonstrate the improvement in the final log likelihoods due to the NL specification, as opposed to the logit model.

4.5 Summary

This chapter presents a practical scheme for the application and assessment of tractable route choice models. It builds upon the current state of the art and identifies a modeling paradigm, where different levels of aggregation are targeted for different purposes of analysis.

We demonstrate the derivation of relevant disaggregate and aggregate indicators for the

Table 4.5: Estimation results

	Logit	NL	EC
Parameter	value (rob. t-test)*	value (rob. t-test)*	value (rob. t-test)*
dummy_{AV}	3.93 (5.81)	3.77 (6.45)	6.70 (3.10)
dummy_{Around}	1.80 (3.37)	2.24 (4.08)	3.99 (2.26)
$\text{dummy}_{Around_{CL}}$	2.50 (3.16)	2.72 (4.26)	4.77 (2.40)
$\text{dummy}_{Around_{CO}}$	3.27 (4.48)	3.09 (4.97)	5.40 (2.77)
dummy_{B2}	-1.43 (-1.94)	-0.824 (-1.33)	-1.16 (-1.21)
$\beta_{TravelTime}$	-0.991 (-7.47)	-0.790 (-7.52)	-1.43 (-4.88)
μ_{Around}	×	2.36 (2.75)	×
σ_{Around}	×	×	3.13 (2.71)
# draws	×	×	1000
# observations	239	239	239
# parameters	6	7	9
$\mathcal{LL}(0)$	-392.742	-392.742	-392.742
$\mathcal{LL}(\hat{\beta})$	-112.440	-105.053	-106.867

*t-test against 0 for all the parameters except for μ_m , for which the reported t-test is against 1.

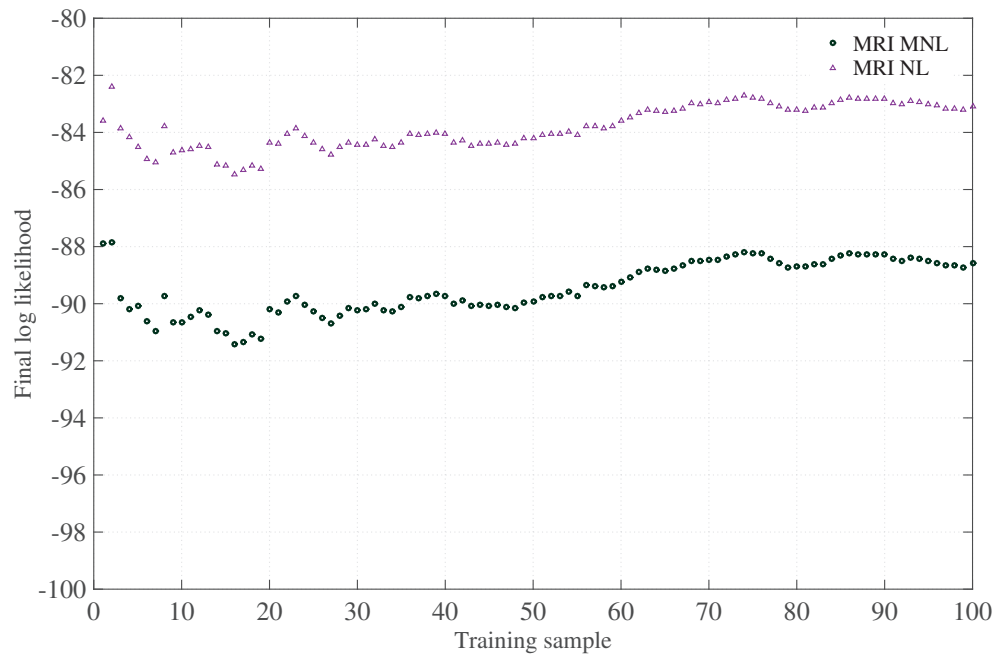


Figure 4.14: Log likelihood of the training samples.

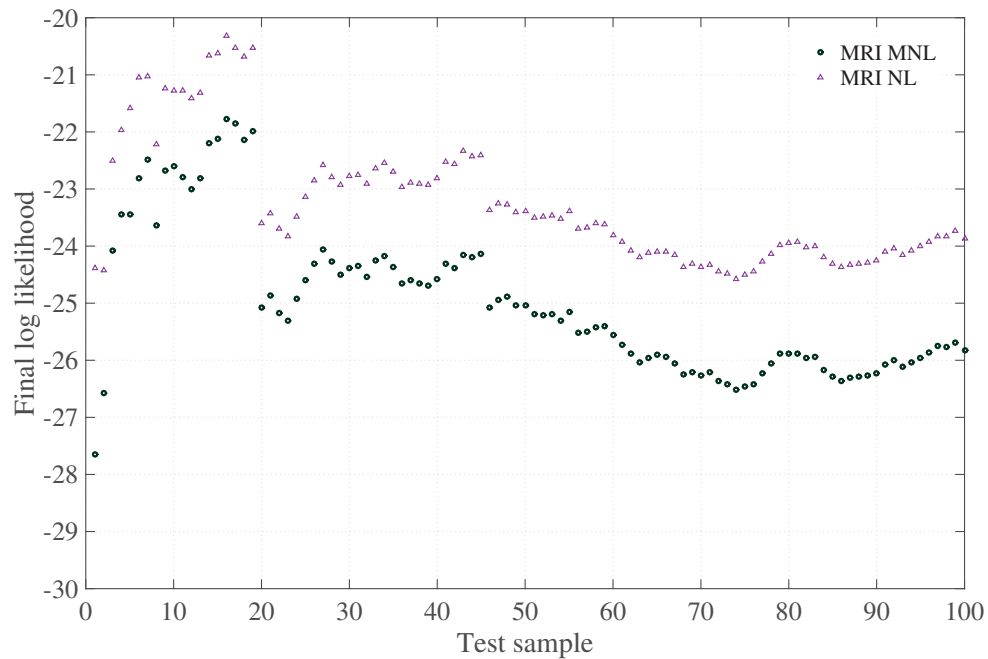


Figure 4.15: Predicted log likelihood of the test samples.

application of route choice models. The derivation of indicators from a model corresponding to a different level of aggregation than the one required from the application is not straightforward. Therefore, we present methods to derive aggregate indicators from a disaggregate model and vice versa.

The RL and the MRI models are investigated and their performance is tested on real data. Despite the limited specification of the MRI model, the results indicate that it can capture the strategic route choices of individuals, and be used for a meaningful aggregate analysis. In comparison with the RL model, its performance at the aggregate level is found to be at the same, and slightly better, level of sufficiency. This is important as the MRI approach enables the development of models for areas without an existing or an inadequate detailed network model, where the disaggregate approach would not be possible.

5

Route choice in a large network: Québec city

This chapter is based on the article

Kazagli, E. and Bierlaire, M. (2017). Route choice in a large network: Québec city. Working paper.

The work has been performed by the candidate under the supervision of Prof. Michel Bierlaire.

In this chapter we apply the MRI approach to a large network. The motivation comes from (i) the additional complexity in the definition of the model due to the size of the city of interest, and (ii) the lack of a detailed disaggregate network model. The goal is the definition of a conceptual model that is realistic and meaningful, that can be operationalized using simple techniques and applied to aggregate route choice analysis.

We present concrete model specifications that are compatible with the standard estimation procedures. We demonstrate the capability of the framework to adapt to a complex choice context — while remaining computationally affordable — using RP data from the city of Québec, in Canada. The proposed model provides a description of the aggregate route choice of individuals, and by integration with the RL model, is readily applied to the prediction of flows on the major segments of the network.

The chapter is organized as follows. Section 5.1 presents the modeling steps for the

application of the MRI approach to the city of Québec. Section 5.2 provides estimation and prediction results, and applies the model to compute aggregate element flows. Section 5.3 discusses assumptions and specific features of the model. Section 5.4 summarizes the outcomes of the analysis.

5.1 Modeling

In this section, we start by providing a short description of the available data and identifying the prominent elements of the area of study, relevant to the determination of the MRIs. We proceed with a detailed description of the modeling steps for the definition and operationalization of the MRI model for the city of Québec. We follow the same methodological steps as in Section 3.1 for the definition of the MRI framework. The specifics of each step are adapted according to the needs of the current application. The whole analysis is elaborated at the aggregate level — based on the definition of the MRI graph — yet its output can be directly interpreted on representative segments of the physical network.

5.1.1 Available dataset

This case study exploits a dataset from the city of Québec, in Canada. It has been collected through *Montraject*, a smartphone application for recording and analyzing route GPS data (Miranda-Moreno et al., 2015). The campaign involved around 4000 individuals. The data collection spanned over a three-week-period (April 25 to May 16, 2014), providing more than 20000 trajectories for analysis. The GPS trajectories were map-matched on the Québec city’s OpenStreetMap¹⁸ road network using TrackMatching (Marchal, 2015) — a cloud based map-matching service. Subsequently, each observation is expressed as an ordered sequence of links of the OpenStreetMap network model. For more details regarding the data processing and relevant applications we refer the reader to Stipancic et al. (2017).

We use a sample of 2321 trips, with a minimum length of 10 km, for which the map-matching provided complete trajectories¹⁹. Figure 5.1 depicts the map of the city and the origins and destinations of the trips in the sample. The highlighted area indicates the center of the city, including the old part that is still surrounded by walls (old city fortress). Figure 5.2 shows the trajectories of the 2321 trips and indicates the extent of the study area.

¹⁸We use the OpenStreetMap network model for all the illustrations of the physical network in the remainder of this chapter.

¹⁹There are instances for which the map-matched trajectories have gaps, i.e. there are missing segments in the sequence resulting in discontinuities. In order to avoid additional biases, and given the abundance of data, we keep only complete trajectories.

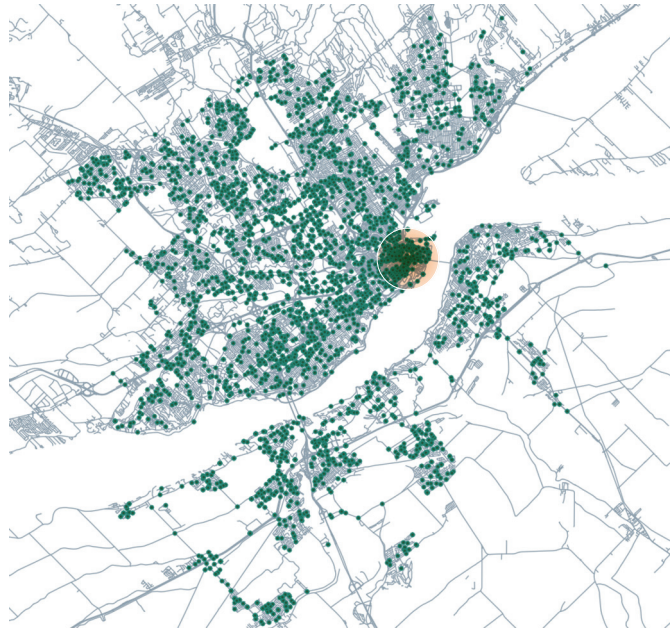


Figure 5.1: Québec city: origins and destinations in the data sample.



Figure 5.2: Observed trajectories and boundaries of the study area.

5.1.2 The mobility image in Québec city

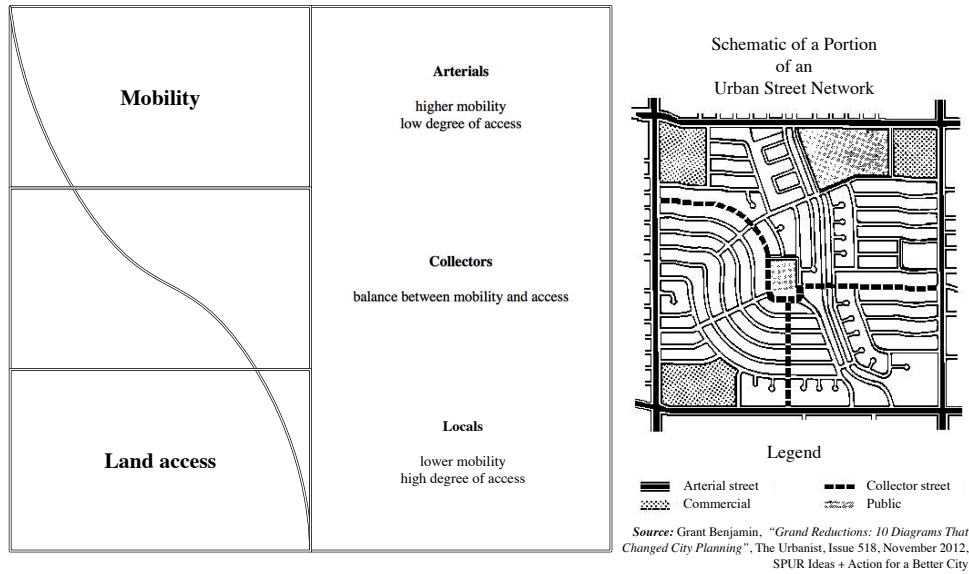
The roadway network of Québec city is part of a big system of “Autoroutes” (highways) that connects the major cities in the province of Québec. The city has an extended network of expressways that serves the everyday commuting needs of the inhabitants. Two bridges and a ferry line provide connections to the city of Lévis, in the south shore of the Saint Lawrence river.

Figure 5.3 depicts the most visited segments of the network — as observed in the data. They are characterized by darker shades. They correspond to the highways, the major primary streets that run across the city and the two bridges. These segments approximately form a grid system. Their schematic, emerging from Figure 5.3, resembles the schematic of the urban road network shown in Figure 5.4, that follows the functional classification of roads of the U.S. Federal Highway Administration guidelines. Indeed, the highways and the major arterials serve the bulk of the mobility in the city, while the streets of lower types grant access to important locations, such as home and work.

We build upon these observations regarding the mobility scheme in Québec city, to formulate the principles of the aggregate route choice model. The “Autoroutes”, the primary arterials and the two bridges listed in Table 5.1 are identified as the prominent



Figure 5.3: Most visited segments in the data sample.



Adapted from the Functional Classification Guidelines: U.S. Department of Transportation, Federal Highway Administration.

Figure 5.4: Mobility versus accesibility.

elements of the city's mobility. They are used as the basis for the definition of the MRIs and the MRI graph. We elaborate on the level of aggregation with the respect to these definitions in the following section. The ferry line is omitted, as that there are only very few observed trips that presumably use it — i.e. with records in the proximity of the ferry platforms in the two sides of the river and a loss of signal in between.

Table 5.1: The prominent routes in Québec city

	reference	road type	side (river reference)
1	Autoroute 40	motorway	upper
2	Autoroute 73	motorway	upper/ lower
3	Autoroute 40; 73	motorway	upper
4	Autoroute 573	motorway	upper
5	Autoroute 440	motorway	upper
6	Autoroute 740	motorway	upper
7	Autoroute 540	motorway	upper
8	Autoroute 973	motorway	upper
9	Route 175	primary	upper/ lower
10	Route 138	primary	upper
11	Route 136	primary	upper
12	New bridge	bridge/ motorway	river pass
13	Old bridge	bridge/ primary	river pass
14	Autoroute 20	motorway	lower
15	Route 132	primary	lower
16	Route 116	primary	lower

5.1.3 Definitions

In this section, we determine the level of aggregation in the representation of the alternatives, and we define accordingly the MRI elements and the MRI graph.

5.1.3.1 The MRIs of Québec city

Several of the elements identified in the previous Section are several kilometers long, running all across the city. For this reason we divide them into segments. We define representative segments of each element in Table 5.1 based on the bounds of the city, i.e. north (N), south (S), east (E), west (W), while taking into account the main intersections/ interchanges, where transfers from one route to another are possible. Consequently, each element listed in Table 5.1 is either associated with one MRI, or segmented to two, three or a maximum of four MRIs. The segmentation is detailed in Table 5.2, along with information regarding the length and the speed limit of each segment. All the segments are bidirectional, yet there is no consideration of direction with respect to the attributes of the segments. The direction of movement is captured implicitly by the definition of the MRI graph that is presented in the following section.

There are in total 30 elements: 19 running across the upper side of the river, 9 in the lower part and *two* bridges granting the connection between the two shores. Each of them corresponds to a motorway or a primary road segment. Figure 5.5 depicts the *geographical span* of each element. It is associated with the corresponding roadway segment and defined as a set of links \mathcal{H} of the OpenStreetMap network model. On the same figure, we illustrate the aggregation of the trip origin (o) and destination (d) nodes into O and D zones, respectively. Natural barriers such as the shores, the city walls, railway tracks, etc. are taken under consideration for the aggregation of the trip origins and destinations. The OD zones are represented by the light-grey shaded polygons and the black circles denote their centroids. There are in total 138 aggregate OD zones, 101 in the upper and 37 in the lower side. Finally, the round shaded areas represent the central part of the city as well as the major interchanges, where additional costs (travel time) are incurred when transferring among the segments. A bigger diameter signifies higher costs of transfer. The features depicted in Figure 5.5 are relevant for the definition of the attributes in Section 5.1.4.

5.1.3.2 The MRI graph of Québec city

The MRI graph is depicted in Figure 5.6. It is defined as $\mathcal{G}^{\mathcal{M}} = (\mathcal{L}', \mathcal{M}')$, where

1. \mathcal{M}' is the set of nodes including the set of MRIs \mathcal{M} , the set of origin zones \mathcal{O} and the set of destination zones \mathcal{D} , that is $\mathcal{M}' = \mathcal{M} \cup \mathcal{O} \cup \mathcal{D}$.
2. \mathcal{L}' is the set of links determining the possible transfers among the nodes of \mathcal{M}' , that is the incidence matrix of the graph.

Table 5.2: The MRIs in Québec city

reference	segment MRI id	length [km]	maximum speed [km/ h]	side (river reference)
Autoroute 40	40E	3.1	100	upper
Autoroute 40	40W	4.8	100	upper
Autoroute 73	73N	5.9	100	upper
Autoroute 73	73S_Upper	3.1	90	upper
Autoroute 40; 73	4073_40	3.6	100	upper
Autoroute 40; 73	4073_73	2.2	90	upper
Autoroute 573	573	4.8	100	upper
Autoroute 440	440E	2.7	100	upper
Autoroute 440	440M	2.3	100	upper
Autoroute 440	440W	2.0	100	upper
Autoroute 740	740	3.7	100	upper
Autoroute 540	540	2.8	100	upper
Autoroute 973	973	3.0	70	upper
Route 175	175N	4.5	50	upper
Route 138	138E	3.2	70	upper
Route 138	138M_E	3.7	70	upper
Route 138	138M_W	3.1	70	upper
Route 138	138W	5.2	70	upper
Route 136	136	5.3	60	upper
New bridge	NB	2.3	90	river pass
Old bridge	OB	2.0	50	river pass
Autoroute 20	20E	5.9	100	lower
Autoroute 20	20M	2.3	100	lower
Autoroute 20	20W	6.1	100	lower
Route 132	132E	5.9	50	lower
Route 132	132M	3.1	50	lower
Route 132	132W	5.6	70	lower
Autoroute 73	73S_Lower	5.8	90	lower
Route 175	175S	5.4	70	lower
Route 116	116	7.9	70	lower

For clarity reasons, we omit the illustration of the nodes corresponding to the *OD* zones from the graph presented in Figure 5.6. An illustration of the detailed list of the *OD* zones is provided in Figure C5, of Appendix C. The following assumptions pertain to the definition of $\mathcal{G}^{\mathcal{M}}$:

1. Trips are generated in $\mathbf{o} \in \mathcal{O}$ and attracted by $\mathbf{d} \in \mathcal{D}$. In particular, each $\mathbf{o} \in \mathcal{O}$ has only outgoing links and each node in $\mathbf{d} \in \mathcal{D}$ has only incoming links²⁰.
2. By using the local network, individuals from any node in \mathcal{O}/\mathcal{D} are assumed to be able to reach any $m \in \mathcal{M}$ that is located at the same side of the river.

The two big interchanges highlighted in Figure 5.5 can be identified on the graph in Figure 5.6 by the radial scheme that they form, involving transfers among several MRIs. The city center is also represented by an area where connections from the NE to the SW MRIs, and vice versa, allow individuals to transfer among MRIs that do not physically

²⁰Note that all zones serve both as origin and destination zones. Two nodes are then defined for each zone to distinguish between its use as an \mathbf{o} and as \mathbf{d} .

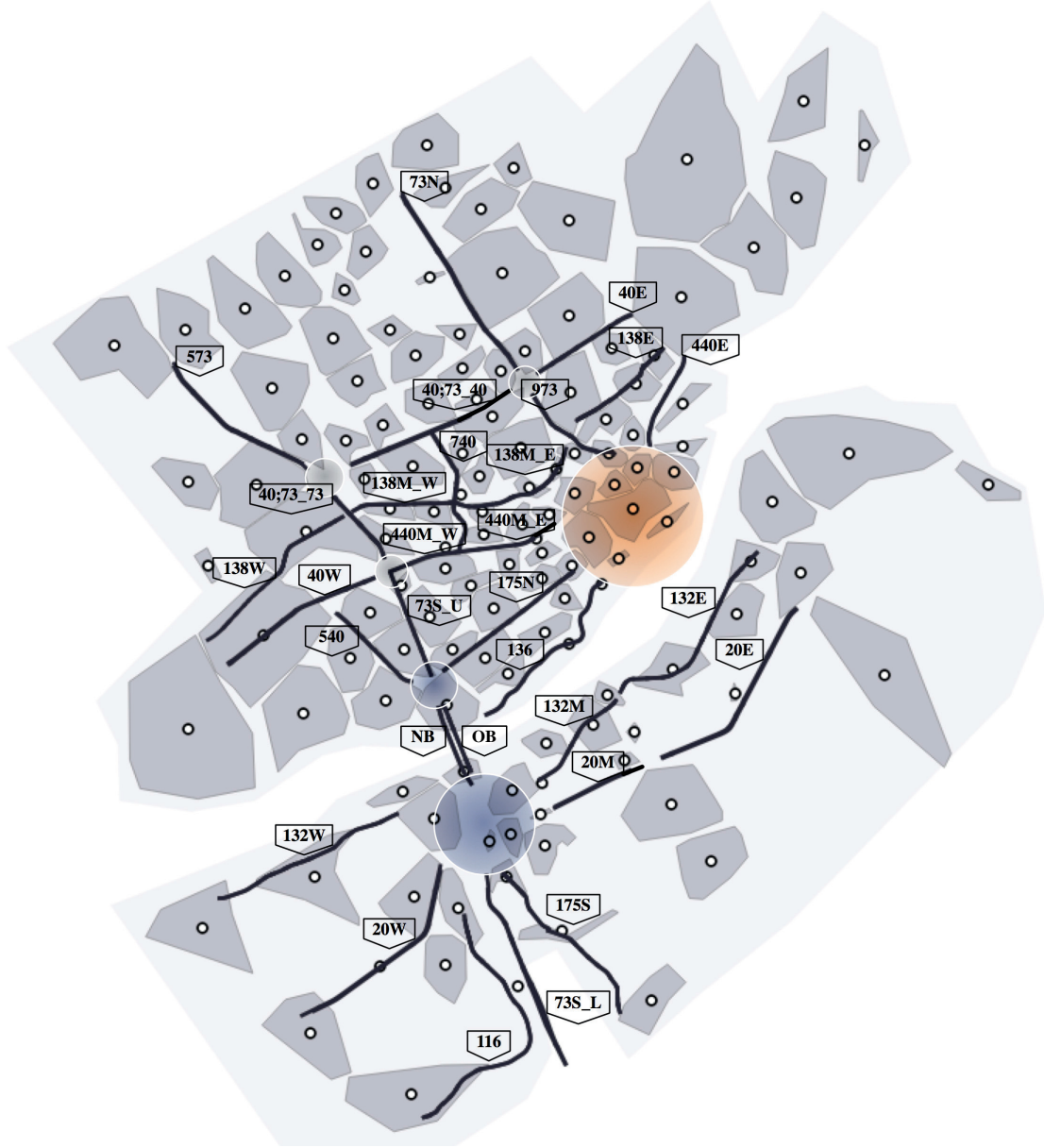


Figure 5.5: Geographical span of the MRIs and the *OD* zones in Québec city.

intersect.

Finally, in accordance with the definition of the MRI framework, the 30 elements illustrated in Figure 5.6 constitute the building blocks of the alternatives of the aggregate model. An alternative r is an ordered sequence of MRI nodes in \mathcal{M}' that connects the $o \in \mathcal{O}$ and the $d \in \mathcal{D}$ of the trip, such that $r = o, m_1, \dots, m_h, d$, where $m_i \in \mathcal{M}$ and h the number of nodes in the sequence.

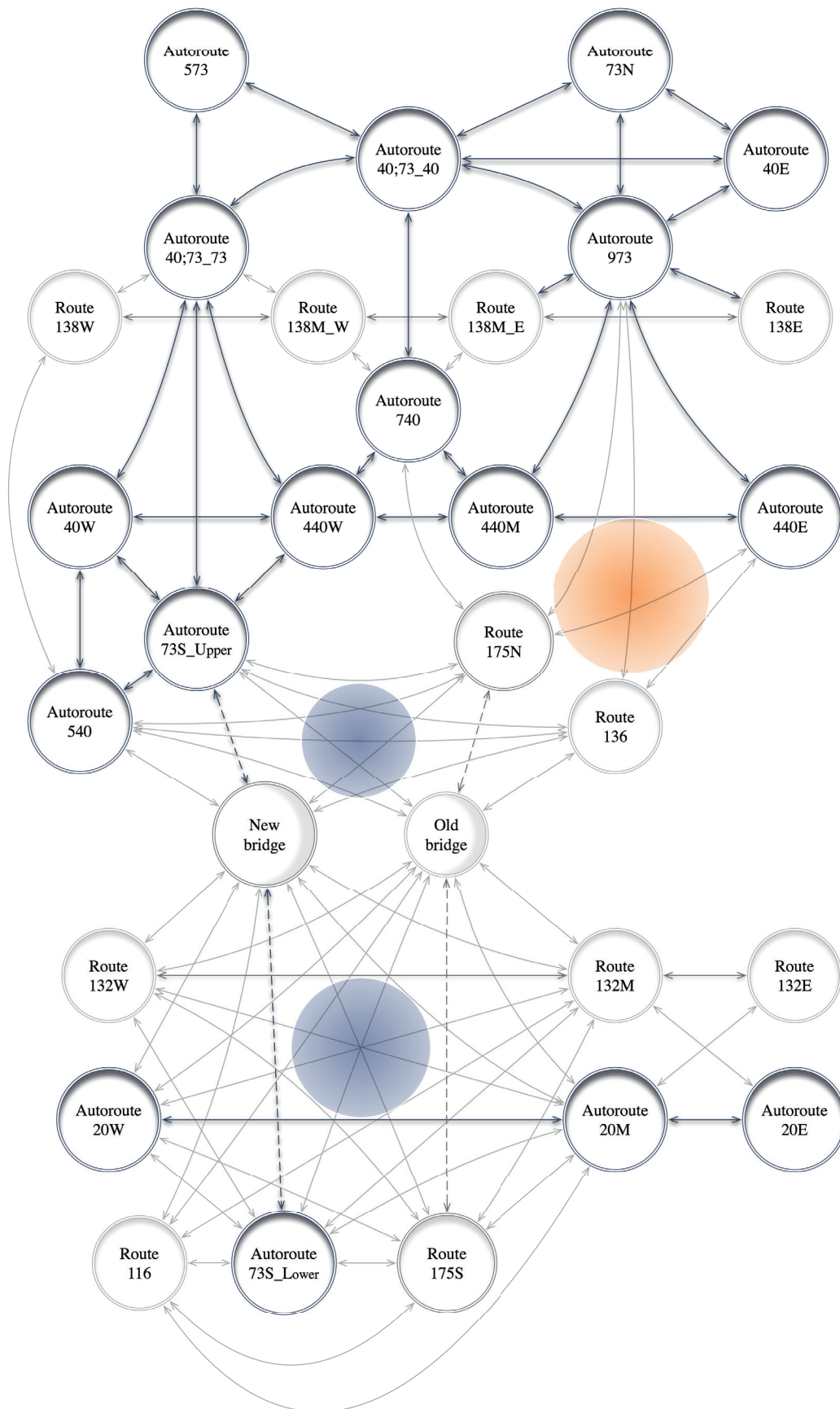


Figure 5.6: The MRI graph of Québec city.

5.1.4 Attributes

The main feature for the operationalization of $\mathcal{G}^{\mathcal{M}}$ is the geographical span of the elements. Element additive attributes are associated with each node in \mathcal{M} and each transfer between pairs of nodes in \mathcal{M}' . More specifically, each node $m \in \mathcal{M}$ is associated with a

Travel time that is computed as

$$\text{Time}(m) = \frac{\text{Length}(m)}{\text{maxSpeed}(m)}$$

the ratio of the length and the maximum allowed speed on the corresponding segment (second column of Table 5.3).

Type of road two dummy variables related to the type of the segment, i.e. *motorway* and *primary*, are defined for each element (third and fourth columns of Table 5.3). That is, $\text{Motorway}(m) = 1$ if the segment corresponds to a motorway, and zero otherwise, and $\text{Primary}(m) = 1$ if the segment corresponds to a primary, and zero otherwise

Cognitive load following the ideas of Gallotti et al. (2016) and Rosvall et al. (2005) — who use a measure of entropy as a proxy for the accumulated *cognitive load* associated with a trip that characterizes the complexity of the navigation task — we define an attribute representing the amount of information that an individual needs to process at any given node $m \in \mathcal{M}$ along a route. Gallotti et al. (2016) and Rosvall et al. (2005) intend to characterize the overall complexity of the city network. We make use of their principles to characterize the complexity of a given route across the city network. The underlying assumption is that the higher the connectivity of a node is, the higher its complexity and hence the cognitive load that it entails for the individual. In that sense, individuals are expected to minimize the cognitive load of their routes, by selecting “simpler” nodes and routes with less transfers. The cognitive load is approximated by the measure of entropy of each node and is equal to

$$\text{CognitiveLoad}(m) = \log_2(c_m),$$

where c_m is the degree of connectivity of node m . An illustrative example is given in Figure 5.7. Node m_1 requires $\log_2(3)$ bits of information, while node m_2 requires $\log_2(7)$, in order to locate the desired exit to the destination.

The cognitive load attribute is reported in the last two columns of Table 5.3. Same as in Gallotti et al. (2016) and Rosvall et al. (2005), the degree of connectivity is discounted by one for every node along a route except for the first one, in order to take into account the information that is gained by traveling along the route; that is, at each node m an individual has a choice among $c_m - 1$ nodes, assuming that she will not visit again the previous node. As all $m \in \mathcal{M}$ located in each side of the river are connected to all

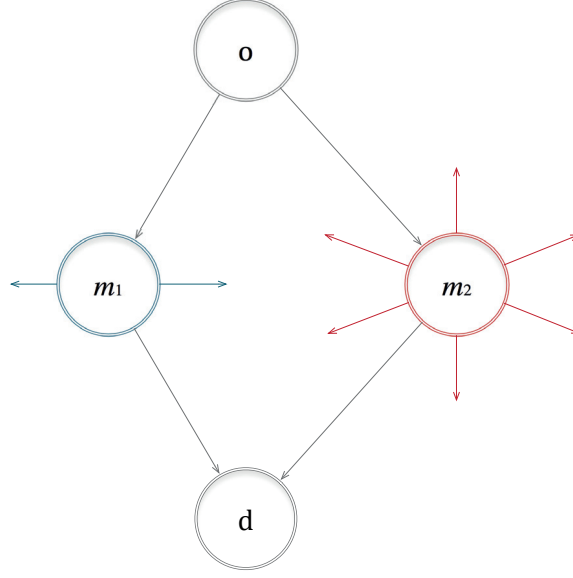


Figure 5.7: Illustration of a simple (m_1) and a complex (m_2) node.

$o \in \mathcal{O}$ and $d \in \mathcal{D}$ of the same side, the connections to the o/d nodes are not counted in c_m (fifth column of Table 5.3). We only measure the cognitive load while traveling throughout the part of the \mathcal{G}^M that is illustrated in Figure 5.6.

The attributes of each element are reported in Table 5.3. Additionally,

Transfer time transfer times are defined for each pair of nodes $m', \nu \in \mathcal{M}'$. More specifically:

1. if both m' and $\nu \in \mathcal{M}$, then $\text{TransferTime}(\nu | m') = 0$, except if m' and ν are involved in the two major interchanges or the city center area. In this case, the transfer times are set to 5, 10 or 15 minutes, depending on the transfer. Table D2, of Appendix D, reports the detailed list of transfer times between each pair of nodes in \mathcal{M} ;
2. else if $m' \in \mathcal{O}$ and $\nu \in \mathcal{M}$, or alternatively if $m' \in \mathcal{M}$ and $\nu \in \mathcal{D}$, then the $\text{TransferTime}(\nu | m')$ is computed using the Google Maps Distance Matrix API. A total of 5034 distances were computed to derive the corresponding transfer times.

5.1.5 Model specification and estimation approach

The MRI model is specified on \mathcal{G}^M and estimated using *maximum likelihood estimation* through the recursive logit (RL) formulation (Fosgerau et al., 2013a)²¹. For this purpose, dummy states d' are defined for every destination node $d \in \mathcal{D}$. They correspond to the

²¹We refer the reader to Section 4.1.1 for a detailed description of the RL model.

Table 5.3: The MRI attributes

MRI	travel time	# of connections			measure of entropy	
	[min]	motorway	primary	c_m	first node after origin: $\log_2(c_m)$	node in the sequence: $\log_2(c_m - 1)$
40E	1.83	1	0	3	1.58	1.00
40W	2.87	1	0	4	2.00	1.58
73N	3.53	1	0	3	1.58	1.00
73S_Upper	2.04	1	0	8	3.00	2.81
4073.40	2.15	1	0	6	2.58	2.32
4073.73	1.46	1	0	7	2.81	2.58
573	2.86	1	0	2	1.00	0.00
440E	1.78	1	0	4	2.00	1.58
440M	1.38	1	0	4	2.00	1.58
440W	1.22	1	0	5	2.32	2.00
740	2.43	1	0	6	2.58	2.32
540	1.89	1	0	7	2.81	2.58
973	2.54	1	0	9	3.17	3.00
175N	5.46	0	1	7	2.81	2.58
138E	3.17	0	1	2	1.00	0.00
138M_E	3.15	0	1	4	2.00	1.58
138M_W	2.63	0	1	4	2.00	1.58
138W	4.49	0	1	3	1.58	1.00
136	5.31	0	1	6	2.58	2.32
NB	1.55	1	0	11	3.46	3.32
OB	2.38	0	1	11	3.46	3.32
20E	3.52	1	0	2	1.00	0.00
20M	1.39	1	0	9	3.17	3.00
20W	3.65	1	0	6	2.58	2.32
132E	7.06	0	1	2	1.00	0.00
132M	3.78	0	1	9	3.17	3.00
132W	4.77	0	1	6	2.58	2.32
73S_Lower	3.86	0	1	8	3.00	2.81
175S	4.60	0	1	8	3.00	2.81
116	6.81	0	1	6	2.58	2.32

absorbing states with no successors. The set of dummy states is denoted by \mathcal{D}' , and the set of nodes \mathcal{M}' is further extended to include them, that is $\mathcal{M}'' = \mathcal{M}' \cup \mathcal{D}'$.

At each state, that is at each node $m \in \mathcal{M}'$, the traveler chooses the next state (next node) $\nu \in \mathcal{M}'$ that maximizes the sum of the instantaneous utility $u_n(\nu \mid m)$ and the expected downstream utility $V^{\mathcal{D}'}(m)$ to the destination, where

$$u_n(\nu \mid m) = v_n(\nu \mid m) + \mu \varepsilon_n(\nu), \text{ and} \quad (5.1)$$

$$V^{\mathcal{D}'}(m) = \mu \ln \sum_{\nu \in \mathcal{M}} \delta(\nu \mid m) e^{\frac{1}{\mu}(v_n(\nu \mid m) + V^{\mathcal{D}'}(\nu))} \quad \forall m \in \mathcal{M}. \quad (5.2)$$

ε_n is i.i.d. extreme value type I with zero mean; μ is the scale parameter of the model; $v_n(\nu \mid m)$ is the deterministic part of the node-pair-utility that is equal to $v(x_{n,\nu \mid m}; \beta)$, with $x_{n,\nu \mid m}$ being the vector of attributes associated with the node pair (m, ν) and β the vector of parameters to be estimated. $V^{\mathcal{D}'}(m)$ are the value functions representing the downstream utility to the destination. The rest follows the RL formulation, with the next node choice probabilities given by the logit model and the probability of a MRI sequence r being the product of the node probabilities in the sequence.

5.1.5.1 Model specifications

We test four specifications of the MRI model, given by (5.3)-(5.6). We use the attributes described in Section 5.1.4. Additionally, the departure time of the trip is interacted with the travel time and the type of road attributes, in order to implicitly capture the effect of congestion on the choice between motorways or primary roads. In order to do so, we define for each individual n two socioeconomic variables, namely the OffPeak_n and the Peak_n , as dummy variables. The Peak periods take place between 7 and 9 am and 4 and 8 pm, accordingly for the morning and afternoon commuting (Figure 5.8). The RL formulation allows to incorporate this effect by defining observation dependent attributes. That is, for each observation the travel time attribute is interacted with the dummy variables denoting the departure time period.

$$v(\nu \mid m) = \beta_{\text{time}} \text{Time}(\nu) + \beta_{\text{TransferTime}} \text{TransferTime}(\nu \mid m). \quad (5.3)$$

$$\begin{aligned} v(\nu \mid m) = & \beta_{\text{time}, \text{Motor}} \text{Time}(\nu) \text{Motorway}(\nu) + \beta_{\text{time}, \text{Prim}} \text{Time}(\nu) \text{Primary}(\nu) + \\ & + \beta_{\text{TransferTime}} \text{TransferTime}(\nu \mid m). \end{aligned} \quad (5.4)$$

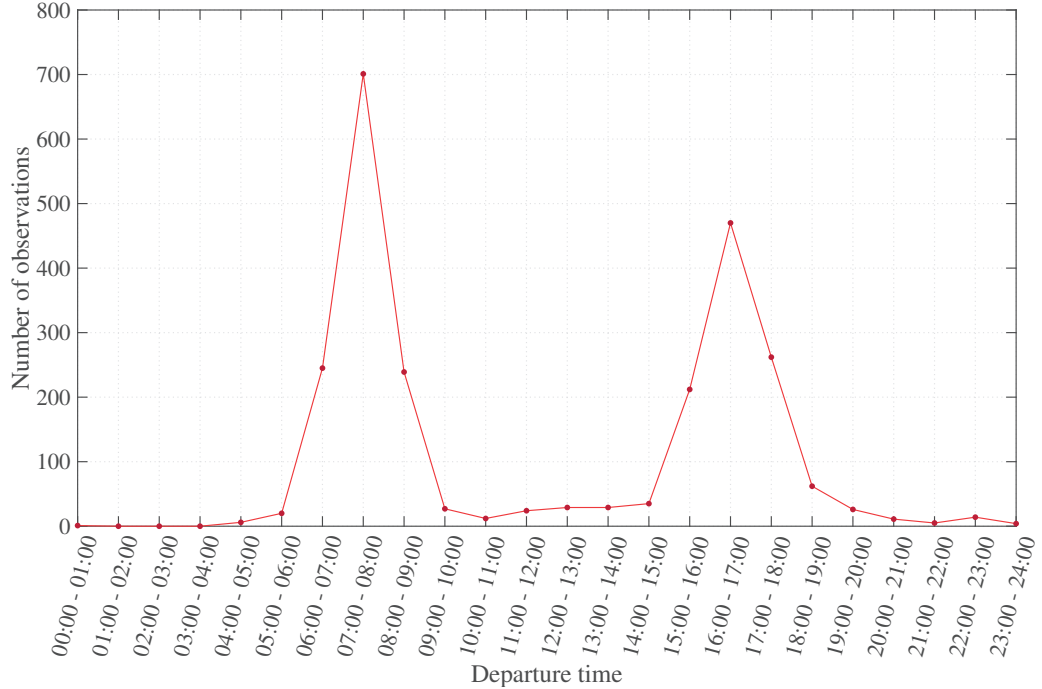


Figure 5.8: Distribution of departure time in the data sample.

$$\begin{aligned}
v(\nu \mid m) = & \beta_{time, Motor} \text{Time}(\nu) \text{Motorway}(\nu) + \beta_{time, Prim} \text{Time}(\nu) \text{Primary}(\nu) + \\
& + \beta_{TransferTime} \text{TransferTime}(\nu \mid m) + \beta_{Load} \text{CognitiveLoad}(\nu).
\end{aligned} \tag{5.5}$$

$$\begin{aligned}
v(\nu \mid m) = & \beta_{time, Motor, Off} \text{Time}(\nu) \text{Motorway}(\nu) \text{OffPeak}_n + \\
& + \beta_{time, Motor, Peak} \text{Time}(\nu) \text{Motorway}(\nu) \text{Peak}_n + \\
& + \beta_{time, Prim, Off} \text{Time}(\nu) \text{Primary}(\nu) \text{OffPeak}_n + \\
& + \beta_{time, Prim, Peak} \text{Time}(\nu) \text{Primary}(\nu) \text{Peak}_n + \\
& + \beta_{TransferTime} \text{TransferTime}(\nu \mid m) + \\
& + \beta_{Load} \text{CognitiveLoad}(\nu).
\end{aligned} \tag{5.6}$$

5.1.5.2 Measurement model

The available data is map-matched on the OpenStreetMap model of Québec city; each observation y is expressed as an ordered sequence of links. This provides the representation of the chosen alternatives at the disaggregate level. Their mapping at the aggregate level is necessary for the estimation of the MRI model. Following the same reasoning as in the previous case studies, each observation y is deterministically associated with an ordered MRI sequence r , according to the geographical span of the elements that it traverses. Recall that, at the disaggregate level, $\mathcal{G} = (\mathcal{A}, \mathcal{V})$ gives the mathematical representation of the physical network, defined in terms of a set of links \mathcal{A} and a set of nodes \mathcal{V} . At the aggregate level, each node $m \in \mathcal{M}$ is associated with the geographical span \mathcal{H}_m of the corresponding MRI, which is defined as a set of links of \mathcal{G} .

Let $\mathcal{H} = \{\mathcal{H}_1, \dots, \mathcal{H}_{|\mathcal{M}|}\}$ denote the set of the geographical spans of the MRIs, where $|\mathcal{M}|$ is the number of MRIs in the choice context and $\mathcal{H}_j \subset \mathcal{A}$, $\forall j \in \{1, \dots, |\mathcal{M}|\}$. One can then associate each y with an ordered sequence of \mathcal{H}_j and consequently with an ordered sequence of nodes $m \in \mathcal{M}$. Algorithm 2 summarizes the mapping process. The algorithm assumes that the MRIs are disjoint. The *od* of the trip is assigned to the corresponding nodes $\mathbf{o} \in \mathcal{O}$ and $\mathbf{d} \in \mathcal{D}$ and added in the sequence. An example of the mapping, from the disaggregate to the aggregate graph, is given in Figure 5.9. The dark line denotes the observed trajectory on the physical network. The labels of the MRIs that are traversed along the trip are indicated on the plot. In this example, the traveler follows the sequence: $573 \rightarrow 40;73_73 \rightarrow 73S_{Upper} \rightarrow \text{NB} \rightarrow 20W$.

5.1.6 Model application

The model is applied to compute MRI element flows using the routine proposed by Fosgerau et al. (2013a) for the computation of link flows. The output of the RL model consists in destination specific state transition probability matrices, denoted by $P^{\mathbf{d}'}$.

Algorithm 2: Mapping of an observed map-matched trajectory y to a MRI sequence r .

Input: $y = k_0, \dots, k_I$, where $k_{i+1} \in \mathcal{A}(k_i)^*$, $\forall i < I$

Input: $\mathcal{H} = \{\mathcal{H}_1, \dots, \mathcal{H}_{|\mathcal{M}|}\}$, where $\mathcal{H}_j \subset \mathcal{A}$, $\forall j \in \{1, \dots, |\mathcal{M}|\}$

Input: a function H , such that $H(m) = \mathcal{H}_m$, $\forall m \in \mathcal{M}$, where $\mathcal{H}_m \in \mathcal{H}$

Output: r as an ordered sequence of $m \in \mathcal{M}$

1 Initialize r as an empty ordered sequence

2 **for** $\forall k_i \in y$ **do**

3 **for** $\forall m \in \mathcal{M}$ **do**

4 **if** $k_i \in H(m)$ **and** $m \notin r$ **then**

5 $r = r, m$

6 **end**

7 **end**

8 **end**

* $\mathcal{A}(k_i)$ is the set of outgoing links from link k_i .



Figure 5.9: Observed trajectory and the corresponding mapping on $\mathcal{G}^{\mathcal{M}}$.

The expected flow $F(\nu)$ on element ν is the summation of the flow originating at ν and the expected incoming flow. It is given by

$$F^{d'}(\nu) = G^{d'}(\nu) + \sum_{m \in \mathcal{M}} P^{d'}(\nu | m) \cdot F^{d'}(m). \quad (5.7)$$

where $G^{d'}(\nu)$ is the demand originating at ν and ending at destination d' .

MRI element flows can be computed *for a specific destination* and multiple origins using the element transition probabilities by solving the following system of linear equations (Fosgerau et al., 2013a)

$$(I - P^T)F = G, \quad (5.8)$$

where I is the $|\mathcal{M}'| \times |\mathcal{M}'|$ identity matrix, P is the d' specific $|\mathcal{M}'| \times |\mathcal{M}'|$ element transition probability matrix, F is a $|\mathcal{M}'| \times 1$ vector representing the expected element flow given by (5.7) and G is a $|\mathcal{M}'| \times 1$ vector representing the demand $G(\nu)$. Subsequently, element flows for multiple destinations can be computed by summation over the elemental flows.

5.2 Results

In this section we estimate and apply the proposed model. We present the results of the four model specifications described in Section 5.1.5.1. A cross-validation approach is performed to evaluate the performance of the model with respect to (i) the predicted choice probabilities and (ii) the aggregate element flows $F(\nu)$.

5.2.1 Estimation results

The estimation results for the four model specifications are reported in Table 5.4. All parameter estimates are significant and have the expected signs. The transfer time parameter is stable across the model specifications. A significant improvement in the final log likelihood $\mathcal{LL}(\hat{\beta})$ is observed due to the interaction of the travel time variable with the type of the road. The inclusion of the cognitive load attribute in the specification further improves the final log likelihood.

The cognitive load factor appears to absorb part of the effect of the travel time attribute. This may be related to the fact that this attribute in the utility penalizes “complex” nodes but also itineraries with many nodes. Many nodes, i.e. longer sequences, may be associated with longer travel times. As the travel time attribute is computed for each representative segment based on the length and the maximum speed, it may not fully represent the travel time experienced by the travelers. It is then possible that part of this effect is captured by the cognitive load coefficient.

Table 5.4: Estimation results

Parameter	Model 1 value (t-test)	Model 2 value (t-test)	Model 3 value (t-test)	Model 4 value (t-test)
$\beta_{TransferTime}$	-0.56 (-72.17)	-0.58 (-78.62)	-0.54 (-72.04)	-0.54 (-72.10)
β_{time}	-1.12 (-152.25)	×	×	×
$\beta_{time,Motor}$	×	-1.24 (-148.41)	-0.50 (-28.94)	×
$\beta_{time,Prim}$	×	-0.85 (-75.39)	-0.52 (-38.37)	×
$\beta_{time,Motor,OffPeak}$	×	×	×	-0.48 (-25.60)
$\beta_{time,Motor,Peak}$	×	×	×	-0.51 (-27.78)
$\beta_{time,Prim,OffPeak}$	×	×	×	-0.54 (-25.28)
$\beta_{time,Prim,Peak}$	×	×	×	-0.51 (-32.95)
β_{Load}	×	×	-0.70 (-40.65)	-0.70 (-40.68)
# observations	2321	2321	2321	2321
# parameters	2	3	4	6
$\mathcal{LL}(\hat{\beta})$	-8145.1	-7593.6	-6935.0	-6930.7
Estimation time (min)	2.5	3.1	4.0	7.2

Finally, the interaction of the travel time, type of road and departure time variables significantly improves the final log likelihood. Individuals appear to be more sensitive to travel time on highways during peak hours in comparison to off-peak hours.

We consider Model 4 to be the best model and use it to perform further analysis. We compute the choice probabilities for each observation in the data sample. The choice probability of an observed MRI sequence r is computed as the product of the node transition probabilities in the sequence. Figure 5.10 shows the distribution of the choice probabilities for the chosen alternative. The model is characterized by many small probabilities. This is expected given the big state space of each node, and the large number of alternatives in the choice set²², and the level of aggregation in the attributes of the model. Even one low state probability in the sequence may downgrade significantly the likelihood of the observed sequence. Indeed, the distribution of the observed state choice probabilities in Figure 5.11 shows that the model performs quite well, that is the distribution of the observed state probabilities is shifted on the right side — of high probabilities.

5.2.2 Forecasting results and validation

We perform a cross validation approach. We generate 100 training samples by randomly drawing 80% of the observations. We use these samples to estimate the model. The remaining 20% of the observations of each draw are used to apply the model and evaluate its prediction capabilities.

²²We simulate a random walk on $\mathcal{G}^{\mathcal{M}}$ based on $P^{d'}$ for one od pair. Even after drawing more than 100000, the number of unique sequences kept increasing, reaching a level of ~ 2000 sequences. A null model, assigning equal probabilities to all alternatives, would forecast the probability of the chosen alternative to be in the order of $\frac{1}{2000} = 5.000e-04$. Only 6% of the observations are predicted with probability lower than $5.000e-04$ by the model.

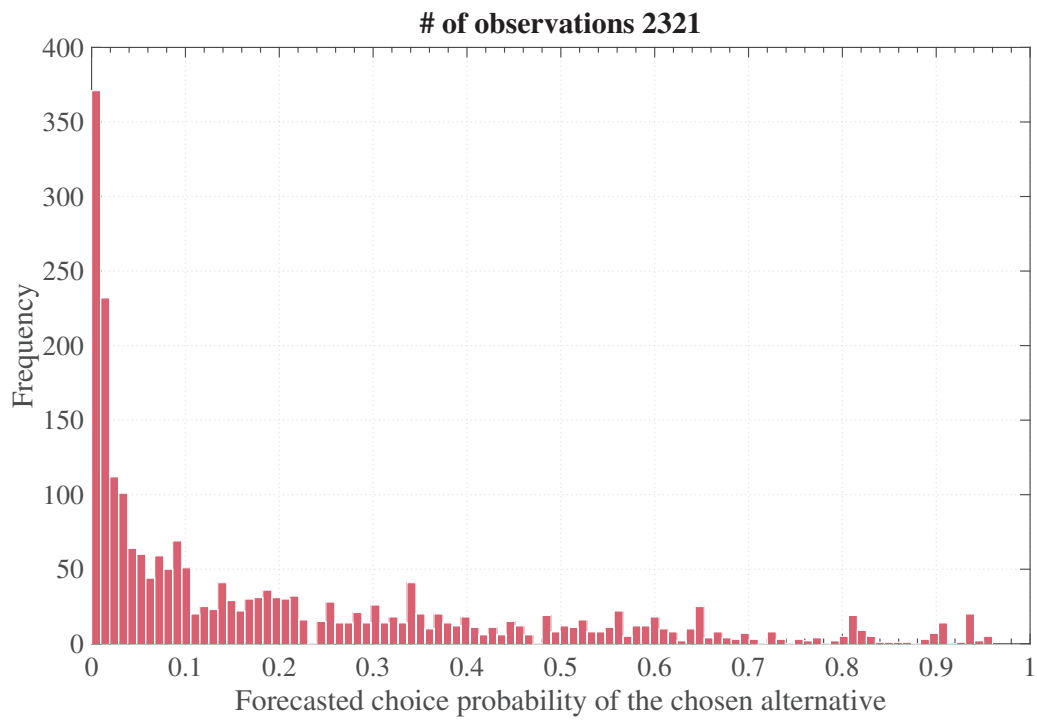


Figure 5.10: Distribution of the forecasted choice probabilities of the chosen alternative.

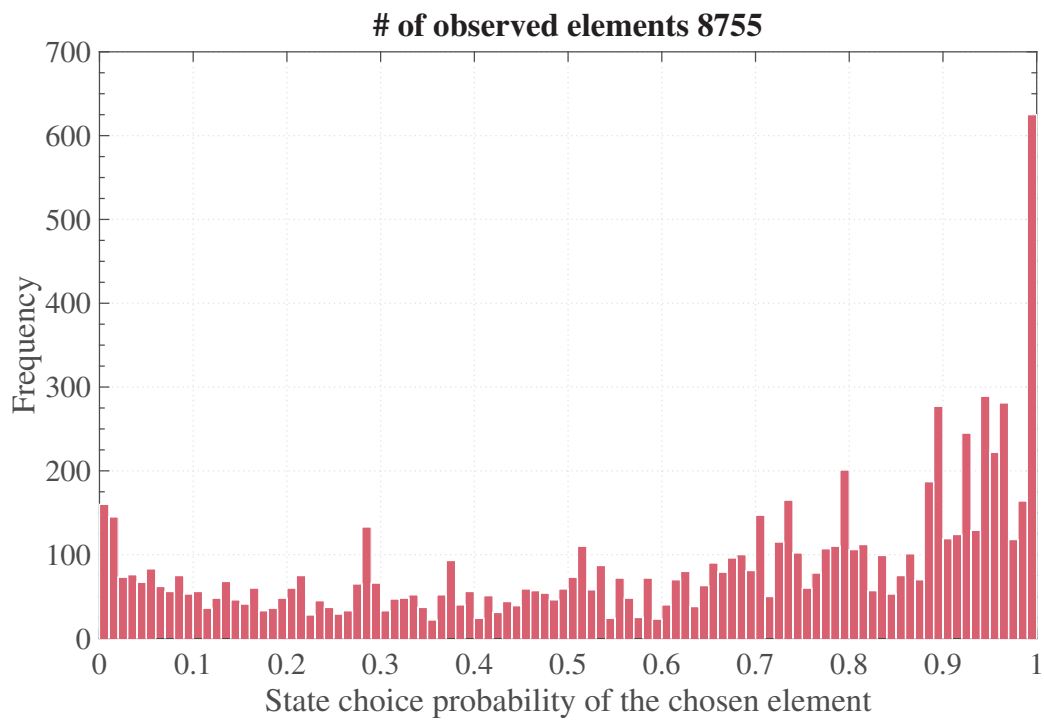


Figure 5.11: Distribution of the state (next node) choice probabilities.

Same as in Mai et al. (2015), we use the log likelihood loss to further evaluate the prediction performance of the model. That is, for each training and test sample s we use the vector of the estimated parameters to compute the errors err_s

$$err_s = \frac{1}{|S_s|} \sum_{r \in S_s} \ln P(r, \beta_s), \quad (5.9)$$

where $|S_s|$ is the size of sample s . We use Model 1, with the effect of the time variables only, as a benchmark for comparison. The average test error values for the two models are depicted in Figure 5.12 and in Figure 5.13, for the training and the test samples respectively. Model 4 is characterized by a lower test error in comparison with the benchmark model.

5.2.3 Aggregate element flows

The model is applied for the prediction of flows $F(\nu)$ on the MRI elements $m \in \mathcal{M}$. We use the observed *OD* demands in the data sample as a proxy of the real demand and apply (5.8). Figure 5.14 illustrates the observed flow on each element ν against the element flow predicted from the model by applying (5.8).

We now adapt the same cross validation approach as in the previous section, to investigate the performance of the model with respect to the prediction of element flows. The procedure observes the following steps

1. We compute the element flows based on each training sample.
2. We compute the element flows based on each test sample.
3. We sum the element flows computed from the corresponding training and the test samples to derive the flows for the full dataset.

Figure 5.15 depicts for each element (i) the observed flow and (ii) the box plots that summarize the outputs of each of the 100 samples following the procedure described above. There are instances for which the model over/ underestimates the observed flows. Despite these instances, the model is able to capture the patterns in the observed flows and for several instances it provides an approximation very close to the real flow.

5.3 Discussions

In this section, we elaborate on specific features of the MRI model for the city of Québec, that differentiate it from the one developed for Borlänge.

The two case studies for Borlänge use the representative paths approach (Section 3.1.3), for the operationalization of the utility functions of the MRI model. The selection of the

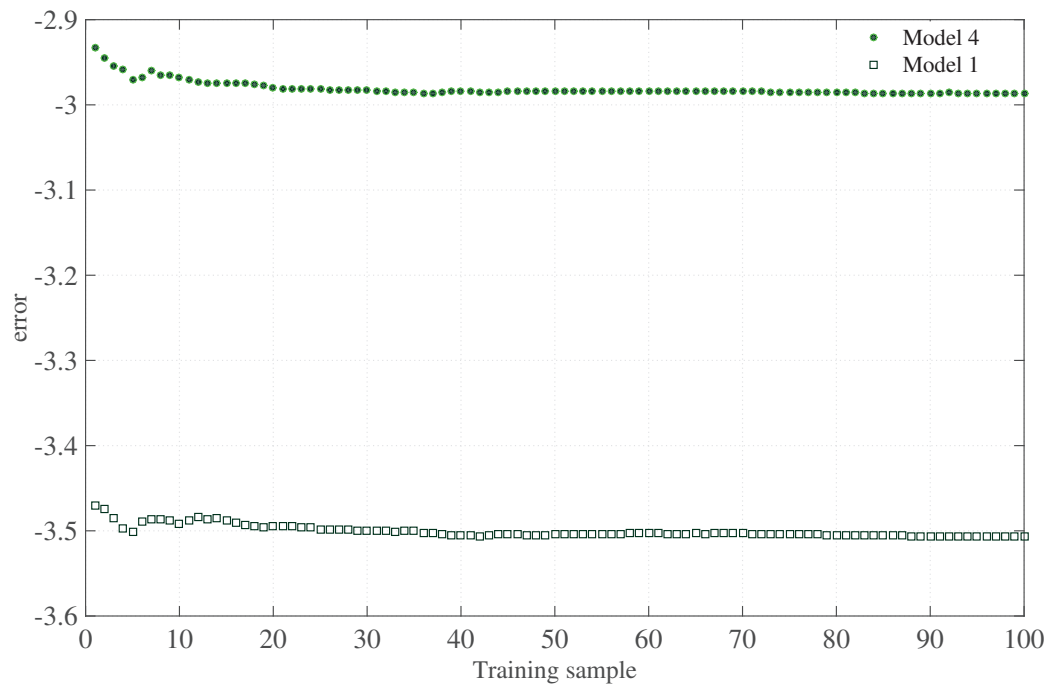


Figure 5.12: Average test error over the training samples.

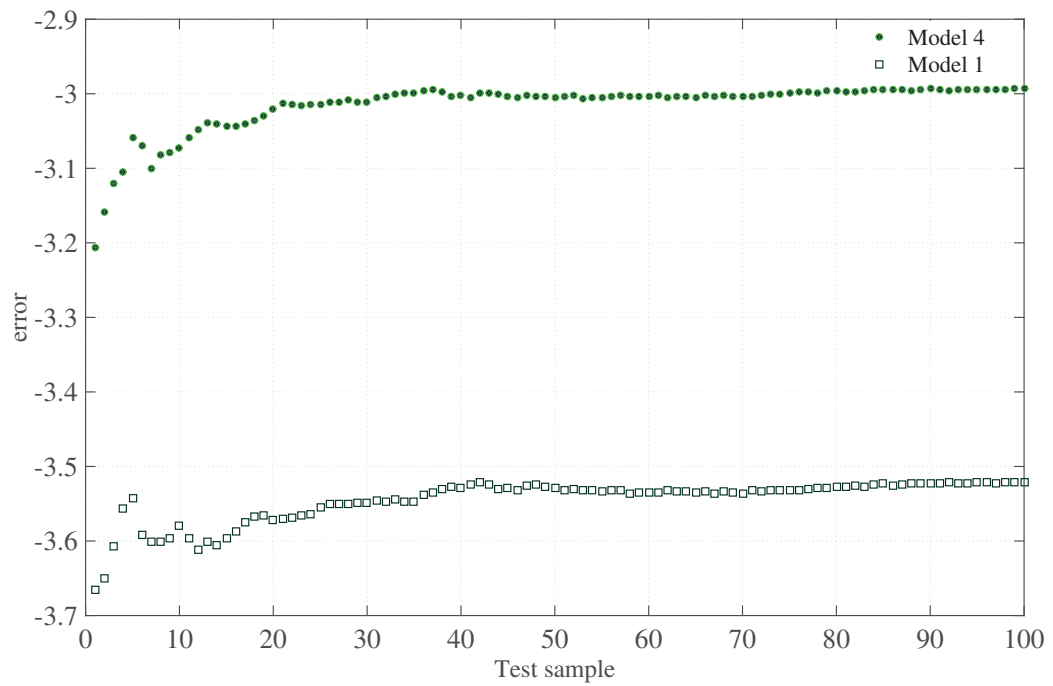


Figure 5.13: Average test error over the test samples.

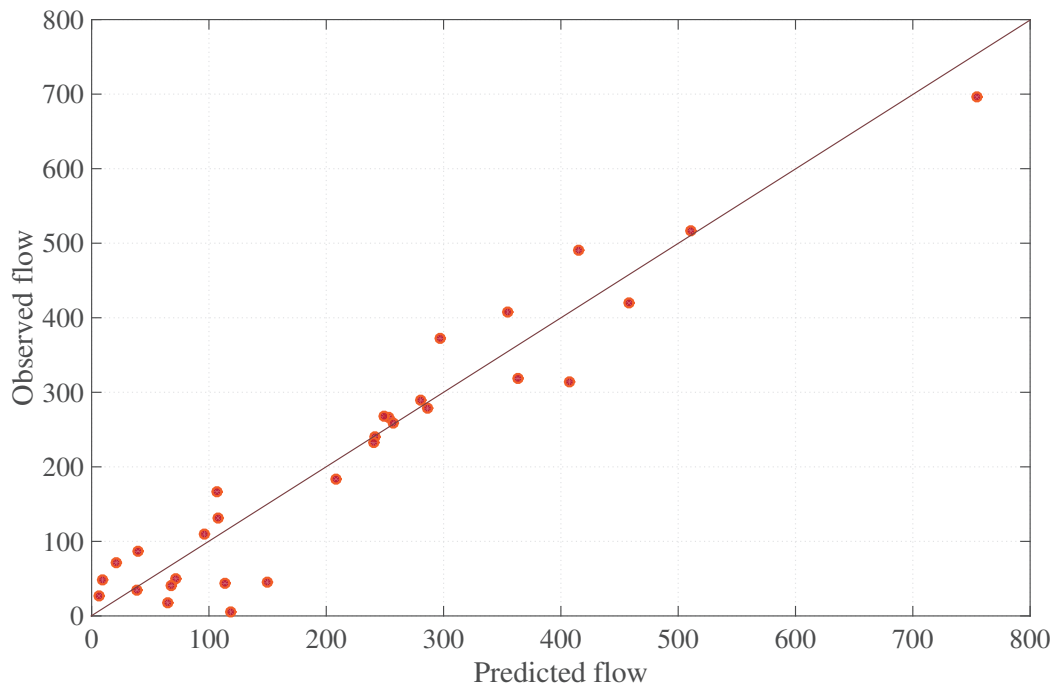


Figure 5.14: Aggregate element flows.

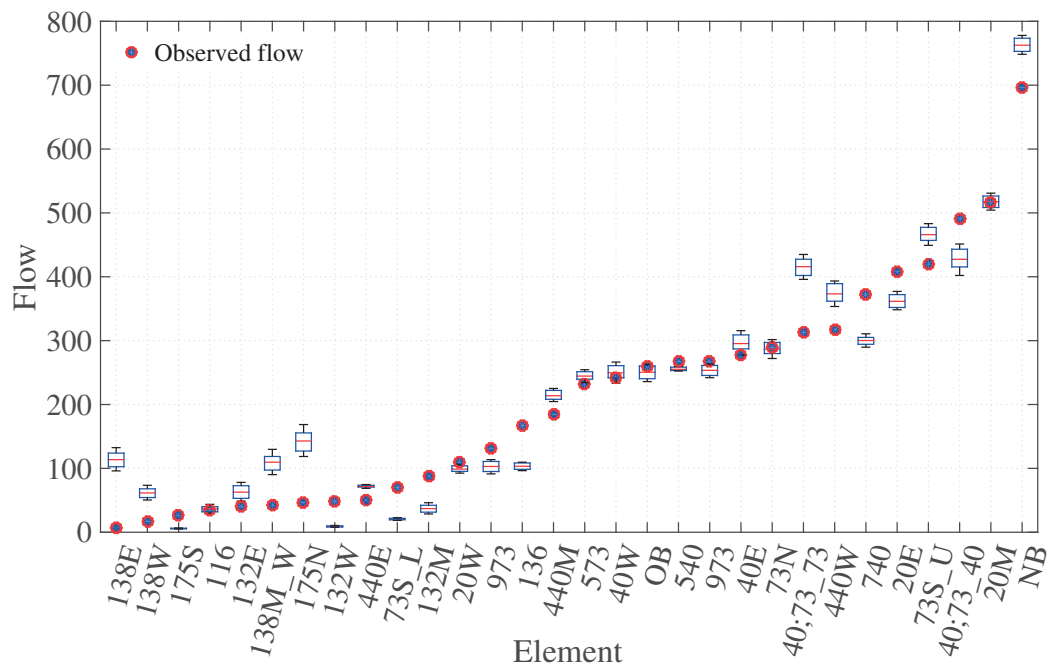


Figure 5.15: Boxplot of the aggregate element flows over the validation samples.

representative points for a large network with complex interactions and interdependencies of the elements, such as the one of Québec city, is not straightforward; it entails the complexity of the path approach²³. In order to tackle this challenge, we have investigated in the direction of the “*network-free*” approach, already identified in Section 3.1.3. We have used a “*path-free*” approach which (i) is less dependent on detailed network data, such as link travel times, and (ii) allows for low model complexity and computational times. In this context, the representative points are not used for the definition of the MRI model and the geographical span is the only important component for its operationalization. On the other hand, this approach lowers the precision in the derivation of the attributes. This is one aspect of the model that needs to be further investigated.

As discussed in Section 5.1.3.1, several of the elements identified as potential MRIs are several kilometers long, running all across the city. Associating them with a single MRI would be too restrictive, in other words, too aggregate. This is where a modeling decision regarding the level of aggregation had to be made. Dividing the segments in every existing intersection would correspond to the disaggregate approach. Instead, only the major intersections in each part of the city (N, S, E, W) have been considered for the segmentation. With respect to the *OD* zones, the idea is to keep the origins and destinations as disaggregate as possible. This is because the $o \in \mathcal{O}$ and the $d \in \mathcal{D}$ don’t constitute part of the decision process, they are merely the locations where trips are generated and absorbed. Hence, they do not affect the efficiency of the model with respect to the estimation time. Yet, some sort of aggregation has been applied in order to facilitate the computation of the transfer times using the Google Maps Distance Matrix API in Section 5.1.4.

Finally, one principal difference of the present MRI model from the ones of the two previous case studies is that explicit enumeration of alternatives is not possible. Despite the fact that the model is therefore more complex than the initial MRI models, it has a cardinal asset in comparison with the disaggregate approach. Note that the physical network of the city that falls under the area of study is composed of 17883 links. On the other hand, the \mathcal{G}^M is composed of 30 (MRIs) + 138 (*O* zones) + 138 (*D* zones) + 138 (dummy nodes) = 444 nodes, out of which only the 30 constitute part of the choice problem. Even if it is not possible to enumerate all the alternatives in \mathcal{G}^M — due to the high connectivity and the existence of loops that characterize the graph — the dimension of the problem is significantly smaller, allowing for the fast computation of the model. As reported in Table 5.4 the estimation time ranges from ~ 2 to ~ 8 minutes. Figure 5.16 shows for each trip in the data sample, the number of links in the map-matched (OpenStreetMap network model) trajectory versus the number of nodes in corresponding MRI sequence (\mathcal{G}^M). There is a remarkable reduction in the length of the description of each observation when transferred in \mathcal{G}^M .

²³This issue applies to a much lesser extent in the Borlänge case, given the small size of the city and the low complexity of the network.

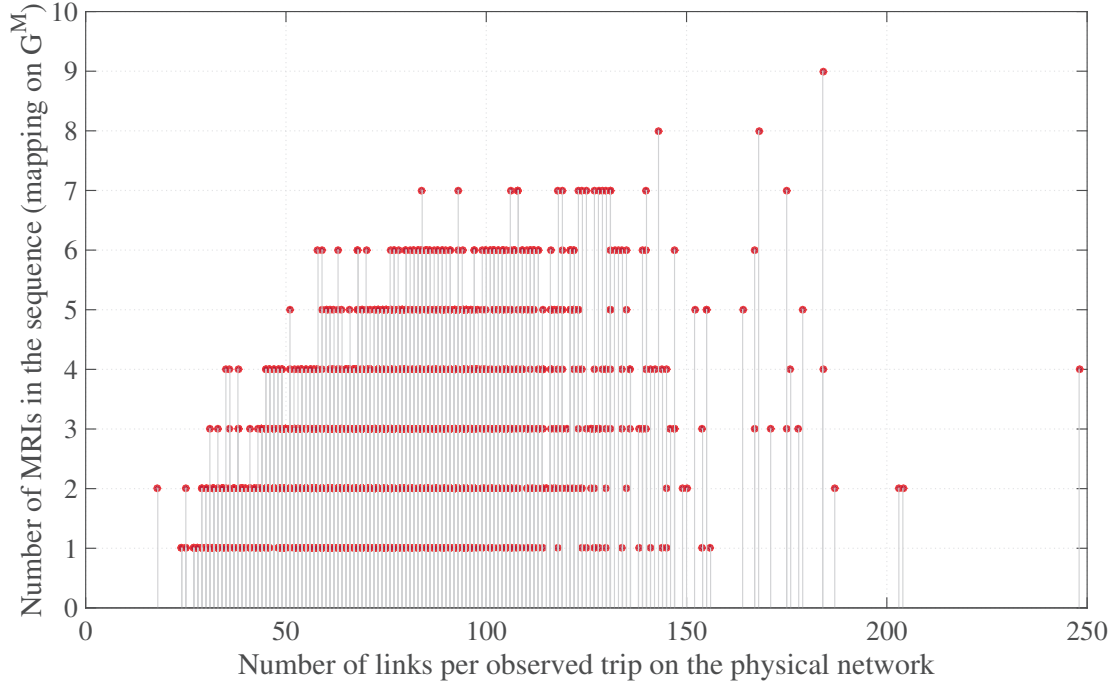


Figure 5.16: Number of links in the map-matched trajectory versus the corresponding number of nodes of the MRI sequence.

5.4 Summary

In this chapter, we combine the knowledge acquired from the previous case studies with the tools that were developed, in order to advance the framework and generalize its applicability. More specifically, we tackle the operational challenges related to the specification of the utility functions — entailed by the path-based approach — and develop a model that is not as simple as the first MRI model presented in Section 3.3, yet still of much lower structural complexity in comparison with the disaggregate approach.

To illustrate the proposed model, we use a smartphone dataset from the city of Québec, in Canada. We introduce a variable representing the complexity of a route, that is associated with the cognitive load that individuals are expected to minimize. We use the departure time of the trip and interact it with the travel time and the road type variables in order to investigate different sensitivities and implicitly capture the effect of congestion. These inclusions in the specification have significantly improved the fit of the model. In summary, the model provides reasonable results, is fast to compute and readily applied to the prediction of flows on the major segments of the city's network.

6

Conclusion

This chapter summarizes the main findings of the research (Section 6.1), discusses its scientific and practical implications (Section 6.2), and identifies aspects and features that require further investigation (Section 6.3).

6.1 Research summary

The research conducted in this thesis has shown that it is possible to circumvent the inherent complexity of route choice models. The analyst can explicitly control the trade-off between complexity and realism, and obtain operational models that are useful and applicable in practice. This has been accomplished by allowing for flexibility and creativity in the representation of the alternatives towards the aggregation of the model. The thesis presents such a modeling paradigm, within which the modeling elements are not dictated by the network model. They are rather inspired by the individuals' mental representations of the physical space. Their definition relies on a modeling decision, consistent with the level of aggregation that the analyst identifies as adequate.

The framework that we have developed contributes significantly towards the simplification of route choice models and facilitates their application to large networks. The validity and applicability of the approach has been demonstrated using two case studies. In Chapter 3, we introduce the concept of a mental representation item (MRI) as a modeling element in route choice analysis. This is the key feature of the aggregate and flexible approach that we design. Subsequently, a route is defined as a sequence of

MRIs. Each MRI is characterized by a name, a description, a geographical span and a list of representative points. The last two components allow to associate the conceptual elements with a network model and/ or a map for the operationalization of the model. In this context, we have presented the methodology for the definition of random utility models based on MRIs. We have proposed simple methods for the specification of the utility functions and have presented an importance sampling approach for the application of the model to traffic assignment.

Through the definition of the MRIs the analyst has control over the level of aggregation in the representation of the route choice alternatives. The definition of the MRIs for the first case study, for the city of Borlänge, allows to obviate the need for sampling of alternatives for the generation of the choice set. The two main features of this model are (i) the common choice set for all individuals in the data, and (ii) the assumption of representative paths for the specification of the utility functions of the alternatives of each individual. These two features have been justified by the small size of the city and the ease to identify the high level decisions of individuals, given the limited and distinct options that the network offers; that is to go through the central part of the city, to go around it or to completely avoid it. As such, the identification of the representative points for each MRI and the generation of the corresponding representative paths for each individual have been straightforward tasks for the town of Borlänge. The results, based on RP data, have demonstrated the validity of the approach.

In Chapter 4, we present the definition of a graph composed of MRI elements. Same as for the disaggregate models specified on $\mathcal{G} = (\mathcal{A}, \mathcal{V})$, the MRI graph is the basis for (i) the generation of the MRI alternatives of each individual and (ii) the application of the model. We have also shown how the MRI model tackles the correlation of alternatives. To further explore and exploit the capabilities of the proposed approach we have tested its performance in deriving disaggregate and aggregate route choice indicators, namely element (link and MRI) and route (path and MRI sequence) flows. In parallel, we have demonstrated the derivation of the same indicators using a disaggregate model. We have used the RL model as a benchmark. The results demonstrate that for the purposes of aggregate applications, the MRI model provides an adequate result that is at the same, and slightly better, level of performance in comparison with the RL model that is subjected to aggregation.

To show the capability of the approach to adapt to more complex choice contexts, we have tested the methodology in a large network and data sample (Chapter 5). We have exploited the idea of the “network-free” approach — previously discussed in Chapter 3 — for the specification of the utility functions. We have used a method that relies on the geographical span of the MRIs, instead of representative paths, and yields a simple model specification. The MRI model is integrated for estimation and application with the RL formulation. The proposed model is not as simple as the first MRI model — enumeration of alternatives is not possible in this case — yet still of much lower

complexity in comparison with the disaggregate approach, and therefore fast to estimate. In addition, thanks to the integration with the RL approach, the model is readily applied to the prediction of flows on the major segments of the city's network. The results demonstrate that the model is capable of capturing the observed patterns in the flows.

To conclude, the MRI concept is sufficiently general to capture a great deal of behaviorally meaningful aspects of route choice, yet sufficiently specific to yield operational models. The framework has to be adapted on a case by case basis. We have shown, using real case studies and RP data, that the use of simple methods leads to meaningful models that can be estimated and used in practice. If relevant data is available, the approach can handle, and more importantly simplify, model specifications such as NL, CNL and EC models tackling the correlation of alternatives, and mixed logit models tackling trade-offs between major variables, i.e. length and time, and taste heterogeneity. Finally, the approach may be of great use for (i) applications without an existing or an inadequate detailed network model and (ii) large scale applications, such as the European Transport Model²⁴ (TransTools) or national models, where a detailed network representation of cities is not realistic.

The framework opens the door to more modeling opportunities and has important practical implications. We discuss about these extensions in the following Section.

6.2 Theoretical and practical implications

In comparison with the state of the art route choice models, the MRI framework is of greater generality. For instance, it is possible to define a MRI model that is independent from a network model. Along the same lines, the framework does not require detailed route choice observations. The data may be expressed in terms of locations, areas, major segments. Therefore, the analysis is not constrained by the availability of detailed data.

The integration of the MRI approach with the RL model has a great potential to simplify the consolidation of route choice models within simulation frameworks. As an example, this integration maybe be particularly useful for the dynamic traffic assignment component of a traffic simulator (see e.g. Yildirimoglu et al., 2015), by allowing for significant memory savings and a realistic representation of the regions. In this context, macroscopic traffic assignment that is currently researched (see Batista et al., 2016) may benefit to from the tractability of the MRI approach.

The concept of MRI and its attributes is extremely relevant to the provision of travel information and route guidance. As complexity and congestion in today's metropolises keep increasing, the provision of information, in a manner that can easily be handled by the individuals and allow them to reduce the uncertainty about their travel, is essential. Helbing (2004) discusses the potential of optimal guidance for traffic optimization. Using

²⁴<http://energy.jrc.ec.europa.eu/transtools/index.html>

decision experiments on day-to-day route choice, he proposes guidance strategies to reach user equilibrium based on empirical transition and compliance probabilities. His work is employed by (Stark et al., 2008) in an experimental study that investigates cooperation strategies in route choice. The MRI representation of route choices would exactly fit the implementation of such strategies in practice.

Finally, the MRI approach is particularly relevant and can be extended to pedestrian route/ activity choice. Similar to the case of vehicular traffic, the MRI model can support pedestrian simulation models for major hubs that are currently researched (see e.g. Molyneaux et al., 2017).

6.3 Future research directions

In this Section we discuss specific aspects of the MRI approach that can be further investigated. Starting by the *definition* of the MRI elements, an interesting direction of research would be to investigate *data-driven* approaches in two different dimensions, i.e.

1. the *traditional approach*: to conduct specific surveys where travelers describe their routes and the perception of the performance of the identified alternatives;
2. the *algorithmic approach*: to automate the identification of MRIs using data mining or machine learning techniques, such as clustering analysis;

and compare the consistency of their output with the elements identified by the analyst. The extension to new case studies would then be of interest.

With respect to the *specification* of the model an important aspect concerns the *attributes in the utility functions*. In Chapter 5 we have tackled the operational challenges that the representative paths approach entails, by defining aggregate attributes for the MRI elements. The proposed “network-free” approach allows the model to be operational even under low data availability, yet lowers the precision in the derivation of the attributes of the alternatives. This has a direct impact on the model’s performance. A higher precision in the derived attributes would justify the extension of the representative paths approach. Keeping in mind that

1. the selection of the representative points for a large network, with complex interactions and interdependencies of the elements, is not straightforward, and that
2. the model parameters may be sensitive to the selection of these points,

simulation techniques, such as Monte-Carlo, could be investigated to test the stability of the estimates’ across various instances of representative point configurations. A comparison of the model’s performance using the “network-free” and the simulation-based-representative-paths approach could then provide further insights into the use of a specific technique, once again, depending on the needs of the application and the data

availability.

Finally, a future research direction with respect to the *application* of the model may concern its use for traffic assignment. More advanced specifications of the assignment model presented in Appendix A should be explored and tested on the basis of a detailed demand input — i.e. origin-destination matrix. In addition, the investigation of statistical tools, such as bootstrapping, to assess the effect of sampling on the results of the assignment at the disaggregate level, would be an asset.



Specification of the assignment model

This appendix presents a simple example for the specification of the assignment model defined by (3.2) in Section 3.1.5.

Let s_v^r be a real number representing the consistency of node v with MRI r . The determination of s_v^r reflects the definition of the MRIs on the basis of the geographical span and the representative points. In particular, if a node is contained in the MRI's geographical span it has a consistency equal to 1, and 0 otherwise. The nodes corresponding to the representative points of a MRI may receive a consistency value higher than 1.

Each path p consists in a sequence of nodes. We can then compute the score $s_p^r = \sum_{v \in p} s_v^r$ of each path for every MRI $r \in \mathcal{C}_n$, where $\sum_{v \in p} \cdot$ represents the sum over all nodes v contained in path p . s_p^r denotes the consistency of a path p with a MRI r .

The path choice probability from the universal path choice set given a MRI r is then, apart from normalization, specified as

$$P(p \mid r) \sim \exp \left(\kappa \frac{s_p^r}{\sum_{j \in \mathcal{C}_n} s_p^j} + \lambda t_p \right) \quad (\text{A.1})$$

where $\sum_{j \in \mathcal{C}_n} \cdot$ spans over all MRIs in \mathcal{C}_n , t_p is the travel time on path p , and $\kappa > 0$, $\lambda < 0$ are real-valued coefficients. The consistency favors paths that have relatively high node overlap with MRI r . It represents, at the path level, the individual's operational decisions leading at the link-by-link level to an implementation of MRI r . The second

factor favors paths that are faster. Some cost-dependency of this type is needed because otherwise it becomes more important to stay in the MRI than to reach the destination.

Now, the link choice probabilities defined by (3.2) need to be computed. The number of paths with nonzero probability of being selected given that MRI r was chosen may be too high to be enumerated and used in the traffic assignment context. We propose to use the Metropolis-Hastings Algorithm of Flötteröd and Bierlaire (2013) to draw, for each MRI r , a large number of Q_r paths from the unnormalized distribution (A.1). Letting p_r^q be the q th path drawn for MRI r , $P(a | r)$ is then approximated by

$$\hat{P}(a | r) = \frac{1}{Q_r} \sum_{q=1}^{Q_r} \mathbf{1}(a \in p_r^q). \quad (\text{A.2})$$

This is, for a given MRI r , the ratio of the number of times link a is contained in a sampled path divided by the total number of sampled paths. The MRI-unconditional link probabilities (3.2) are then approximated through

$$\hat{Prob}(a | C_n, x_{rn}, z_n) = \sum_{r \in \mathcal{C}_n} \hat{P}(a | r) \cdot P(r | C_n, x_{rn}, z_n). \quad (\text{A.3})$$

B

Description of a work trip in Athens

This appendix provides a qualitative example in support of the MRI assumption. The case study area is located in Athens, Greece. Athens is a big city and its transportation network is very dense and complicated. The characteristics of the driver are:

- Male;
- 54 years old;
- Familiar with the route as he has been doing this trip for more than 20 years;
- Experienced driver with very good knowledge of the network (living in Athens all his life and driving from the age of 18);
- He either uses a motorcycle or a car for his transportation.

Figure B1 depicts all the relevant components that we discuss hereafter. We asked the driver to describe his regular route from home to work. He said that there are two alternatives: either to go through the *city center* (red-shaded area) or to take the *peripheral* road (green polyline).

After asking the driver to give more details regarding the two itineraries, he described different options associated to each of these two alternatives. Given that he chooses to go through the peripheral he has several ways to reach it: (i) neighbourhood *Y* and then neighbourhood *V*, or (ii) neighbourhood *I*. Continuing describing his route, he stated that after exiting the peripheral and a while before reaching the destination he has another two options: (i) either through a main arterial (extension of the green line),

or (ii) through cutting through neighbourhood P (blue line). The name of the peripheral road (Katechaki) came up several times during the description as it is associated with all of these itineraries.

When he chooses to go through the city centre, he regularly follows one specific itinerary along main arterials. He only pointed one minor deviation to a minor street in order to avoid a traffic light in cases of congestion. After being explicitly asked, the driver mentioned that he adjusts his itinerary in the level of minor streets, mainly due to bottlenecks that he may encounter. In this case though, he did not refer to the exact options.

Being asked what defines his choice, he said that it depends on his mood and on the current traffic conditions. He prefers to go through the city centre as it is more pleasant for him than the peripheral, that he called monotonous. The city centre alternative is also the shorter option with respect to kilometres, but it is usually more congested in the morning. For this reason he usually takes the peripheral road on his way to work. On the other hand, on his way back home in the evening he always chooses to go through the centre as it is not congested during this time of day. It is worth noticing that apart from abstraction in the representation of the possible alternatives, there is abstraction in the association of attributes to them. It is highlighted by the use of adjectives, like fast, pleasant etc.

While talking, the respondent made use of major streets' names and neighbourhoods as described above, but he also referred to schools in one of the neighbourhoods, park in another, squares, an ancient stadium which is a landmark in Athens, a cemetery (the first and biggest of the city), several churches that are located along these routes, a cinema, the tower of Athens, and also home location of friends and relatives that signify reference points (anchor points and landmarks) along the way. When asked if locations such as the stadium play any role in his choice of route the answer was: "*No, I just meet them on my way*". These elements facilitate the description of his route. They are used to improve communication and understanding, and they characterize the alternative routes. It should be underlined that there is a distinction between these reference points and landmarks along the way and the representations that consist alternatives. The former though can be used to construct explanatory variables. For instance, areas with increased number of landmarks and points of interest might be more attractive, or more familiar, to travelers. They may also serve as representative points for the definition of the MRIs that we discuss in this paper.



Figure B1: Sketch of the described route alternatives.



Additional figures

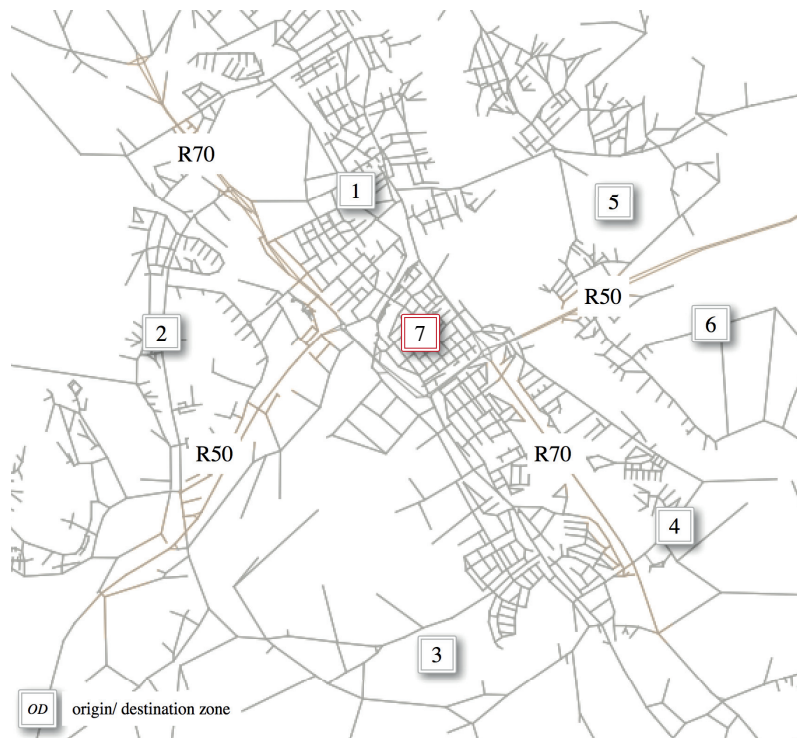


Figure C1: The *OD* zones in Borlänge.



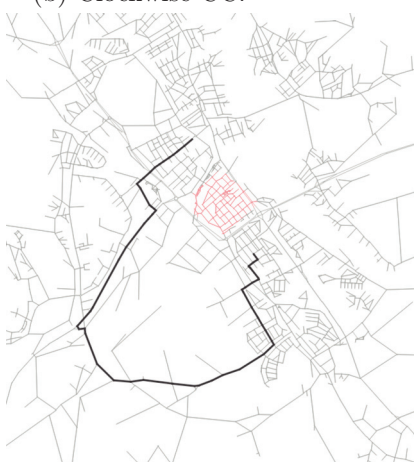
(a) Through CC.



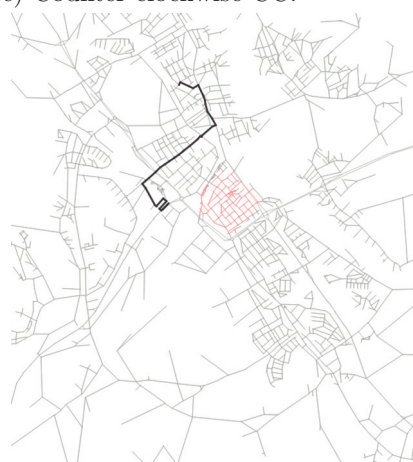
(b) Clockwise CC.



(c) Counter-clockwise CC.



(d) Avoid CC.



(e) Avoid CC.

Figure C2: Characteristic examples of observed trajectories in Borlänge.

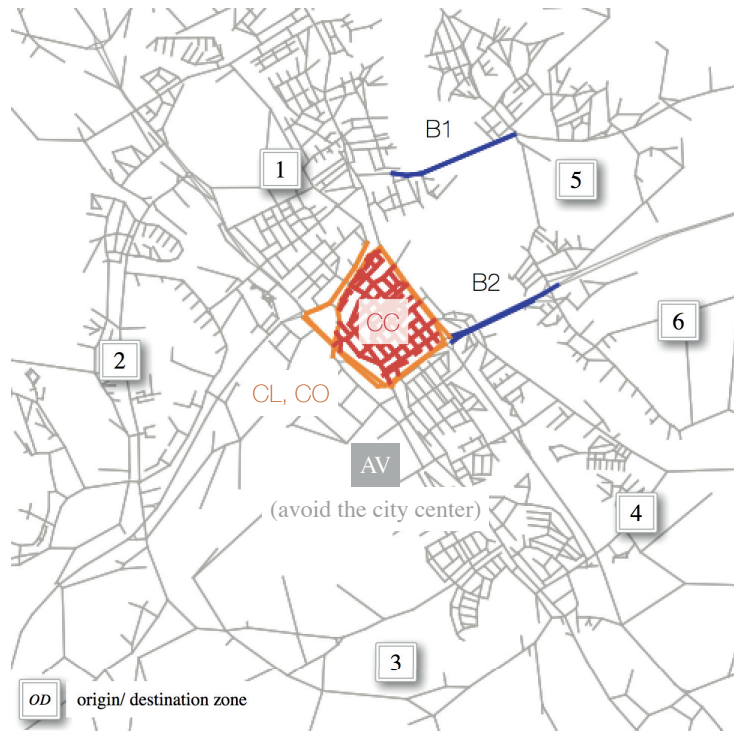


Figure C3: The geographical span of the MRIs in Borlänge.

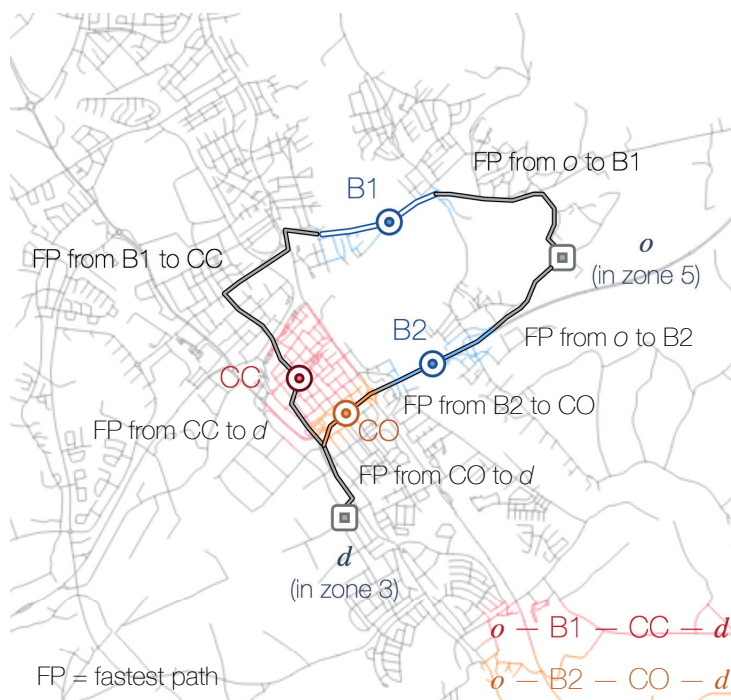


Figure C4: Example of MRI sequences in Borlänge.



Figure C5: The *OD* zones in Québec city.

D

Additional tables

Table D1: List of alternatives of the MRI model (Borlänge)

a/a	MRI choice set	<i>OD</i> pairs
1	{CC, CL, CO, AV}	[12, 13, 14, 21, 23, 24, 31, 32, 34, 41, 42, 43]
2	{CC, CL, CO, AV} ¹ → {B1, B2} ²	[15, 25, 35, 45, 16, 26, 36, 46]
3	{B1, B2} ¹ → {CC, CL, CO, AV} ²	[51, 52, 53, 54, 61, 62, 63, 64]
4	{B1, B2}	[57, 67, 75, 76]

{MRI1, MRI2}¹: first step decision, {MRI3, MRI4}²: second step decision

Table D2: Transfer times (non zero) between MRI pairs (Québec)

from MRI	to MRI	transfer time [min]
73S_Upper	540	5
73S_Upper	175N	5
73S_Upper	136	5
440E	440M	10
440E	973	5
440E	175N	10
440E	136	10
440M	440E	10
440M	973	10
740	175N	5
540	73S_Upper	5
540	175N	5
540	138W	5
540	136	5
973	440E	5
973	440M	10
973	175N	10
973	136	15
175N	73S_Upper	5
175N	440E	10
175N	740	5
175N	540	5
175N	973	10
138W	540	5
136	73S_Upper	5
136	440E	10
136	540	5
136	973	15
NB	132M	5
NB	132W	5
NB	175S	5
NB	116	5
OB	20M	5
OB	20W	5
OB	132M	5
OB	132W	5
OB	73S_Lower	10
OB	175S	10

continued ...

... continued

from MRI	to MRI	transfer time [min]
OB	116	10
20E	132M	5
20M	OB	5
20M	20W	5
20M	132E	5
20M	132W	10
20M	73S_Lower	5
20M	175S	5
20M	116	10
20W	OB	5
20W	20M	5
20W	132M	10
20W	73S_Lower	5
20W	175S	5
132E	20M	5
132M	NB	5
132M	OB	5
132M	20E	5
132M	20W	10
132M	132W	10
132M	73S_Lower	5
132M	175S	5
132M	116	10
132W	NB	5
132W	OB	5
132W	20M	10
132W	132M	10
132W	73S_Lower	5
132W	175S	10
73S_Lower	OB	10
73S_Lower	20M	5
73S_Lower	20W	5
73S_Lower	132M	5
73S_Lower	132W	5
73S_Lower	175S	5
73S_Lower	116	5
175S	NB	5
175S	OB	10
175S	20M	5

continued ...

Appendix D. Additional tables

...continued

from MRI	to MRI	transfer time [min]
175S	20W	5
175S	132M	5
175S	132W	10
175S	73S_Lower	5
175S	116	10
116	NB	5
116	OB	10
116	20M	10
116	132M	10
116	73S_Lower	5
116	175S	10

Bibliography

- Abdel-Aty, M. a., Kitamura, R., and Jovanis, P. P. (1997). Using stated preference data for studying the effect of advanced traffic information on drivers' route choice. *Transportation Research Part C: Emerging Technologies*, 5(1):39–50.
- Akamatsu, T. (1996). Cyclic flows, markov process and stochastic traffic assignment. *Transportation Research Part B: Methodological*, 30(5):369–386.
- Arentze, T. a. and Timmermans, H. J. P. (2005). Representing mental maps and cognitive learning in micro-simulation models of activity-travel choice dynamics. *Transportation*, 32(4):321–340.
- Axhausen, K. W., Schönfelder, S., Wolf, J., and Oliveira, M. (2003). 80 weeks of GPS-traces: Approaches to enriching the trip information. *Transportation Research Record*, 1870:46–54.
- Azevedo, J., Santos Costa, M., Silvestre Madeira, J., and Vieira Martins, E. (1993). An algorithm for the ranking of shortest paths. *European Journal of Operational Research*, 69(1):97–106.
- Baillon, J.-B. and Cominetti, R. (2008). Markovian traffic equilibrium. *Mathematical Programming*, 111(1–2):33–56.
- Batista, S., Mariotte, G., and Leclercq, L. (2016). The physics of traffic in urban areas at a macroscopic scale. In *FISICA 2016, 20 Conferencia Nacional de Fisica*, page 15, Braga, Portugal.
- Bekhor, S., Ben-akiva, M. E., and Ramming, M. S. (2002). Adaptation of Logit Kernel to Route Choice Situation. *Transportation Research Record: Journal of the Transportation Research Board*, pages 78–85.
- Bekhor, S., Ben-Akiva, M. E., and Ramming, S. M. (2006). Evaluation of choice set generation algorithms for route choice models. *Annals of Operations Research*, 144(1):235–247.
- Bellman, R. (1957). *Dynamic Programming*. Princeton University Press, Princeton, NJ, USA, 1 edition.

- Ben-Akiva, M., Bergman, M. J., Daly, A., and Ramaswamy, V. (1984). Modeling interurban route choice behavior. In *Proceedings of the 9th International Symposium on Transportation and Traffic Theory*, pages 299–330, Utrecht, The Netherlands.
- Ben-Akiva, M. and Bierlaire, M. (1999). Discrete choice methods and their applications to short-term travel decisions. In Hall, R., editor, *Handbook of Transportation Science, Operations Research and Management Science*, pages 5–34. Kluwer. ISBN:0-7923-8587-X.
- Ben-Akiva, M. and Bierlaire, M. (2003). Discrete choice models with applications to departure time and route choice. In Hall, R., editor, *Handbook of Transportation Science, 2nd edition*, Operations Research and Management Science, pages 7–38. Kluwer. ISBN:1-4020-7246-5.
- Ben-Akiva, M. and Lerman, S. R. (1985). *Discrete Choice Analysis: Theory and Application to Travel Demand*. MIT Press Series in Transportation Studies. The MIT Press, Cambridge, MA.
- Bierlaire, M. (2003). BIOGEME: A free package for the estimation of discrete choice models. In *3rd Swiss Transportation Research Conference*, Ascona, Switzerland.
- Bierlaire, M. (2006). A theoretical analysis of the cross-nested logit model. *Annals of Operations Research*, 144(1):287–300.
- Bierlaire, M., Chen, J., and Newman, J. P. (2013). A probabilistic map matching method for smartphone GPS data. *Transportation Research Part C: Emerging Technologies*, 26:78–98.
- Bierlaire, M. and Frejinger, E. (2008). Route choice modeling with network-free data. *Transportation Research Part C: Emerging Technologies*, 16(2):187–198.
- Boarnet, M., Kim, E., and Parkany, E. (1998). Modeling Route Choice Behavior: How Relevant Is the Composition of Choice Set? *Transportation Research Record: Journal of the Transportation Research Board*, 1634:93–99.
- Bolduc, D. and Ben-Akiva, M. (1991). A multinomial probit formulation for large choice sets. In *Proceedings of the 6th International Conference on Travel Behaviour*, volume 2, pages 243–258.
- Bovy, P. and Fiorenzo Catalano, S. (2007). Stochastic route choice set generation: behavioral and probabilistic foundations. *Transportmetrica*, 3(3):173–189.
- Bovy, P. H. L. and Stern, E. (1990). *Route Choice: Wayfinding in Transport Networks*. Studies in Industrial Organization, Kluwer Academic Publishers.
- Broach, J., Dill, J., and Gliebe, J. (2012). Where do cyclists ride? a route choice model developed with revealed preference gps data. *Transportation Research Part A: Policy and Practice*, pages 1–11.

- Büchner, S. J. (2011). *Environmental Structure, Mental Representations and Path Choice Heuristics-Information Processing in Wayfinding*. PhD thesis, Albert-Ludwigs-Universität Freiburg.
- Cascetta, E., Nuzzolo, A., Russo, F., and Vitetta, A. (1996). A modified logit route choice model overcoming path overlapping problems: specification and some calibration results for interurban networks. In *Proceedings of the Thirteenth International Symposium on Transportation and Traffic Theory*, pages 697–711, Lyon, France.
- Chase, W. G. (1983). *D. A. Rogers & J. A. Sloboda (Eds.), The acquisition of symbolic skills*, chapter Spatial representations of taxi drivers, pages 391–405. New York: Plenum.
- Chen, J. and Bierlaire, M. (2013). Probabilistic multimodal map-matching with rich smartphone data. *Journal of Intelligent Transportation Systems*.
- Cottrill, C., Pereira, F. C., Zhao, F., Dias, I., Lim, H. B., Ben-Akiva, M., and Zegras, C. (2013). Future mobility survey: Experience in developing a smart-phone-based travel survey in singapore. *Transportation Research Record: Journal of the Transportation Research Board*.
- Couclelis, H., Golledge, R. G., Gale, N., and Tobler, W. (1987). Exploring the anchor point hypothesis of spatial cognition. *Journal of Environmental Psychology*, 7:99–122.
- Daganzo, C. F. and Sheffi, Y. (1977). On stochastic models of traffic assignment. *Transportation Science*, 11:253–274.
- de la Barra, T., Perez, B., and Anez, J. (1993). Multidimensional path search and assignment. In *Proceedings of the 21st PTRC Summer Annual Meeting*, Manchester, England.
- Dial, R. B. (1971). A probabilistic multipath traffic assignment model which obviates path enumeration. *Transportation Research*, 5(2):83 – 111.
- Dijkstra, E. W. (1959). A note on two problems in connexion with graphs. *Numer. Math.*, 1(1):269–271.
- Eagle, N. and Pentland, A. (2006). Reality mining: sensing complex social systems. *Journal Personal and Ubiquitous Computing*, 10:255 – 268.
- Flötteröd, G. and Bierlaire, M. (2013). Metropolis-Hastings sampling of paths. *Transportation Research Part B: Methodological*, 48:53–66.
- Fosgerau, M., Frejinger, E., and Karlstrom, A. (2013a). A link based network route choice model with unrestricted choice set. *Transportation Research Part B: Methodological*, 56(0):70 – 80.

- Fosgerau, M., McFadden, D., and Bierlaire, M. (2013b). Choice probability generating functions. *Journal of Choice Modelling*, 8:1–18.
- Frank, L. D., Sallis, J. F., Saelens, B. E., Leary, L., Cain, K., Conway, T. L., and Hess, P. M. (2009). The development of a walkability index: application to the Neighborhood Quality of Life Study. *British Journal of Sports Medicine*, 44:924–933.
- Frejinger, E. (2008). *Route choice analysis: data, models, algorithms and applications*. PhD thesis, Ecole Polytechnique Fédérale de Lausanne, Switzerland.
- Frejinger, E. and Bierlaire, M. (2007). Capturing correlation with subnetworks in route choice models. *Transportation Research Part B: Methodological*, 41(3):363–378.
- Frejinger, E., Bierlaire, M., and Ben-Akiva, M. (2009). Sampling of alternatives for route choice modeling. *Transportation Research Part B: Methodological*, 43(10):984–994.
- Friedrich, M., Hofsaess, I., and Wekeck, S. (2001). Timetable-based transit assignment using branch and bound techniques. *Transportation Research Record: Journal of the Transportation Research Board*, pages 100–107.
- Gallotti, R. and Barthelemy, M. (2014). Anatomy and efficiency of urban multimodal mobility. *Nature*, 4:6911.
- Gallotti, R., Porter, M. A., and Barthelemy, M. (2016). Lost in transportation: Information measures and cognitive limits in multilayer navigation. *Science Advances*, 2(2).
- Golledge, R. G. (1999). *Wayfinding Behavior: Cognitive Mapping and Other Spatial Processes*. Johns Hopkins University Press, Baltimore, MD.
- Golledge, R. G. and Gärling, T. (2003). Cognitive Maps and Urban Travel. *University of California Transportation Center*.
- González, M. C., Hidalgo, C. a., and Barabási, A.-L. (2008). Understanding individual human mobility patterns. *Nature*, 453(7196):779–82.
- Guevara, C. A. and Ben-Akiva, M. E. (2013). Sampling of alternatives in multivariate extreme value models. *Transportation Research Part B: Methodological*, 48(0):31 – 52.
- Halldórsdóttir, K., Rieser-Schussler, N., Axhausen, K. W., Nielsen, O. A., and Prato, C. G. (2014). Efficiency of choice set generation methods for bicycle routes. *European journal of transport and infrastructure research*, 14(4):332–348.
- Hannes, E., Janssens, D., and Wets, G. (2008). Destination Choice in Daily Activity Travel: Mental Map’s Repertoire. *Transportation Research Record: Journal of the Transportation Research Board*, 2054:20–27.

- Hato, E. and Asakura, Y. (2001). New approach for collection of activity diary using mobile communication systems. In *Proceedings of the 80h Annual Meeting of the Transportation Research Board*.
- Helbing, D. (2004). Dynamic decision behavior and optimal guidance through information services: Models and experiments. In Schreckenberg, M. and Selten, R., editors, *HUMAN BEHAVIOUR AND TRAFFIC NETWORKS*, pages 47–95. Springer.
- Hoogendoorn-Lanser, S. (2005). *Modelling Travel Behavior in Multi-modal Networks*. PhD thesis, Technology University of Delft.
- Jan, O., Horowitz, A. J., and Peng, Z.-R. (2000). Using gps data to understand variations in path choice. *Transportation Research Record*, pages 37–44.
- Jenelius, E. and Koutsopoulos, H. N. (2013). Travel time estimation for urban road networks using low frequency probe vehicle data. *Transportation Research Part B: Methodological*, 53:64–81.
- Lai, X. and Bierlaire, M. (2015). Specification of the cross-nested logit model with sampling of alternatives for route choice models. *Transportation Research Part B: Methodological*, 80:220 – 234.
- Li, H., Guensler, R., and Ogle, J. (2005). Analysis of Morning Commute Route Choice Patterns Using Global Positioning System-Based Vehicle Activity Data. *Transportation Research Record: Journal of the Transportation Research Board*, 1926:162–170.
- Lynch, K. (1960). *The Image of the City*. M.A.: MIT Press, Cambridge.
- Mahmassani, H., Joseph, T., and Jou, R.-C. (1993). Survey approach for study of urban commuter choice dynamics. *Transportation research record*, (1412):80–89.
- Mai, T. (2016). A method of integrating correlation structures for a generalized recursive route choice model. *Transportation Research Part B: Methodological*, 93, Part A:146 – 161.
- Mai, T., Bastin, F., and Frejinger, E. (2016). A decomposition method for estimating complex recursive logit based route choice models. *EURO Journal on Transportation and Logistics*, pages 1 – 23.
- Mai, T., Fosgerau, M., and Frejinger, E. (2015). A nested recursive logit model for route choice analysis. *Transportation Research Part B: Methodological*, 75:100 – 112.
- Mai, T., Frejinger, E., Fosgerau, M., and Bastin, F. (2017). A dynamic programming approach for quickly estimating large network-based {MEV} models. *Transportation Research Part B: Methodological*, 98:179 – 197.

- Manley, E., Addison, J., and Cheng, T. (2015a). Shortest path or anchor-based route choice: a large-scale empirical analysis of minicab routing in london. *Journal of Transport Geography*, 43:123 – 139.
- Manley, E., Orr, S., and Cheng, T. (2015b). A heuristic model of bounded route choice in urban areas. *Transportation Research Part C: Emerging Technologies*, 56:195 – 209.
- Marchal, F. (2015). TrackMatching.
- McFadden, D. L. (1978). Modelling the choice of residential location. In et al., A. K., editor, *Spatial Interaction Theory and Residential Location*, pages 75–96. North Holland, Amsterdam, The Netherlands.
- Miranda-Moreno, L. F., Chung, C., Amyot, D., and Chapon, H. (2015). A System for Collecting and Mapping Traffic Congestion in a Network Using GPS Smartphones from Regular Drivers. In *Proceedings of the 94th Annual Meeting of the Transportation Research Board*.
- Molyneaux, N., Scarinci, R., and Bierlaire, M. (2017). Pedestrian management strategies for improving flow dynamics in transportation hubs. In *17th Swiss Transportation Research Conference*, Ascona, Switzerland.
- Murakami, E., Bricka, S., Rodriguez, S., Hathaway, K., Hoffman, C., Lawe, S., Cottrill, C., Whitmore, R., and Kizakevich, P. (2012). Using smartphones for travel behavior studies. In Members and of the Transportation Research Boards Travel Survey Methods Committee (ABJ40), F., editors, *The Online Travel Survey Manual: A Dynamic Document for Transportation Professionals*.
- Murakami, E. and Wagner, D. P. (1999). Can using Global Positioning System (GPS) improve trip reporting? *Transportation Research Part C: Emerging Technologies*, 7:149–165.
- Prato, C. and Bekhor, S. (2007). Modeling Route Choice Behavior: How Relevant Is the Composition of Choice Set? *Transportation Research Record: Journal of the Transportation Research Board*, 2003:64–73.
- Prato, C., Rasmussen, T., and Nielsen, O. (2014). Estimating value of congestion and of reliability from observation of route choice behavior of car drivers. *Transportation Research Record: Journal of the Transportation Research Board*, (2412):20–27.
- Prato, C. G. and Bekhor, S. (2006). Applying branch and bound technique to route choice set generation. *Transportation Research Record*, pages 19–28.
- Prato, C. G., Bekhor, S., and Pronello, C. (2011). Latent variables and route choice behavior. *Transportation*, 39(2):299–319.

- Quddus, M. A., Ochieng, W. Y., and Noland, R. B. (2007). Current map-matching algorithms for transport applications: State-of-the art and future research directions. *Transportation Research Part C: Emerging Technologies*, 15:312–328.
- Rahmani, M. and Koutsopoulos, H. N. (2013). Path inference from sparse floating car data for urban networks. *Transportation Research Part C: Emerging Technologies*, 30:41 – 54.
- Ramming, M. S. (2002). *Network Knowledge and Route Choice*. PhD thesis, Massachusetts Institute of Technology (MIT).
- Ramos, G. D. M. (2015). *Dynamic Route Choice Modelling of the Effects of Travel Information using RP Data*. PhD thesis, Delft University of Technology.
- Rasmussen, T., Anderson, M., Nielsen, O., and Prato, C. (2016). Timetable-based simulation method for choice set generation in large-scale public transport networks. *European Journal of Transport and Infrastructure Research*, 16(3):467–489.
- Rasmussen, T., Nielsen, O., Watling, D., and Prato, C. (2017). The restricted stochastic user equilibrium with threshold model: Large-scale application and parameter testing. *European Journal of Transport and Infrastructure Research*, 17(1):1–24.
- Rosvall, M., Trusina, A., P Minnhagen, P., and Sneppen, K. (2005). Networks and cities: An information perspective. *Physical Review Letters*, 94(2). Paper id:: doi: 10.1103/PhysRevLett.94.028701.
- Sheffi, Y. (1984). *Urban Transportation Networks: Equilibrium Analysis With Mathematical Programming Methods*. Prentice-Hall.
- Sheffi, Y. and Powell, W. B. (1982). An algorithm for the equilibrium assignment problem with random link times. *Networks*, 12(2):191–207.
- Stark, H.-U., Helbing, D., and Schönhof, M. (2008). Alternating cooperation strategies in a route choice game: Theory, experiments, and effects of a learning scenario. In Innocenti, A. and Sbriglia, P., editors, *Games, Rationality and Behaviour*, pages 256–273. Houndmills and New York: Palgrave MacMillan.
- Stipancic, J., Miranda-Moreno, L., and Saunier, N. (2017). The impact of congestion and traffic flow on crash frequency and severity: An application of smartphone-collected gps travel data. Technical report.
- Stopher, P., Jiang, Q., and FitzGerald, C. (2007). Deducing mode and purpose from GPS data. In *paper presented at the 11th TRB National Transportation Planning Applications Conference*, Daytona Beach.
- Suttles, G. (1972). *The Social Construction of Communities*. The University of Chicago Press, Chicago.

- Taylor, H. A. and Tversky, B. (1992). Spatial mental models derived from survey and route descriptions. *Journal of Memory and Language*, 31(2):261 – 292.
- Tolman, E. C. (1948). Cognitive maps in rats and men. *Psychological Review*, 55:189–208.
- Train, K. (2003). *Discrete Choice Methods with Simulation*. SUNY-Oswego, Department of Economics.
- van der Zijpp, N. J. and Fiorenzo Catalano, S. (2005). Path enumeration by finding the constrained K-shortest paths. *Transportation Research Part B: Methodological*, 39(6):545–563.
- Venigalla, M., Zhou, X., and Zhu, S. (2016). Psychology of route choice in familiar networks: Minimizing turns and embracing signals. *Journal of Urban Planning and Development*, 143(2):04016030.
- Vovsha, P. and Bekhor, S. (1998). Link-Nested Logit Model of Route Choice: Overcoming Route Overlapping Problem. *Transportation Research Record: Journal of the Transportation Research Board*, 1645:133–142.
- Vrtic, M., Schüssler, N., Erath, A., Axhausen, K., Frejinger, E., Bierlaire, M., Stojanovic, S., Rudel, R., and Maggi, R. (2006). Including travelling costs in the modelling of mobility behaviour. Technical report, Final report for SVI research program Mobility Pricing: Project B1, on behalf of the Swiss Federal Department of the Environment, Transport, Energy and Communications, IVT ETH Zurich, ROSO EPF Lausanne and USI Lugano.
- Yang, J. and Juang, G. (2014). Development of an enhanced route choice model based on cumulative prospect theory. *Transportation Research Part C: Emerging Technologies*, 47, Part 2(0):168–178.
- Yildirimoglu, M., Ramezani Ghalenoei, M., and Geroliminis, N. (2015). Equilibrium analysis and route guidance in large-scale networks with MFD dynamics. *Transportation Research Part C: Emerging Technologies*, 59:404–420.

Evanthia Kazagli

Transport and Mobility Laboratory – TRANSP-OR
School of Architecture, Civil and Environmental Engineering, Station 18
Ecole Polytechnique Fédérale de Lausanne, CH-1015 Lausanne, Switzerland

☎ +41 (0) 76 273 27 31 • 📞 +41 (0) 21 693 24 29
✉ evanthia.kazagli@epfl.ch • 🌐 evanthia-kazagli

Education

École Polytechnique Fédérale de Lausanne (EPFL) <i>Ph.D. in Civil and Environmental Engineering, Dissertation: Aggregate route choice models</i>	Lausanne 2012–present
KTH Royal Institute of Technology <i>Master in Transport Systems, Master thesis: Arterial travel time estimation from automatic number plate recognition data</i>	Stockholm 2010–2012
National Technical University of Athens (NTUA) <i>Diploma in Rural and Surveying Engineering, Diploma thesis: Assessment of the design of reverse horizontal curves to accommodate heavy vehicles based on simulation</i>	Athens 2003–2009

Professional experience

École Polytechnique Fédérale de Lausanne (EPFL) <i>Research and Teaching Assistant, Transport and Mobility Laboratory</i>	Lausanne 2012–present
KTH Royal Institute of Technology <i>Undergraduate Student, iMobility Lab, Division of Transport and Logistics Research assistant, Master level coursework (TEMPUS IV European project)</i>	Stockholm 2011–2012
Roadinfo Europe AB <i>Part-time Traffic Engineer, External partner</i>	Stockholm 2011–2012
ANKA Consulting Engineers <i>Road Design Engineer</i>	Athens 2008–2010

Teaching assistant

École Polytechnique Fédérale de Lausanne <i>Mathematical Modeling of Behavior (Master course)</i>	2013–2016
<i>Decision-Aid Methodologies in Transportation (Master course)</i>	2013–2016
<i>Discrete Choice Analysis: Predicting Demand and Market Shares (postgraduate one-week program)</i>	2013–2017

Student supervision

Master thesis.....

École Polytechnique Fédérale de Lausanne

Plourde, M. <i>Modeling heterogeneity of drivers route choice behavior in Québec</i>	Spring 2017
Buisson, A. <i>Individual activity-travel analysis based on smartphone WiFi data</i>	Spring 2014
Friederich, M. N. X. <i>Mode choice analysis using smartphone data</i>	Spring 2014

Semester projects.....

École Polytechnique Fédérale de Lausanne

Montesinos, M. F. and Ortelli, N. M. <i>Simplicity in drivers' behavior</i>	Spring 2017
Montesinos, M. F. and Richard, T. G. M. <i>Data analysis and route guidance with limited information</i>	Fall 2016
Plourde, M. <i>Modeling route choice in the city of Québec using the MRI approach</i>	Fall 2016
Plourde, M. <i>Modeling route choice in Québec city using mental representations</i>	Spring 2016
Arriagada, D. A. <i>Development of an aggregate route choice model for a big network</i>	Spring 2015
Buisson, A. <i>Identify users' locations of interest from smartphone WiFi data</i>	Fall 2013
Babel, H. L. <i>Exploring pedestrian mobility using video tracking data in Lausanne train station</i>	Fall 2013
Friederich, M. N. X. <i>Mode choice analysis from a large smartphone dataset</i>	Fall 2013
Friederich, M. N. X. <i>Exploration of smartphone users trip data to investigate travel behavior</i>	Fall 2013
Kissling, L. <i>Enhancement of Naville's press delivery regulation tool: An exploratory analysis</i>	Spring 2013
Buisson, A. <i>Mobility learning from smartphone WIFI data</i>	Spring 2013

Selected publications

Publications in peer reviewed journals.....

1. Kazagli, E., Bierlaire, M., and Flötteröd, G. (2016). *Revisiting the route choice problem: A modeling framework based on mental representations*, **Journal of Choice Modelling**, Vol. 19, pp- 1–23.
2. Kazagli, E., and Koutsopoulos, H. N. (2013). *Estimation of Arterial Travel Time from Automatic Number Plate Recognition Data*, **Transportation Research Record**, Vol. 2391, pp- 22–31.

Books and contributions to books.....

1. Kazagli, E., Chen, J., and Bierlaire, M. (2014). *Individual Mobility Analysis Using Smartphone Data*, in Soora Rasouli and Harry Timmermans, eds., **Mobile Technologies for Activity-Travel Data Collection and Analysis**, IGI Global, chapter 12, pp.187-208.

Working papers.....

Submitted to journals

1. Kazagli, E., Bierlaire, M., and Lapparent, M.(de) (2017). *Operational route choice methodologies for practical applications*, submitted to **Transportation**

Ongoing papers

1. Kazagli, E., Bierlaire, M. (2017). *Route choice in a large network: Québec city*.

Technical reports.....

1. Kazagli, E., Bierlaire, M., and Lapparent, M.(de) (2017). *Operational route choice methodologies for practical applications*. Technical report TRANSP-OR 170526. Transport and Mobility Laboratory, ENAC, EPFL.
2. Kazagli, E., Bierlaire, M., and Flötteröd, G. (2015). *Revisiting the route choice problem: A modeling framework based on mental representations*. Technical report TRANSP-OR 150824. Transport and Mobility Laboratory, ENAC, EPFL.

Conference proceedings.....

1. Montesinos, M. F, Ortelli, N. M, Bellocchi, L., Kazagli, E., and Geroliminis, N. (2017). *Modeling simplicity in drivers' route choice behavior*. Proceedings of the 17th Swiss Transport Research Conference (STRC) 17-19 May, 2017.
2. Kazagli, E., and Bierlaire, M. (2016). *Assessing complex route choice models using mental representations*. Proceedings of the 16th Swiss Transport Research Conference (STRC) May 19-20, 2016.
3. Kazagli, E., and Bierlaire, M. (2015). *A route choice model based on mental representations*. Proceedings of the Proceedings of the 15th Swiss Transport Research Conference (STRC) April 15-17, 2015.
4. Kazagli, E., and Bierlaire, M. (2014). *Revisiting route choice modeling: A multi-level modeling framework for route choice behavior*. Proceedings of the Proceedings of the 15th Swiss Transport Research Conference (STRC) April 15-17, 2015.
5. Kazagli, E., Chen, J., and Bierlaire, M. (2013). *Incorporating "Mental Maps" in route choice modeling: Preliminary ideas*. Proceedings of the 13th Swiss Transport Research Conference (STRC) 24-26 April, 2013.
6. Kazagli, E., and Koutsopoulos, H. N. (2013). *Arterial travel time estimation from automatic number plate recognition data*. Proceedings of the 92nd Annual Transportation Research Board Meeting January 13-17, 2013.

Invited talks and seminars.....

1. May 24, 2017: Ecole des Ponts Paris-Tech, Paris, France. *Modeling route choice using aggregate models*.
2. May 12, 2016: Ecole des Ponts - ParisTech, France. *Dealing with structural correlation in discrete choice models: The complex case of route choice*.
3. Kazagli, E., Bierlaire, M., and Lapparent, M.(de) (2017). *Modeling route choice in Québec city using mental representations*. 17th Swiss Transport Research Conference (STRC) May 18, 2017, Ascona, Switzerland.

4. Kazagli, E., Bierlaire, M. (2016). *Assessing complex route choice models using an abstracted network based on mental representations*. hEART 2016, 5th Symposium of the European Association for Research in Transportation, Delft University of Technology, September 16, 2016, Delft, Netherlands.
5. Kazagli, E., Bierlaire, M. (2016). *Assessing complex route choice models using an abstracted network based on mental representations*. Ninth Triennial Symposium on Transportation Analysis (TRISTAN IX), June 16, 2016, Oranjestad, Aruba.
6. Kazagli, E., Bierlaire, M., and Flötteröd, G. (2015). *Assessment of A Route Choice Model Based on Mental Representations for Practical Applications*. hEART 2015, 4th Symposium of the European Association for Research in Transportation, Technical University of Denmark (DTU) September 11, 2015, Copenhagen, Denmark.
7. Kazagli, E., Bierlaire, M. (2015). *Revisiting the route choice problem: A modeling framework based on mental representations*. International Choice Modelling Conference, May 12, 2015, Austin, Texas - USA.
8. Kazagli, E., Bierlaire, M. (2014). *Revisiting route choice modeling: A multi-level modeling framework for route choice behavior*. hEART 2014, 3rd Symposium of the European Association for Research in Transportation, Institute for Transport Studies, University of Leeds, September 12, 2014, Leeds, United Kingdom.
9. Kazagli, E. (2014). *A route choice modeling framework based on mental representations*. Short program course: Modeling and Simulation of Transportation Networks 2014, May 23, 2014, Naples, Italy.
10. Kazagli, E. (2013). *Incorporating Travelers' mental representations in route choice modeling*. DATA SIM Summer School 2013, Mobility Modeling and Big Data Sources, Hasselt University, July 15, 2013, Hasselt, Belgium.

Reviewing

1. EURO Journal on Transportation and Logistics
2. Transportation
3. Transportation Research Part C: Emerging Technologies

Languages

Greek: Native

English: Fluent

Certificate of Proficiency in English, The University of Michigan

French: Intermediate

Diplome d'Etude en Langue Francaise 1^{er} Degré (Delf 1)

Awards and distinctions

Best Master Thesis in the field of Operations Research

Stockholm

SOAF - Svenska Operationsanalytiseringsföreningen (Swedish Operations Research Association)

2012

Thomaideio Award of Sciences and Arts for Publications of Graduate Students

Athens

Publication of NTUA Diploma Thesis, in *Advances in Transportation Studies: An International Journal*, Twenty-third issue, April, 2011

2009

Thomaideio Award for the Participation of Graduate Students in Conferences

Athens

Presentation of NTUA Diploma Thesis, in the 2nd International Conference Road Safety and Simulation (RSS 2009) in Paris, France

2009

